

Review

Material design and structure optimization for rechargeable lithium-sulfur batteries

Yiju Li¹ and Shaojun Guo^{1,2,*}

SUMMARY

With the merits of low cost, abundant resources, environment friendliness, and high energy density, the Li-S battery is recognized as a promising alternative to the Li ion battery and is anticipated to play an important role in high-energy-density electrochemical storage systems. In this review, we first review the development process of Li-S batteries and briefly introduce the working principle of Li-S batteries. The scientific problems existing in the Li-S batteries, such as sulfur cathode, separator, electrolyte, and Li anode, and the corresponding countermeasures, are then summarized. Subsequently, main research advancements of Li-S batteries are comprehensively reviewed, and the critical concerns about commercialization of Li-S batteries are discussed. Finally, we give our perspectives on the development of high-performance Li-S batteries. We hope this review can provide the timely and comprehensive information on the future research direction of Li-S batteries and offer the guidance for material design and structure optimization of Li-S batteries.

INTRODUCTION

The exhaustion of fossil energy and aggravation of environmental pollution have become two major challenges that greatly restrict the sustainable development of today's society. To mitigate these two issues, alternative energy technologies based on clean and renewable sources have been extensively developed. However, renewable energies, such as solar, wind, geothermal, and tidal, are regionally limited, intermittent, and unpredictable. Therefore, it is necessary and significant to develop efficient and economical electrochemical energy storage technologies for rational and reliable utilization of the electricity produced by these renewable sources. Among the available electrochemical energy storage devices, rechargeable batteries, such as lead-acid, nickel-cadmium, and nickel metal hydride batteries have been successfully applied in various applications, e.g., consumer electronics and vehicles, for several decades. With the complexification, miniaturization, and lightweighting of portable electronics and the increasing demand for electric vehicles, advanced secondary batteries with higher energy density, longer cycle lifespan, higher safety, and lower environmental impact need to be explored and developed. As an innovative energy storage technology, Li ion batteries have been the most prominent battery technology over the latest three decades.^{1–3} Since the first commercial production of Li ion batteries configured with lithium cobalt oxide cathodes and graphite anodes in 1991, the rechargeable Li ion battery technology has been constantly achieving important progress both in power and energy density and dominating the energy storage market worldwide. Nevertheless, very recently, it has been argued that the Li ion battery systems based on the intercalation mechanism encounter a “bottleneck”: the overall energy density is approaching the limit

Progress and potential

Conventional lithium (Li) ion batteries are more and more difficult in satisfying the ever-growing energy demand because they are approaching their theoretical energy density limits. Owing to the high theoretical energy density, lithium-sulfur (Li-S) batteries are a promising alternative in the era of post Li ion battery chemistry. However, the practical application of Li-S batteries is hindered by their low sulfur utilization, severe self-discharge, inferior cycling stability, and high safety hazards. Rational material design and structure optimization are thus highly desired to address these issues. This review summarizes current challenges facing the development of Li-S batteries, including sulfur cathode, separator, electrolyte, and Li anode, and the corresponding strategies, are comprehensively discussed. The concerns regarding the commercialization of Li-S batteries are then briefly presented. Finally, some perspectives on the directions for future research on Li-S batteries are provided.



(300–350 Wh kg⁻¹).^{4–6} The limit of energy density is usually determined on electrode capacity and cell voltage. In the existing Li ion battery technology route, the capacity of insertion-type oxide cathodes has reached a maximum value of ~250 mAh g⁻¹, and the capacity of graphite anodes is also limited to 372 mAh g⁻¹. On the other hand, the voltage window of currently available liquid organic electrolytes can barely operate stably beyond ~4.3 V. Therefore, pushed by the requirement of higher energy density, the development of alternative battery chemistries that can either offer higher capacity or a wider electrochemical stability window or both are urgently needed.

Among various alternatives, Li-S batteries assembled with the earth-abundant (0.048 wt % in the earth's crust) and low-toxic sulfur cathodes and lightweight lithium anodes (0.534 g cm⁻³) are considered as one of the most promising next-generation electrochemical energy storage systems that possess the advantages of low cost and high energy density.^{7–14} At the anode, the Li metal based on the stripping/plating mechanism can provide the lowest redox potential of -3.04 V and a high theoretical specific capacity of 3,860 mAh g⁻¹. For the cathode, due to the multi-electron conversion chemistry, the cost-efficient active sulfur is able to display a high theoretical specific capacity of 1,675 mAh g⁻¹. As a result, the Li-S batteries can deliver an ultrahigh theoretical gravimetric energy density of ~2,510 Wh kg⁻¹ (based on the average discharge voltage of 2.15 V), much higher than that of the conventional Li ion batteries.

The emergence of Li-S batteries can be traced back to 1962. Herbert and colleagues¹⁵ first proposed the primary cell models using Li and Li alloys as anodes, and sulfur, selenium, and halogens, etc., as cathodes. In the patent, the alkaline or alkaline earth perchlorates, iodides, sulfocyanides, bromides, or chlorates dissolved in a primary, secondary, or tertiary saturated aliphatic amine are selected as the electrolyte. In 1968, Bhaskara¹⁶ specifically patented high-energy-density metal-sulfur batteries assembled with light metals (Li, Ca, Be, Mg, and Al) and a mixture of inert conductors with sulfur in organic electrolytes. The organic solvents, including propylene carbonate, γ -butyrolactone, dimethylsulfoxide, and *N,N*-dimethylformamide were first proposed in the electrolytes, and these battery systems can achieve cell voltages of 1.16–2.52 V. In addition, the theoretical gravimetric and volumetric energy densities of the proposed metal-sulfur batteries were systematically presented. In the following 20 years, primary Li-S batteries based on various organic solvents, such as tetrahydrofuran and dioxolane (DOL), have been continually developed.^{17–19} In 1989, a notable work by Peled et al.²⁰ demonstrated the feasibility of developing a rechargeable Li-S battery system in DOL-rich electrolytes: a Li-S battery with a configuration of Li foil//0.1 M Li₂S₈ in a mixture of ethers//Teflon-bonded porous carbon was built. In most cases, the charge capacity is 20%–100% higher than the discharge capacity, and maximum number of cycles to failure is 50 at a discharge rate of 6 mA. Although the reversibility of the proposed Li-S cell model is not high enough, it inspired the researchers to put much effort into the explorations of rechargeable Li-S batteries in the subsequent period. With the extensive investigation of solid-state electrolytes since the 1990s, polymer- and ceramic-based electrolytes have been successfully applied in the rechargeable Li-S batteries.²¹ A patent granted in 1998 described a poly(ethylene oxide) (PEO)-based solid-state Li-S battery, of which the positive electrode contains 20–80 wt % active sulfur, acetylene black, and PEO with Li salt.²² The proposed PEO-based gel-state rechargeable Li-S battery with an active sulfur of 50 wt % delivered a high capacity of 1,500 mAh g⁻¹ under 90°C.

¹School of Materials Science and Engineering, Peking University, Beijing 100871, China

²BIC-ESAT, College of Engineering, Peking University, Beijing 100871, China

*Correspondence: guosj@pku.edu.cn

<https://doi.org/10.1016/j.matt.2021.01.012>

To further prevent dissolution of polysulfides and enhance the active sulfur utilization, two important works, presented by Wang et al., in 2002,^{23,24} first demonstrated that the sulfur/active carbon and sulfur/polyaniline nano-composites are two highly effective cathode materials to improve the specific capacity and cycling stability. The elemental sulfur embedded and trapped in the nanopores of high-specific-area active carbon shows a reversible capacity of 440 mAh g⁻¹ based on the composite (sulfur:active carbon, 3:7) and sulfur utilization reaches ~90%. The molecular level mixed sulfur/polyaniline composite contains a highly electronically conductive polymer matrix, in which active sulfur is homogeneously embedded. This structure can effectively prevent sulfur from aggregating and suppress the dissolution of polysulfides. As a result, the sulfur/polyaniline composite electrode can be stably operated for 50 cycles with a capacity retention above 600 mAh g⁻¹. Another significant progress in inhibiting dissolution of polysulfides was achieved by Nazar and colleagues.²⁵ They constructed the nanostructured polymer-modified ordered mesoporous carbon (CMK-3)-sulfur composite and demonstrated effective confinement effects at the nanoscale. The mesopores in the CMK-3 carbon acts as numerous reaction microchambers for enhancing the utilization of active sulfur. In addition, the polymer coating helps to retard diffusion of polysulfides out of the composite, decreasing the loss of active mass and improving the cycling stability. The proposed strategy of “physical confinement” in the above-mentioned works have been widely used.^{26–30} Since 2000, some fundamental in-depth studies on the Li-S battery chemistry, particularly in terms of self-discharge characteristics, chemical structure evolution of sulfur species, and optimization of electrolyte system, including organic solvent, additives, and Li salts, have been performed.^{31–37} These fundamental investigations laid a solid foundation for the overall understanding of electrochemical mechanisms of rechargeable Li-S batteries.

After 2010, more efforts have been dedicated to the investigation of rechargeable Li-S batteries, as demonstrated by the dramatically increased number of research publications. In the meantime, many significant breakthroughs have been achieved toward high specific capacity and long cycle life Li-S batteries.^{38–40} Particularly in 2012, some proposed strategies, such as “small sulfur molecule,” interlayer construction, and chemical adsorption enabled by oxides and heteroatom-doped carbons have been proved to be highly effective for boosting the electrochemical performance of Li-S batteries, and shed light on the future research direction on the performance enhancement of sulfur cathodes.^{41–44} Subsequently, in 2015, pushed by the poor reaction kinetics of insulated polysulfides and inspired by the enhanced kinetics of aqueous polysulfides in photoelectrochemical solar cells and redox flow cells using electrocatalytic electrodes, another important strategy of electrocatalytic conversion in Li-S batteries was first reported by Arava and colleagues.⁴⁵ The electrocatalytic conversion reactions of polysulfides have been found to take place on surfaces, such as Pt, Au, and Ni, which can effectively reduce polarization and increase specific capacity.⁴⁶ Meanwhile, in the last 10 years, much progress has also been achieved in the design and preparation of functional separators, binders, and conductive additives to suppress the shuttle effect and improve the utilization of active sulfur.^{47–52}

It should be mentioned that, in addition to the problems of sulfur dissolution and slow conversion kinetics at the cathode, Li dendrite growth and low Coulombic efficiency at the anode could also be the main reasons for the fast performance decay of Li-S batteries, but have not received much attention over that period. On the basis of the previous explorations on Li anode chemistry, in 2014 Liu and colleagues⁵³ constructed an artificial self-regulated solid-state electrolyte interface (SEI) layer of

lithiated graphite on the surface of Li metal, which cannot only supply Li ion on demand, but also minimize the direct contact between the Li anode and polysulfides. The proposed surface engineering strategy for using Li metal anodes effectively suppressed the deleterious side reactions of Li anodes, and resulted in great performance enhancement. The work has triggered much research attention on protection of the Li anode, promoting further development of Li-S battery systems.^{54,55} Although significant progress on addressing the fundamental scientific issues of Li-S battery chemistry has been made, researchers realized that there was still a large gap between academic research and industrial production.⁵⁶ To turn the commercialization of Li-S batteries into reality, more efforts need to be focused on the material design and structure optimization under practical working conditions. Fortunately, some recent works on the construction of high-mass-loading sulfur cathodes and solutions to the passivation of the cathode under a lean electrolyte have shown positive results, which has greatly strengthened researchers's confidence in the commercialization of Li-S batteries.^{57–60}

Looking back on the 60-year development of Li-S batteries (Figure 1), it can be seen that great success has been achieved and that there has been a gradual move toward practical applications. In this review, we first introduce the fundamental reaction mechanisms and scientific challenges in the development of Li-S batteries. Based on the comprehensive understanding of Li-S battery chemistry, we demonstrate representative strategies for material design and structure optimization to address the existing scientific problems in Li-S battery systems. The critical concerns on the commercialization of Li-S batteries are then discussed. Finally, we summarize the current situation with regard to Li-S batteries and present some outlooks on the development of more efficient and application-oriented Li-S batteries featuring high energy density and long-term stability.

FUNDAMENTALS AND CHALLENGES IN THE DEVELOPMENT OF LITHIUM-SULFUR BATTERIES

Reaction mechanism

Li-S batteries based on the conversion mechanisms are expected to be a good alternative in current critical energy storage applications, such as in electric vehicles and in stationary energy storage, due to their potentially higher energy density compared with the currently available Li ion batteries (Figure 2A). Typically, conventional Li-S batteries are composed of a Li metal anode, a sulfur composite cathode, an organic electrolyte, and a porous polymer-based separator. Unlike mainstream Li ion batteries based on the ion-insertion mechanism, Li-S batteries undergo a series of complex electrochemical/chemical reactions under working conditions.⁶¹ Although the working mechanism of Li-S batteries is complicated and still under debate, the common operation principle can be generally summarized as shown in Figure 2B. Of the more than 30 solid sulfur allotropes, the orthorhombic cyclic octasulfur (S_8) is the most stable at ambient temperature, and usually used as the starting material at the cathode. Since the electrode material of S_8 is Li-free, the Li-S batteries commonly start with a discharge process. During the galvanostatic discharge process, the number of S_8 molecules is reduced, and then their "crown structure" opens and combines with Li ions through the mediation of electrons from the external electrical circuit. At the early stage (stage I), the S_8 molecules are successively electrochemically reduced to form high-order soluble lithium polysulfide intermediates (Li_2S_x , $4 \leq x \leq 8$), yielding to an upper voltage plateau at about 2.35 V versus Li/Li^+ (0.5 electron transfer per sulfur atom at the end of stage I). It should be noted that, on the one hand, the soluble polysulfides with a high reactive activity

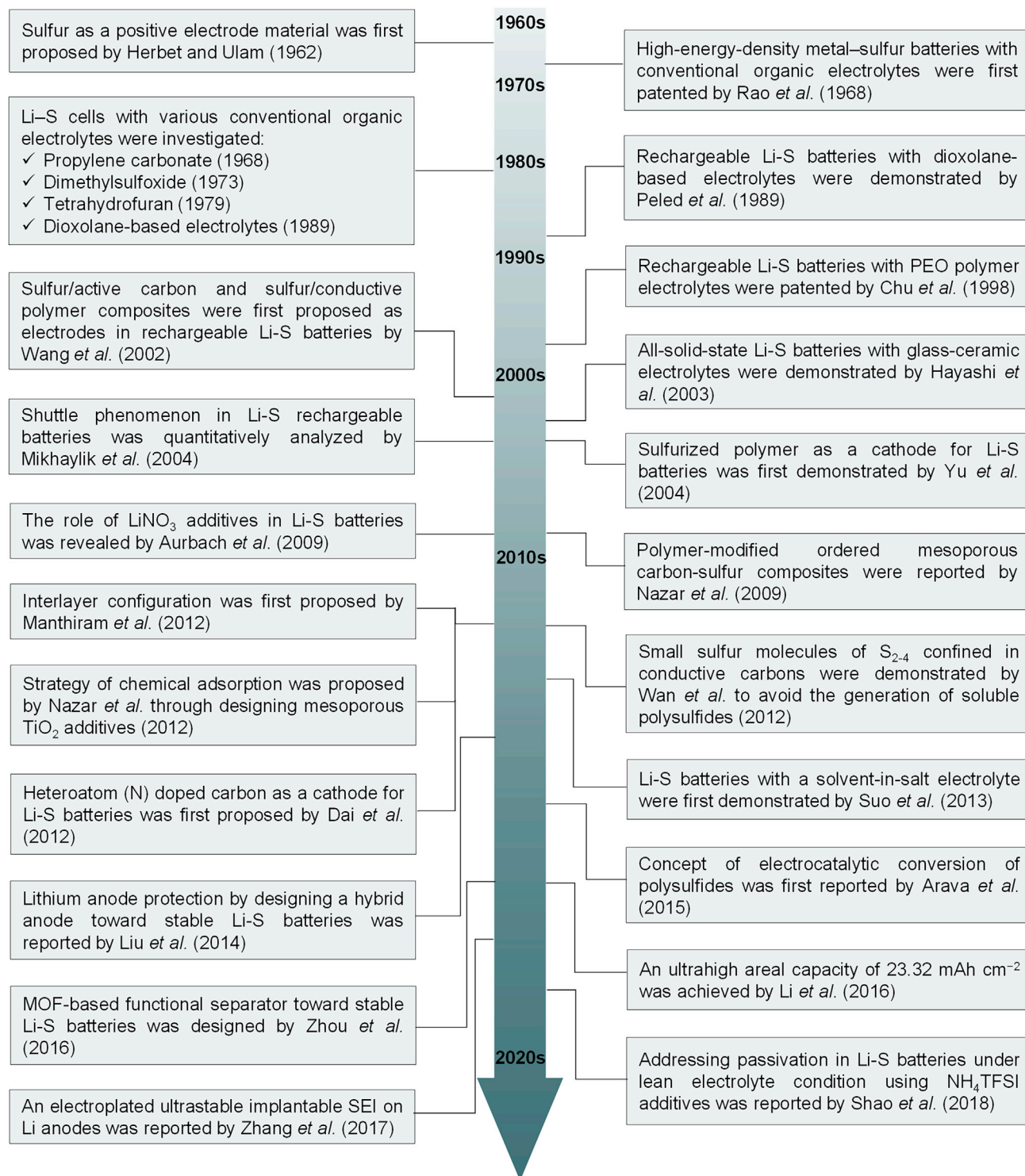


Figure 1. Brief timeline showing the pioneering and key events in the development of Li-S batteries

could continuously expose the reaction interfaces of sulfur electrode, contributing to obtaining fast reaction kinetics and enhancing the utilization of active sulfur. While, on the other hand, the dissolution of high-order polysulfides increases the viscosity

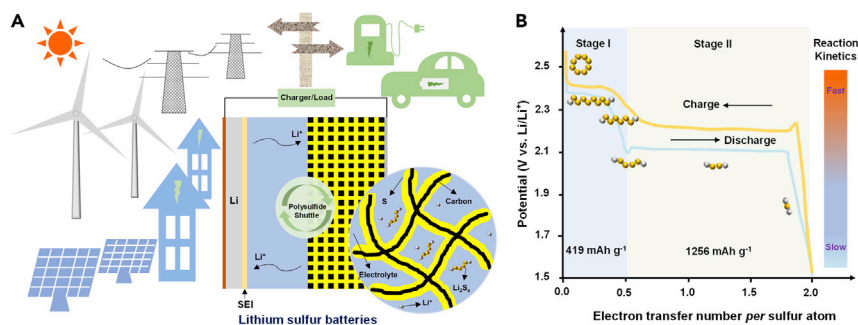


Figure 2. Schematic illustration of the structure and charge/discharge process of Li-S batteries

(A) Schematic showing the structure of a Li-S battery.

(B) Typical voltage profiles of a Li-S battery.

of the electrolyte, resulting in the reduction of ionic conductivity and inevitably causing the loss of active materials.

With discharge taking place, the low-order insoluble lithium polysulfides (Li_2S_x , $1 \leq x < 4$) are produced due to combination with additional Li ions, yielding a lower voltage plateau at about 2.15 V versus Li/Li^+ (1.5 electron transfer per sulfur atom during stage II). It is worth noting that an overpotential is usually observed at the transition region between stage I and II during the discharge process, which is attributed to the motivation toward heterogeneous nucleation of insoluble polysulfides on conductive substrates. In addition, the reaction kinetics during state II is much more sluggish than that during the state I due to the solid-solid conversion reaction between Li_2S_2 and Li_2S .⁶² During the subsequent charge process, the Li_2S is consecutively delithiated to form S_8 through multiple polysulfide intermediates. Because the polysulfide intermediates are gradually identified in ether-based electrolytes, an in-depth understanding of the mechanism of complex sulfur chemistries is established. The redox reactions of sulfur based on solid-liquid-solid conversion are effectively modulated through material design and structure optimization. It should be pointed out that the shape of the galvanostatic charge/discharge profiles can vary with the chemical states of the sulfur-based cathodes and electrolytes, because the voltage plateaus are related to the conversion mechanism, which depends on the form of the polysulfide intermediates. For example, only one single discharge plateau is usually observed for the small molecular sulfur and sulfurized polymers, indicating the solid-solid phase conversion without the formation of soluble polysulfides. Moreover, in the absence of liquid organic solvents for the dissolution of polysulfides, all-solid-state Li-S batteries based on ceramic and polymer electrolytes also commonly follow an alternative solid-solid transformation route between sulfur and Li_2S .

Scientific challenges and strategies

Sulfur cathode

There are still many challenges facing Li-S chemistry (Figure 3). With regard to the sulfur cathode, three main challenges have been identified.⁶³ Firstly, the most obvious challenge is the electrically insulating nature of sulfur ($\sim 10^{-30} \text{ S cm}^{-1}$) and the insoluble intermediate products, such as Li_2S ($\sim 10^{-13} \text{ S cm}^{-1}$).⁶⁴ Their inferior electronic conductivity results in poor utilization of active materials and limits the electron transfer during the reaction process, causing relatively slow kinetics. Another challenge is the well-recognized shuttle effect resulting from the diffusion of soluble sulfur species. The high-order polysulfide intermediates can shuttle to the anode and react with the metallic Li to form low-order polysulfides, and then

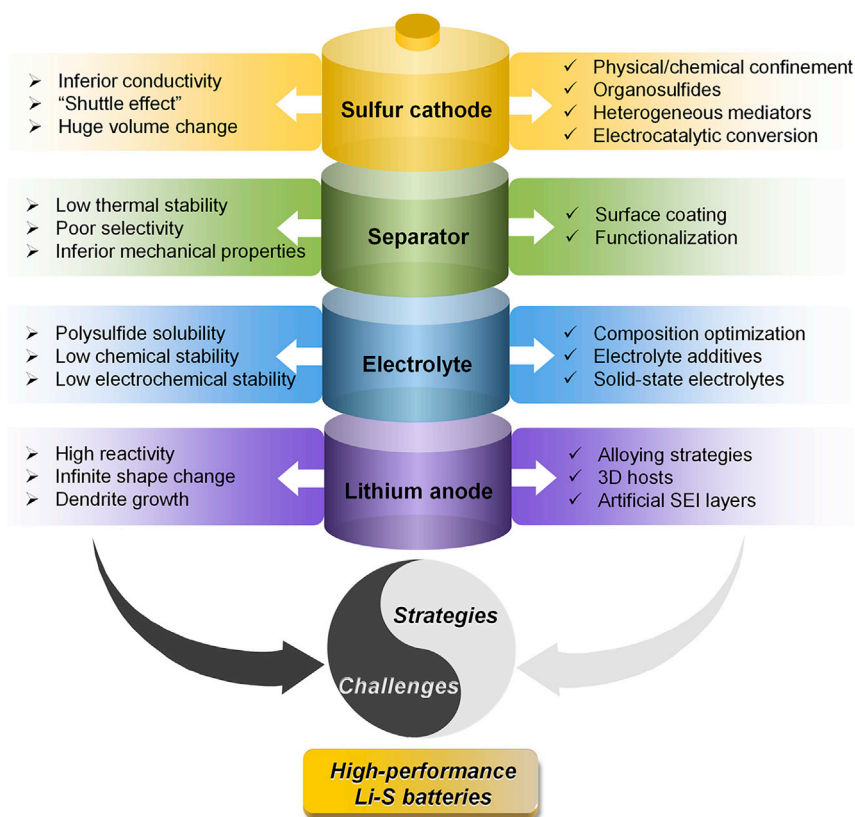


Figure 3. Summarization of scientific challenges and strategies for high-performance Li-S batteries

migrate back to the cathode where they are reoxidized to generate high-order polysulfides.⁶⁵ Severe shuttle phenomena result in rapid self-discharge, infinite charge, low Coulombic efficiency, increased internal resistance, and fast fading of capacity. The last challenge is the huge change in volume during the charge/discharge process, which is commonly neglected in most published works. The "host-less" electrochemical conversion reaction of the sulfur cathode suffers from a significant volume change of ~78%, about eight times higher than that of intercalation-based transition metal oxide-based cathodes in current Li ion batteries.⁶⁶ As a consequence, the cohesion of active sulfur may deteriorate, and the mechanical structure of the sulfur electrode may collapse, leading to the decay of capacity. The adverse evolution of electrode disintegration would be even more significant when the mass loading of sulfur is increased.

To address these problems, the physical confinement of sulfur in well-designed nonpolar porous hosts was first proposed as early as about 10 years ago and has been demonstrated to be an effective strategy to alleviate, to some extent, the diffusion of soluble polysulfide intermediates. To better prevent the shuttle behavior, the concept of chemical adsorption has been subsequently proposed to further enhance the interaction between sulfur species and substrates.⁶⁷ The introduction of polar sites, either on hosts or binders, can lead to a strong chemical bond with the polar polysulfides, and thus well suppress their irreversible dissolution into the electrolyte. The use of heterogeneous mediators as solid additives in sulfur cathodes, which could facilitate polysulfide conversion by changing the polysulfide reaction pathways, has been widely investigated in Li-S batteries.⁶⁸ Because they are important

alternative sulfur-based cathode materials, the organosulfides (R-S_x-R) have also attracted much research attention due to their low cost, favorable sustainability, and highly tunable properties, and are regarded as a potential choice to address the shuttle effect.⁶⁹

In addition to the above-mentioned strategies, researchers have gradually turned their attention toward the electrocatalytic effect of a series of specific materials on the redox of sulfur cathode. Usually, slow transformation kinetics of polysulfides will increase the possibility of their dissolution and diffusion into the electrolyte, causing the shuttle phenomenon to be more serious and accelerating the decay rate of the capacity. Akin to the known oxygen redox reactions in rechargeable metal-air batteries, the introduction of electrocatalytic materials in the sulfur cathode can effectively reduce the charge transfer resistance and decrease the reaction polarization, leading to an accelerated conversion process between soluble and insoluble sulfur species. Of course, two or more of the above-mentioned strategies can be integrated into a single electrode to build a multifunctional sulfur cathode, further enhancing its electrochemical performance.

Separator

An indispensable component in liquid battery systems, the separator acts as a barrier to block internal electron transfer and as a channel to allow ion transport. The most commonly utilized separators in Li-S batteries are porous polyethylene (PE), polypropylene (PP), and a multilayered PP/PE composite. These non-toxic thermoplastic polyolefin-based separators have the advantages of light weight, excellent low temperature resistance (the lowest service temperature can be from as low as -100°C to approximately -70°C), good chemical stability (can withstand acid and alkali erosion), and excellent electrical insulation performance. However, as the conventional PE- and PP-based separators have a low melting point (PE, 92°C ; PP, 165°C), they are apt to shrink and deform at high temperature, leading to internal short circuiting. In addition, the porous PE- and PP-based separators have inferior mechanical properties, such as inferior abrasion resistance and low elasticity modulus (0.84–0.95 GPa). As a result, the polyolefin-based separators in Li-S batteries can barely suppress Li dendrite growth and penetration. Another challenge for these polyolefin-based separators in Li-S batteries is their poor ionic selectivity. The soluble polysulfide ions can easily penetrate the nanopores in the porous polyolefin-based separators, resulting in a severe shuttle phenomenon.

There are usually two main pathways to develop advanced separators: (1) surface coating and (2) functionalization. For the surface coating strategy, the coating layer (interlayer) between the sulfur cathode and the separator can improve the selective ion transport of separators and regulate the polysulfide ions via physical and chemical confinement and electrocatalytic conversion. The interlayer at the interface between the Li anode and the separator can facilitate uniform Li stripping/plating either through regulating the near-surface Li ion distribution on the Li metal anode or homogenizing the current distribution. In addition, it can also suppress the Li dendrite penetration by using high-elasticity-modulus functional materials. Nevertheless, it cannot be ignored that the interlayer will to some extent introduce additional weight and volume, and inevitably lower the energy density of the full cell. Therefore, it is very necessary to minimize the weight and volume of the interlayers without sacrificing their performance. Apart from the interlayer strategy, functionalizing the separators by manipulating their chemical composition and structure is also an effective strategy to tailor the ionic selectivity, mechanical properties, and thermal stability. For example, a separator based on the polymeric materials grafted

with some specific anionic functional groups could retard the polysulfide ion transport through the electrostatic repulsion.⁷⁰ Moreover, the functionalization of separators by introducing additional rigid and fire-resistance polymers into the original matrix via blending or copolymerization could enhance their mechanical properties and thermal stability.⁷¹

Electrolyte

The electrolyte plays a critical role in the development of high-performance Li-S batteries. As mentioned above, the development of a liquid organic electrolyte solvent in Li-S batteries has gone through a process from aliphatic amines to carbonates and then to ethers. The DOL/dimethyl ether (DME)-based binary solvent system has been well developed and is commonly utilized in Li-S batteries. The current popular liquid electrolytes in Li-S batteries mainly contain a DOL/DME binary solvent, Li salts, such as lithium bis(trifluoromethane sulfone) imide (LiTFSI) or lithium bis(fluorosulfonyl) imide (LiFSI), and additives, such as LiNO_3 . It is well accepted that the linear ether solvent, DME, has a relatively high polysulfide solubility, which can provide fast conversion kinetics for the redox reactions of polysulfides.⁷² The cyclic ether solvent of DOL with a low viscosity (0.6 mPa s^{-1}) could contribute to the formation of protective SEI layers on the surface of a Li metal anode. It has been shown that the cyclic DOL could be polymerized by triggering of the trace HTFSI and radical-catalyzed isomerization to form a flexible passivation layer containing ROLi , HCO_2Li , and poly-DOL oligomers terminated with $-\text{OLi}$ groups.⁷³ As well as the organic solvent, Li salts are another vital component of electrolytes. To ensure high ion conductivity, Li salts are required to possess high chemical/electrochemical stability, high solubility, and high degree of dissociation. Among various Li salts, the LiTFSI with high thermal stability and favorable compatibility is one of the most commonly used Li salts in Li-S batteries. The additive LiNO_3 has been widely recognized to have the ability to improve the electrochemical performance of Li-S batteries. Although the exact mechanism by which LiNO_3 contributes to the improvement of the performance of Li-S batteries is still under debate, it is generally believed that LiNO_3 has a positive effect on the formation of robust SEI layers on Li metal anodes.

Despite the extensive utilization of electrolyte systems containing the DOL/DME binary solvent, LiTFSI salt, and LiNO_3 , there are still many challenges facing use of this kind of liquid organic electrolyte. For example, the high dissolution of polysulfides can result in significant loss of active materials. In addition, without effective protection strategies for the Li anode, the soluble polysulfides can migrate to the surface of the Li metal anode and reduce to form insoluble inorganic $\text{Li}_2\text{S}_2/\text{Li}_2\text{S}$ layers. Despite the fact that, to some extent, these insoluble inorganic components can help the formation of SEI layers, the resultant thick $\text{Li}_2\text{S}_2/\text{Li}_2\text{S}$ layers can cause high surface impedance, and the uneven distribution makes the SEI layers more fragile and unstable. Moreover, ether-based electrolytes have a relatively poor anti-oxidation ability, and are liable to have an anodic decomposition, which can lead to increased overpotential. On the other hand, ether-based electrolytes can be also reduced by the highly reactive Li metal anode. In some cases, the resultant inhomogeneous and unstable SEI layers can continuously expose the fresh Li active sites, resulting in continuous electrolyte consumption, thus increasing polarization. Also, gas evolution, such as CH_4 and H_2 induced by side reactions between the Li metal anode and the organic solvent or Li salts can cause a large internal pressure in the cell devices.⁷⁴ This can damage the electrode interface structure and, under some extreme conditions, can cause electrolyte leakage and risk of corrosion. Furthermore, as discussed above, the most commonly used binary ether solvent in Li-S batteries is volatile and flammable. Similar to the components in gunpowder (nitrates, sulfur, and

charcoal), the mixture of LiNO_3 , sulfur, and carbon in Li-S batteries is highly combustible, further increasing potential safety hazards.

To address the above-mentioned problems of use of a liquid organic electrolyte in Li-S batteries, there are, in general, three strategies: (1) optimization of composition; (2) use of electrolyte additives; and (3) use of solid-state electrolytes. The optimization of composition of liquid organic electrolytes discussed here mainly refers to the manipulation of solvent and Li salts. The selection of solvents is critical to regulate the dissolution and diffusion of polysulfides and enhance the chemical/electrochemical stability of Li metal anodes. For instance, compared with traditional ether solvents, fluorinated ether-based solvents, such as 1,1,2,2-tetrafluoroethyl-2,2,3,3-tetrafluoropropylether (TTE), have the advantages of low flammability, low viscosity, and low solubility to polysulfides. The anti-solvent effect of a TTE co-solvent can limit the self-discharge rate of Li-S batteries.⁷⁵ In addition, it has been found that the decomposition of fluorinated ether solvents on Li metal anodes can also help build stable SEI layers during cycling. Another successfully applied electrolyte system is use of the acetonitrile (ACN)-based “sparingly solvating” electrolyte with the co-solvent 1,1,2,2-tetra-fluoroethyl 2,2,3,3-tetrafluoropropyl ether (HFE).⁷⁶ Under the synergistic effect of ACN and HFE solvents, the solubility of polysulfides is greatly suppressed. Ionic liquids (ILs, typical “non-solvent” electrolytes), consisting of coordinated anions and cations, have the advantages of high thermal stability, a wide electrochemical window, and low volatility; these have been also widely investigated in Li-S batteries.⁷⁷ Owing to the lack of free solvent molecules, ILs can be tailored to possess a low solubility to polysulfides by selecting an appropriate anionic component with a weak electron donor ability, thus resulting in decreased polysulfide solubility.

As well as the selection of an appropriate solvent, the optimization of Li salts also plays an important role in designing high-performance organic electrolytes. For example, some electrolytes containing binary Li salts have been investigated with regard to improving the deficiency of single Li salts, thus improving the overall performance of the electrolyte.⁷⁸ Furthermore, the concept of using highly concentrated Li salts in ether solvents was proposed recently and has been proved to be able to decrease the ability of solvating polysulfides and improve the reversibility of Li metal anodes. In addition to the above-mentioned sparingly solvating and non-solvent strategies, an opposite strategy is to develop new electrolytes that can maximize the solubility of polysulfides using high donor number solvents.^{79,80} In this case, fast reaction kinetics can be achieved due to the easily accessible active sites and the existence of trisulfur (S_3) radicals, causing catalytic oxidation of Li_2S . Nevertheless, it should be pointed out that a porous cathode host and protection of the Li anode are necessary in this sort of electrolyte. Therefore, it is believed that, under the premise that the sulfur cathode and Li anode are well protected, utilizing an electrolyte with a high solubility of polysulfides could minimize the amount of electrolyte used and contribute to optimization of the electrode and cell configuration.

The introduction of electrolyte additives to enhance the electrochemical performance of Li-S batteries can be summarized as follows: (1) stabilizing the Li metal anode by facilitating the uniform deposition of Li or the formation of robust SEI layers; (2) enhancing the utilization of sulfur species; and (3) improving the stability of the electrolyte itself. As a typical additive, it is well known that LiNO_3 in ether-based electrolytes can stabilize the Li metal anode by participating in the formation of SEI layers. However, the added LiNO_3 will be continuously consumed during cycling, eventually leading to inferior Coulombic efficiency of Li-S batteries. Recently, the addition of inorganic salts, such as CsNO_3 , KNO_3 , $\text{La}(\text{NO}_3)_3$, and

$\text{Zn}(\text{CH}_3\text{COO})_2$, has been successfully applied in electrolytes of Li-S batteries to enhance the reversibility of the Li metal anode, due to either the electrostatic shield effect or the formation of transition metal/lithium sulfides in the SEI layers.^{81–85} Some other surface-charged inorganic nanoparticles, such as montmorillonites, are also found to have the ability to facilitate uniform Li deposition by regulating the near-surface Li ion distribution.^{86,87} Suitable additives in electrolytes can also help prevent irreversible polysulfide loss and improve the utilization of sulfur. Among various additives for upgrading sulfur utilization, the redox mediators (RMs) are the most commonly investigated, and have been proved to have the ability to facilitate the conversion of polysulfides.⁸⁸ As homogeneous mediators, RMs undergo charge transfer processes directly with sulfur species in the electrolytes, and then transfer the charge to current collectors. They change the charge transfer pathways in solid electrode materials to the more effective charge conduction in the electrolyte. Other additives can be used to enhance the physicochemical properties of the electrolyte itself, including thermal stability, viscosity, and electrochemical window. For example, flame-retardant additives, including phosphites and phosphazenes, are widely investigated with regard to improving the thermal stability of electrolytes.^{89,90} Replacing the liquid organic electrolytes by solid-state electrolytes is another promising strategy for constructing high-performance Li-S batteries.⁹¹ The utilization of solid-state electrolytes based on polymers or ceramics could alleviate or even eliminate the shuttle effect of polysulfides and circumvent the issue of Li dendrites; this is discussed in detail below.

Li anode

Compared with the great progress achieved in the development of sulfur cathodes, the development of Li metal anodes in rechargeable Li-S batteries is only in the initial stages. In terms of energy density, metallic Li is the top priority for the anode in Li-S batteries due to its ultrahigh specific capacity and lowest redox potential. However, there are three main challenges, including high reactivity, infinite shape change, and dendrite growth, facing the development of Li metal anodes. In contrast to graphite, with well-defined interlayers accommodating Li ions, the infinite shape change of highly reactive Li metal anodes during cycling will cause deterioration of the structural stability and aggravate the reconstruction of SEI layers, resulting in accelerated electrolyte consumption. Moreover, the continuous side reactions with the electrolyte on the inhomogeneous Li anode surface would also cause the formation of inactive Li (“dead Li”), which would directly lead to a low Coulombic efficiency. More seriously, the generated Li dendrites may pierce the separator, giving rise to internal short circuiting that could potentially cause thermal runaway and even explosion.

To address these issues, three typical strategies have been proposed, including: (1) alloying strategies; (2) 3D hosts; and (3) artificial SEI layers. The Li alloys can decrease the high reactivity of Li anodes and thus mitigate, to a certain extent, the side reactions with electrolytes. More importantly, some specific Li alloys possess a lower surface diffusion barrier and a higher bulk diffusion coefficient than Li metal, which contributes to the uniform stripping/plating of Li. To address the issue of infinite shape change of Li metal anodes, the effective “3D host” strategy has been proposed recently. Particularly for 3D conductive frameworks, it is believed that the decreased current density in the 3D hosts contributes to the uniform stripping/plating of metallic Li and thus could enhance the reversibility of Li metal anodes. As well as the regulation of *in-situ*-formed SEI layers by manipulating the electrolyte components,⁹² various artificial SEI layers coated onto Li metal anodes before cell assembly have been investigated. In general, these proposed artificial SEI layers have better mechanical or chemical properties than the SEI layers generated by the

decomposition of electrolytes and additives. In addition, the *in-situ*-formed SEI layers in electrolytes usually have complicated components and structures, and limited understanding has been obtained so far on what the specific function is for each component in SEI layers, and how the component distribution affects the SEI properties and Li anode performance. In contrast, artificial SEI layers possess definite compositions and structures, which contributes to establishing a clear structure-activity relationship, in turn guiding the material design and structure optimization of artificial SEI layers.

MATERIAL DESIGN AND STRUCTURE OPTIMIZATION

Design of the sulfur cathode

Encapsulating active sulfur in porous carbon hosts is one of the earliest strategies to improve the performance of sulfur cathodes. The porous carbon hosts can greatly enhance the electronic conductivity of sulfur electrodes, accommodate huge volume change of sulfur species, and immobilize soluble polysulfides. So far, various porous carbons with different dimensions, such as zero-dimensional (0D) hollow carbon spheres,^{93–98} multi-shell carbon spheres,^{99–101} hierarchical porous carbon spheres,^{102–105} 1D carbon tubes and carbon fibers,^{106–110} 2D graphene and carbon sheets,^{111–115} and 3D carbon frameworks,^{116–118} have been extensively investigated (Figure 4A). In a representative example, inspired by the structure of old-fashioned photo albums, the 2D yolk-shell carbon nanosheets were synthesized to construct a novel freestanding sulfur cathode with a high sulfur loading of 5 mg cm⁻² and a high sulfur content of 73 wt %, which can deliver an areal capacity of 5.7 mAh cm⁻² and a volumetric capacity of 1,330 mAh cm⁻³.¹¹⁹ Commonly, the porous carbons can be categorized into macroporous (>50 nm), mesoporous (2–50 nm), and microporous (<2 nm) carbons. Macropores of carbon hosts can provide a large space for achieving high sulfur loading and buffering volume change. Mesopores in carbon hosts could offer short electron and ion pathways and lead to uniform sulfur distribution. As a result, manipulating macropores and mesopores in carbon hosts to optimize the performance of the sulfur cathode is most frequently reported in the literature.^{120–122} Recently, micropores in carbons are found to have a stronger ability to physically confine polysulfides.^{123–125} In particular, when the size of micropores is reduced below ~0.6 nm, only small metastable sulfur allotropes S_{2.4} can be confined in the micropores. Such small micropores can avoid the formation of high-order soluble polysulfides and isolate the accessibility of polysulfides to solvent molecules (0.6–0.8 nm) (Figure 4B).⁴³ As a result, usually only stage II can be observed in the charge/discharge profiles. In addition, owing to the alleviation of dissolution of polysulfides, the confined small S_{2.4} molecules in micropores can display enhanced cycling performance compared with the S₈ molecules loaded in conventional macropores and mesopores.

As a sulfur derivative, organosulfide molecules containing different sulfur chain lengths have attracted extensive research interest in the development of Li-S batteries.^{128,129} Tetraethylthiuram disulfide (TETD) was, in 1988, the first reported organodisulfide molecule to be utilized as the cathode material in Li ion batteries.¹³⁰ It was found that the disulfide bond (R-S-S-R) in TETD can break and regenerate reversibly during the charge/discharge process. However, the low capacity and energy density greatly impair its competitiveness compared with transition metal oxide-based cathodes. Organosulfide molecules with long sulfur chains (R-S_x-R, x ≥ 3), such as dimethyl trisulfide,¹³¹ diphenyl trisulfide,¹³² and dipentamethylene thiuram tetrasulfide,¹³³ could provide a higher capacity. Recently, a novel sulfurized limonene composite, synthesized from S₈ and D-limonene through a one-step chemical

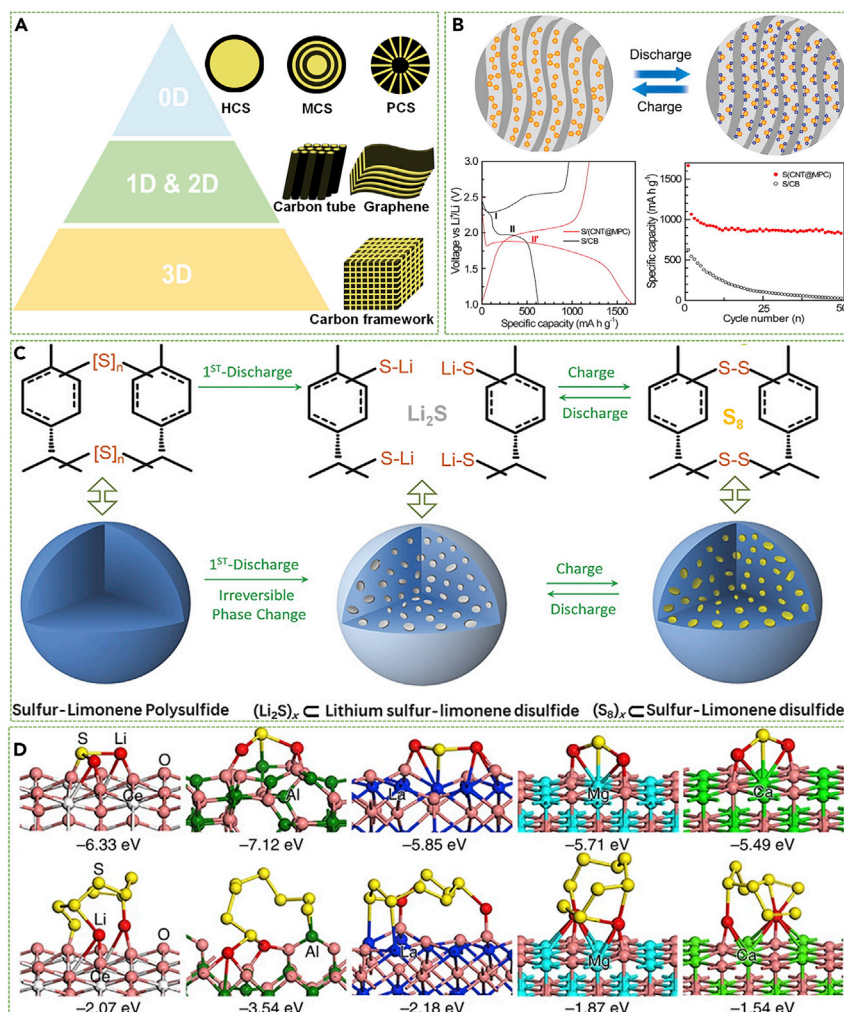


Figure 4. Strategies of physical confinement, small molecular sulfur, covalent sulfur, and chemisorption for advanced sulfur cathodes

(A) Schematic of typical carbon hosts for sulfur cathodes.

(B) Schematic illustration of charge/discharge process of small sulfur molecules (S₂₋₄) and typical charge/discharge profiles and cycling performance of S/CB and S/(CNT@MPC). Reproduced with permission from Xin et al.⁴³ Copyright 2012, American Chemical Society.

(C) Schematic illustration showing the structure evolution of S-S chains and self-protection mechanism. Reproduced with permission from Wu et al.¹²⁶ Copyright 2018, Wiley-VCH Verlag GmbH & Co. KGaA.

(D) Optimized geometries of the most stable Li₂S and Li₂S₈ on CeO₂(111), Al₂O₃(110), La₂O₃(001), MgO(100), and CaO(100) surfaces. Reproduced with permission from Tao et al.¹²⁷ Copyright 2016, Springer Nature.

reaction under high temperature, was demonstrated as a high-performance cathode material in Li-S batteries.¹²⁶ As shown in Figure 4C, during the first discharge, the long S-S chains break and form Li₂S nanoparticles within the limonene disulfide matrix. The embedded structures cannot only ensure contact stability, but also act as ion sieves to allow Li ion transport and block penetration of the solvent. Then, when charging, the Li₂S nanoparticles are reversibly converted back to S₈, and the R-S-Li groups are delithiated to form the R-S-S-R chains. In the following cycles, the S₈ and organosulfide molecules with R-S-S-R chains separately undergo redox reactions. As a result, the sulfur-limonene-based electrodes can display a high

specific capacity of $\sim 1,000$ mAh g⁻¹ at 0.5 C and a low fading rate of 0.008% per cycle. As well as the organosulfide molecules, organosulfide polymers have been also widely investigated as cathode materials in Li-S batteries.¹³⁴ A typical example is sulfurized polyacrylonitrile (SPAN).¹³⁵ It has been shown that sulfur can dehydrogenate PAN under high temperature in an argon atmosphere and is exclusively bonded to carbon atoms. Although the exact chemical structure of SPAN is still under investigation, the superior Li storage capability makes it a potential cathode material in Li-S batteries. Moreover, it is worth mentioning that selenium (Se), a congener of sulfur containing d electrons, possesses a high intrinsic electronic conductivity of $\sim 10^{-3}$ S cm⁻¹, and is usually introduced into the organosulfide matrix to accelerate the redox transformation of sulfur species and enhance cycling stability.^{136,137}

Although the confinement of sulfur in nonpolar carbon hosts can improve the specific capacity of Li-S batteries, their long-term cycle stability remains unsatisfactory due to the weak intermolecular interactions between the polysulfides and the carbon hosts. Researchers gradually realized that the formation of strong polar bonds to immobilize polysulfides can effectively alleviate the shuttle effect and thus greatly enhance cycle life.¹³⁸ To this end, functionalizing carbon materials by heteroatoms, such as O, N, S, P, B, and F atoms, is regarded as one of the effective strategies to strengthen the surface immobilization of sulfur intermediates.^{139–143} The enhancement mechanism is usually based on the electrostatic interaction between the electronegative heteroatoms with lone pairs of electrons and positively charged Li ions. As well as the heteroatom-doped carbon materials, some metal oxides, such as TiO₂, Al₂O₃, SiO₂, and Co₃O₄, have also been extensively investigated as effective polar hosts for the chemisorption of polysulfides.^{144–147} It should be pointed out that, unlike conductive carbon materials, most metal oxides have a poor electronic conductivity, and that strong polysulfide adsorption on the surface of insulated metal oxides can probably block their active sites and reduce the electrochemical performance. Nevertheless, some studies have demonstrated that the obvious enhancement of electrochemical performance has been achieved after introducing the poor conductive metal oxides. To explain this phenomenon, Cui and colleagues¹²⁷ proposed the concept of competition between chemical adsorption and diffusion of polysulfide adsorbates on these metal oxides. Figure 4D shows the optimized geometries of the most stable Li₂S and Li₂S₈ on CeO₂(111), Al₂O₃(110), La₂O₃(001), MgO(100), and CaO(100) surfaces. It was found that Li₂S and Li₂S₈ have a moderate adsorption energy of -5.71 and -1.87 eV on MgO(100), respectively. The diffusion of Li on the surface of these five metal oxides has also been investigated using the density functional theory calculation in their work. Among these samples, the Li on MgO(100) shows the lowest diffusion barrier of 0.45 eV. The optimized balance between adsorption and surface diffusion makes MgO the most favorable for regulation of polysulfide. These theoretical simulation results have been well verified by the experimental specific capacity and cycling performance results. In addition, some other advanced materials with abundant polar active sites, such as metal-organic frameworks (MOFs),¹⁴⁸ covalent organic frameworks (COFs),¹⁴⁹ and MXene,¹⁵⁰ have been also developed to effectively suppress the polysulfide diffusion via strong chemisorption; however, this will not be discussed in detail here.

Introduction of heterogeneous mediators in Li-S batteries is also an effective strategy to enhance the performance of sulfur cathodes. Heterogeneous mediators can bind with the polysulfides and accelerate the polysulfide conversion via their redox reactions with polysulfides, inducing different reaction pathways (Figure 5A).¹⁵¹ To reveal the working mechanism of heterogeneous mediators, the

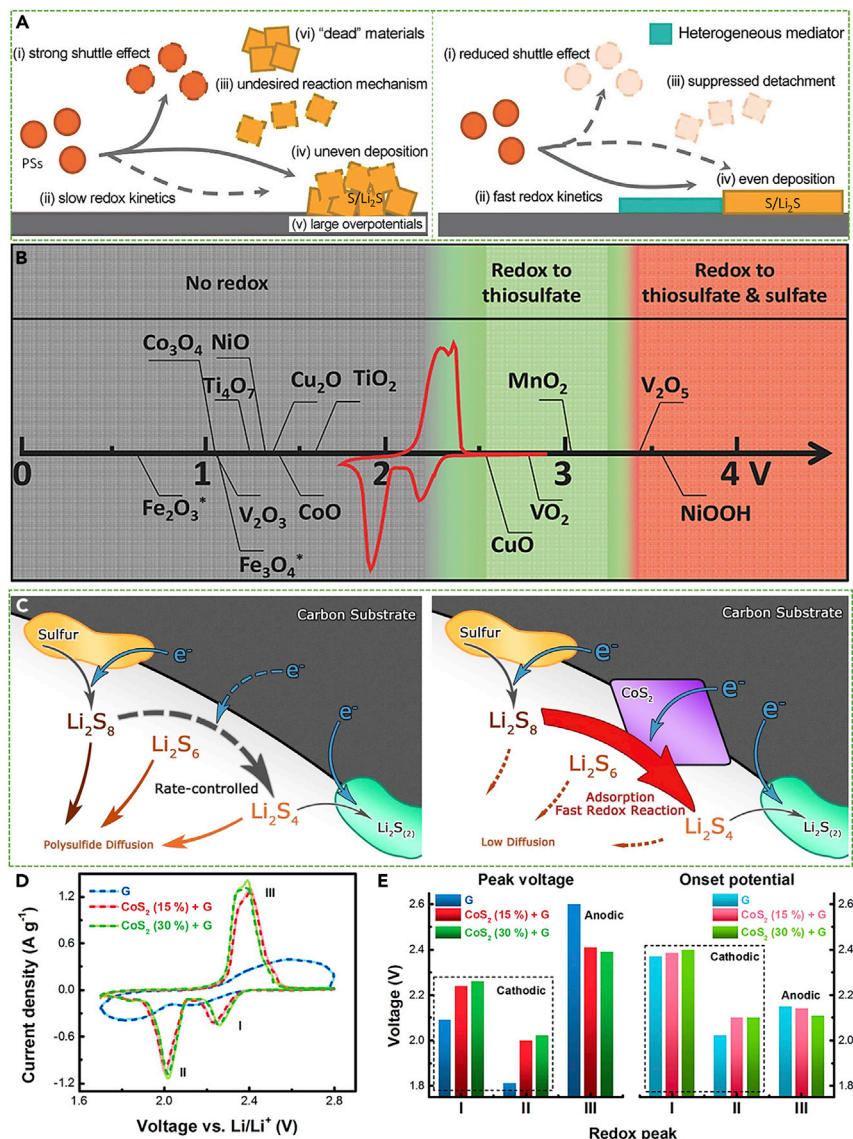


Figure 5. Strategies of heterogeneous mediators and electrocatalytic conversion for advanced sulfur cathodes

(A) Schematic illustration of the working principles of Li-S batteries without and with heterogeneous mediators. Reproduced with permission from Zhang et al.¹⁵¹ Copyright 2018, Wiley-VCH Verlag GmbH & Co. KGaA.

(B) Chemical reactivity of various metal oxides with polysulfides as a function of redox potential versus Li/Li^+ . The typical Li-S CV profile is shown in red. Reproduced with permission from Liang et al.¹⁵² Copyright 2015, Wiley-VCH Verlag GmbH & Co. KGaA.

(C) Schematic illustration of the discharge process in sulfur cathodes without and with the CoS_2 nanocatalysts.

(D) CV profiles of the Li-S batteries using the G, CoS_2 (15%) + G, and CoS_2 (30%) + G hosts.

(E) Corresponding peak voltages and onset potentials derived from the CV profiles. Reproduced with permission from Yuan et al.¹⁵⁷ Copyright 2016, American Chemical Society.

polysulfide conversion pathways on some specific metal oxides were systematically investigated, and a "Goldilocks" principle was proposed by Nazar and colleagues¹⁵² to describe the metal oxide-polysulfide interaction. As shown in Figure 5B, the metal oxides can be divided into three categories based on their chemical reactivity with

polysulfides. When the redox potential of metal oxides is located within the Goldilocks voltage window of 2.4–3.05 V, the polysulfides can be oxidized to thiosulfates on the surface of metal oxides. Subsequently, the thiosulfates react with the high-order polysulfides to generate polythionate complexes $[\text{O}_3\text{S}_2(\text{S})_{x-2}\text{S}_2\text{O}_3]^{2-}$ and low-order polysulfides uniformly distributed within electrodes. The unique conversion pathway of high-order polysulfides to low-order polysulfides based on thiosulfate mediation can bypass the traditional direct high-order to low-order polysulfide conversion in electrolyte and thus suppress the irreversible polysulfide diffusion. Moreover, according to the Goldilocks principle, metal oxides with redox potentials lower than the Goldilocks voltage window are unable to form polythionates, and only have the function of chemisorption, while metal oxides with redox potentials higher than the Goldilocks voltage window over-oxidize active polysulfides to inactive sulfates, causing poor long-term cycling stability. Nevertheless, some metal oxides, such as Fe_2O_3 , Fe_3O_4 , Co_3O_4 , and CoO , with their redox potentials falling outside the Goldilocks voltage window, were still found by other groups to have the ability to promote the transformation of polysulfides.^{153–156} Therefore, owing to the lack of direct evidence at a molecular level, the classification of these solid additives as adsorbents, heterogeneous mediators, and electrocatalysts, which are discussed next, varies in the literature. At present, it is difficult to accurately identify whether these solid additives would change the reaction pathways or lower the activation energy of polysulfide conversion reactions or do both after initial chemical adsorption.

The concept of electrocatalytic conversion of polysulfides has been proposed and has triggered much interest in the field of Li-S batteries in recent years.¹⁵⁸ Polysulfide electrocatalysts are deemed to be able to accelerate the conversion kinetics of polysulfides by lowering the energy barrier during conversion reactions. The acceleration of polysulfide conversion can reduce the accumulation of polysulfides and thus suppress polysulfide shuttle. Also, the accelerated polysulfide conversion rate contributes to the high performance rate for Li-S batteries. So far, a tremendous number of electrocatalytic materials, such as heteroatom-doped carbon materials, noble metals, and metal oxides/sulfides/selenides/carbides/nitrides/phosphides have been developed and utilized in Li-S batteries.^{159–166} The half-metallic cattierite cobalt disulfide (CoS_2 , a typical metal sulfide) was incorporated into the carbon/sulfur cathode and proved to significantly enhance the redox reactivity of polysulfides (Figure 5C).¹⁵⁷ The accelerated polysulfide redox kinetics can be revealed from the CV profiles of Li-S batteries using various sulfur cathodes (Figure 5D). It can be seen that the pure graphene (G)-based sulfur cathode displays broad anodic and cathodic peaks and severe polarization. After incorporation of 15 and 30 wt % CoS_2 , the polarization of the sulfur cathode is greatly mitigated, with the cathodic/anodic peaks positively/negatively shifting by approximately 0.2 V. One sharp anodic peak at ~ 2.35 V and two sharp cathodic peaks at ~ 2.25 and ~ 2.00 V can be seen upon introduction of CoS_2 . In addition, the addition of CoS_2 decreases the onset potential of the anodic peak and increases that of the cathodic peaks compared with the pure G-based sulfur cathode, further proving the acceleration of polysulfide conversion over CoS_2 (Figure 5E).

To take full advantage of electrocatalysts, the emerging concept of single-atom electrocatalysts has been also proposed to improve the utilization of sulfur in Li-S batteries.^{167–170} Experimental and theoretical data verify that these single-atom materials could serve as bifunctional electrocatalysts to accelerate the generation and decomposition of Li_2S during the discharge and charge processes. However, it should be pointed out that, despite the fact that the electrocatalytic effect can be evaluated by experimental data, and that the computational simulation would

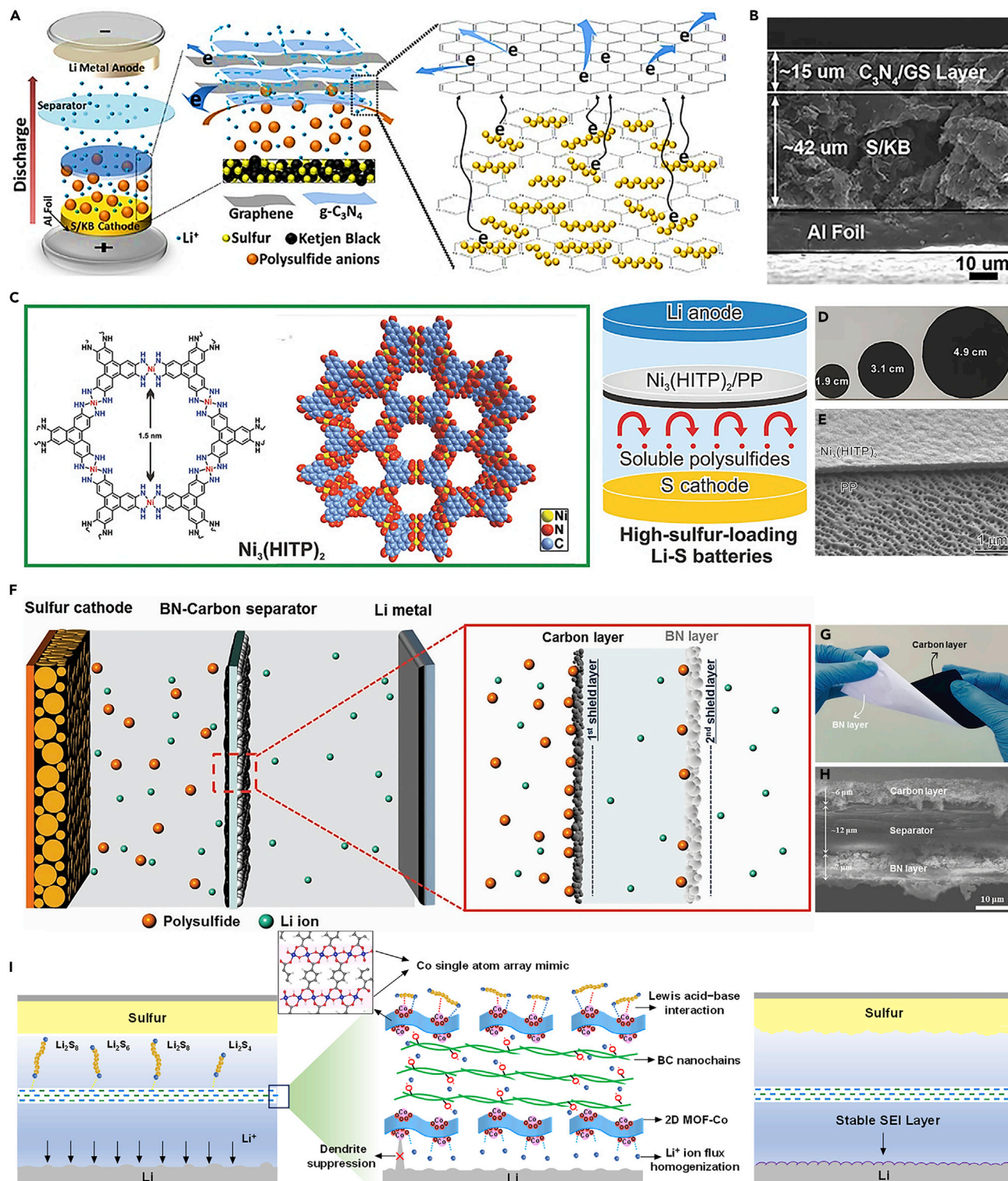


Figure 6. Design of functional interlayers for Li-S batteries

(A) Schematic illustration of a Li-S battery with a laminated $g\text{-C}_3\text{N}_4/\text{GS}$ interlayer.

(B) SEM image of the cross-section of the S/KB@ $\text{C}_3\text{N}_4/\text{GS}$ cathode. Reproduced with permission from Qu et al.¹⁸¹ Copyright 2019, Wiley-VCH Verlag GmbH & Co. KGaA.

(C) Schematic illustration of the chemical structure of $\text{Ni}_3(\text{HITP})_2$ and the structure of a Li-S battery with a $\text{Ni}_3(\text{HITP})_2$ -coated PP separator.

Figure 6. Continued

(D) Photograph of the $\text{Ni}_3(\text{HITP})_2$ -coated PP separators with different sizes.

(E) SEM image showing the cross-section of $\text{Ni}_3(\text{HITP})_2$ -coated PP separator. Reproduced with permission from Zang et al.¹⁸² Copyright 2018, Wiley-VCH Verlag GmbH & Co. KGaA.

(F) Schematic illustration of a Li-S battery with a separator coated with carbon and BN.

(G) Photograph of the twisted functionalized separator.

(H) SEM image showing the cross-section of the functionalized separator. Reproduced with permission from Kim et al.¹⁸³ Copyright 2017, Springer Nature.

(I) Schematic illustration for the Li-S battery with a B/2D MOF-Co separator.¹⁸⁴ Copyright 2020, Wiley-VCH Verlag GmbH & Co. KGaA.

help understand the potential electrocatalytic process, the accurate electrocatalytic mechanism of these materials remains unclear.¹⁷¹ Real-time detection of sulfur intermediates, including species and configuration, to reveal the real electrocatalytic conversion process and structure evolution of electrocatalysts is highly desirable.

Design of the separator

As well as the construction of advanced sulfur cathodes, designing functionalized separators is another feasible and effective strategy to improve the electrochemical performance of Li-S batteries.¹⁷² Conventional porous polyolefin separators have a limited ability to suppress the polysulfide shuttle and inhibit the penetration of Li dendrites. The additional interlayers inserted between the Li anode/sulfur cathode and the separator can act as extra functional layers to regulate the polysulfide diffusion and Li stripping/plating behavior. The concept of the interlayer to intercept polysulfides was first proposed by Su and Manthiram.⁴² A freestanding conductive multi-walled carbon nanotube (MWCNT) interlayer was placed between the sulfur cathode and the separator to boost the electrochemical performance of the Li-S batteries. The self-supported MWCNT interlayer, serving as an “upper current collector,” can help enhance the utilization of active sulfur and alleviate the irreversible polysulfide diffusion. As a result, a high capacity of 804 mAh g^{-1} at a high rate of 1 C can be maintained after 100 cycles. Subsequently, various carbon-based interlayers, such as CNT, graphene, carbon nanofibers, and graphdiyne, have been developed to enhance the utilization of active sulfur and thus improve the cycling stability of Li-S batteries.^{173–176} Given that the effects of adsorbents, heterogeneous mediators, and electrocatalysts in enhancing the performance of sulfur cathodes have been successfully demonstrated, these materials were also considered to be incorporated into interlayers for achieving high-performance Li-S batteries.^{177–180} For instance, a 2D $\text{g-C}_3\text{N}_4$ /graphene sheet ($\text{g-C}_3\text{N}_4$ /GS) was developed as an effective composite interlayer in Li-S batteries (Figure 6A).¹⁸¹ The 2D $\text{g-C}_3\text{N}_4$ and graphene nanosheets stack with each other to generate a laminated structure, which can greatly enhance the interception of polysulfides. In the composite $\text{g-C}_3\text{N}_4$ /GS interlayer, graphene can be used as conductive networks to facilitate the charge transfer, and the $\text{g-C}_3\text{N}_4$ can act as a trapping agent for soluble sulfur species due to the strong chemical adsorption between polysulfides and electronegative N atoms. As a result, the sulfur cathode equipped with a $15\text{-}\mu\text{m}$ -thick $\text{g-C}_3\text{N}_4$ /GS interlayer can deliver a high initial discharge capacity of $1,167.8 \text{ mAh g}^{-1}$ and remain at 612.4 mAh g^{-1} even after 1,000 cycles (Figure 6B).

Considering that the introduction of interlayer would inevitably decrease the energy density of Li-S cells, more and more attention has been devoted to the design of lightweight and thin coating layers with an integrated configuration of interlayers and separators.¹⁸⁵ For example, a large-area, crack-free, and thin-layer conductive MOF, $\text{Ni}_3(\text{HITP})_2$ (HITP = 2,3,6,7,10,11-hexamino-triphenylene), was tightly coated on the separator using an interface-induced growth process.¹⁸² The 2D MOF monolayers are packed with each other by strong π - π interactions to generate uniform 1D

channels. The walls of these well-aligned channels possess abundant polar sites (Figure 6C). It should be mentioned that the thickness of the $\text{Ni}_3(\text{HITP})_2$ interlayer is only about 340 nm and the mass loading is as low as 0.066 mg cm^{-2} , which have a negligible effect on the energy density (Figures 6D and 6E). Benefiting from the high conductivity, uniform 1D microporous channels, and rich polar sites, a Li-S battery equipped with a thin $\text{Ni}_3(\text{HITP})_2$ interlayer can achieve a high capacity of 589 mAh g^{-1} at an ultrahigh rate of 5 C and a high capacity retention of 716 mAh g^{-1} at a rate of 1 C after 500 cycles. Even under a high areal sulfur loading of 8.0 mg cm^{-2} and a high sulfur content of 70 wt %, a high areal capacity of 7.24 mAh cm^{-2} can be achieved after 200 cycles at 0.5 C.

Although various interlayers used for polysulfide immobilization have been extensively reported, the interlayers between anode and separator for manipulation of stripping/plating behavior of Li anodes have been relatively infrequently investigated. Designing advanced interlayers to build a robust shield or regulate the distribution and concentration of near-surface Li ions on the Li metal anode can effectively enhance the electrochemical performance of Li metal anodes. For instance, a multifunctional trilayer film was demonstrated by coating a carbon layer and a boron nitride (BN) layer onto each surface of a conventional polyolefin separator (Figures 6F–6H).¹⁸³ The BN layer facing the Li anode can be used to further block the penetrated polysulfides and manipulate the growth of Li dendrites, contributing to the stable formation of SEI layers and a uniform deposition and dissolution of Li. When the functionalized trilayer separator was utilized in Li-S batteries, the sulfur cathode delivered a high capacity retention of 780.7 mAh g^{-1} over 250 cycles. Another typical example is the ultrathin MOF nanosheet-coated bacterial cellulose-based separator (Figure 6I).¹⁸⁴ The abundant Co-O_4 moieties exposed on the surface of ultrathin MOF nanosheets could homogenize Li ion flux through strong Li ion adsorption with O at the interface between the Li anode and the separator, resulting in uniform Li stripping/plating. Until now, more and more attention has been focused on the construction of bifunctional interlayer-modified separators, which can simultaneously address the problems of polysulfide shuttle and growth of Li dendrites.

Despite the enhanced electrochemical performance of Li-S batteries, adding interlayers on separators more or less results in thickness and weight increase, which, to a certain extent, increases the diffusion resistance of Li ion, causes deterioration of the electrode wetting capability, and decreases the energy density. Designing novel separators without introducing extra interlayers to improve the ionic selectivity, thermal stability, and mechanical properties is another straightforward and effective approach to boost the performance of Li-S batteries. The utilization of abundant, environmentally friendly, and biodegradable natural polymers, such as nanocellulose, bacterial cellulose, and chitin, for the fabrication of separators, has aroused much research interest.^{186–189} Due to the existence of periodically arranged polysaccharide chains on cellulose nanofibers (CNFs), the separators based on CNFs usually exhibit enhanced wettability, permeability, thermal stability, and mechanical properties. Recently, a porous cellulose-based membrane derived from a facial mask has been demonstrated to be a high-performance separator in Li-S batteries.¹⁸⁶ The Fourier transform infrared spectrum shows that the cellulose-based membrane possesses abundant polar oxygen-containing groups, such as -OH and C-O (Figure 7A). The results suggest that the cellulose-based membrane has a better electrolyte uptake and retention capability compared with the commercial Celgard 2500. In addition, it was found that the cellulose-based membrane displays a better thermal stability compared with the Celgard 2500. The shape of the cellulose membrane remains unchanged at 150°C for 12 h, while the Celgard 2500 separator shrinks

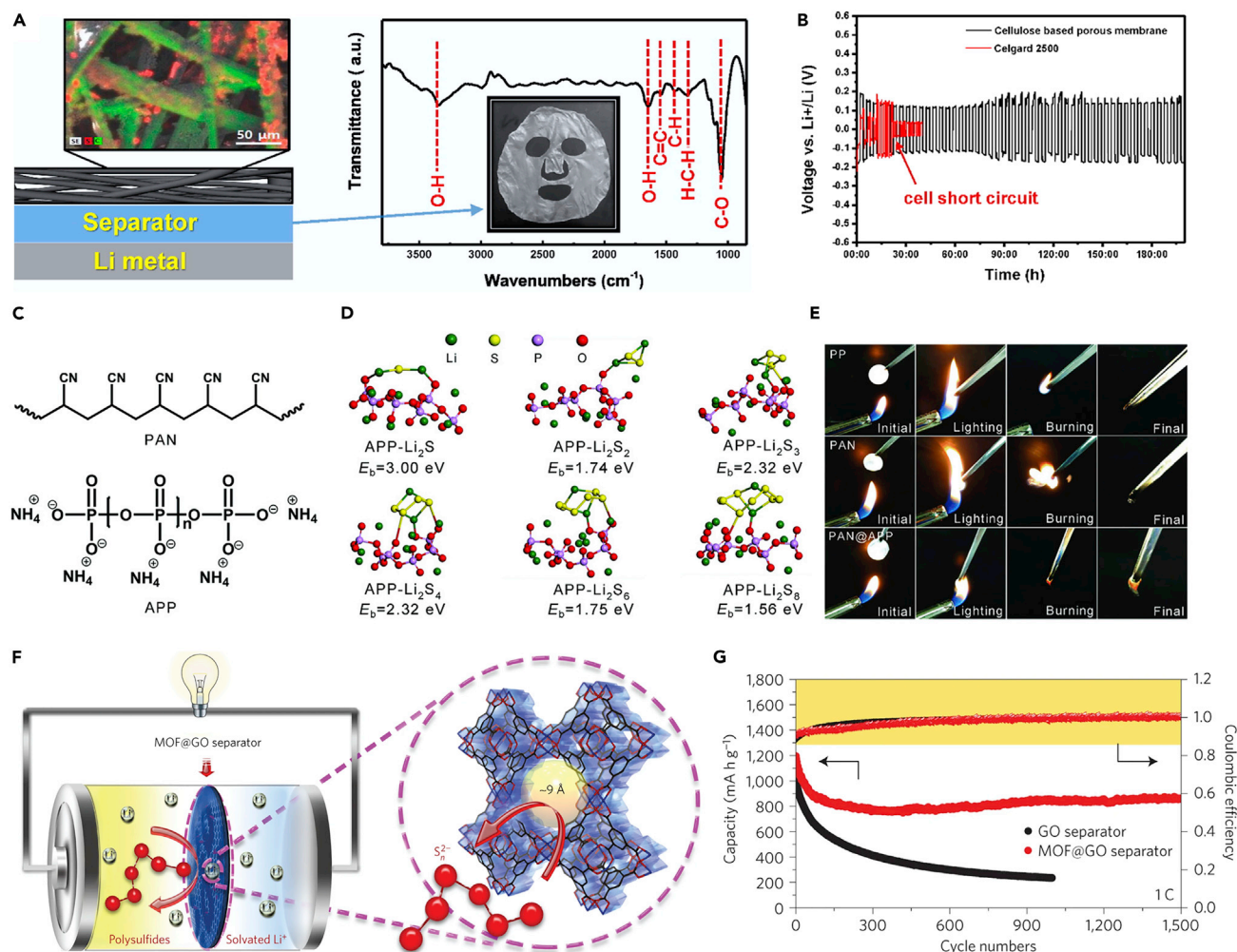


Figure 7. Design of advanced separators for Li-S batteries

(A) Schematic illustration of a Li-S battery with a cellulose separator and corresponding Fourier transform infrared spectrum of the cellulose separator. (B) Voltage profiles of the Li//Li symmetric cells with a Celgard 2500 and a cellulose separator at a current density of 2.4 mA cm⁻² (4.8 mAh cm⁻²).

Reproduced with permission from Yu et al.¹⁸⁶ Copyright 2016, American Chemical Society.

(C) Chemical structures of PAN and APP.

(D) Binding energies between APP and polysulfides.

(E) Photographs showing the fire-retardant properties of PP, PAN, and PAN@APP separators. Reproduced with permission from Lei et al.¹⁹⁰ Copyright 2018, Wiley-VCH Verlag GmbH & Co. KGaA.

(F) Schematic illustration showing the ionic sieve function of the MOF@GO separator toward soluble polysulfides.

(G) Cycling performance of the Li-S batteries with the MOF@GO and GO separators. Reproduced with permission from Bai et al.¹⁹¹ Copyright 2016, Springer Nature.

severely. Benefiting from the rich oxygenic groups and uniform distribution of small nanopores, the symmetric Li//Li cell with a porous cellulose-based separator displays a stable voltage profile of Li stripping/plating over 200 h, suggesting a favorable reversibility of the Li anode with a stable SEI layer. As a comparison, the symmetric Li//Li cell with a Celgard 2500 separator fails after only a few cycles (Figure 7B). Moreover, an Li-S battery with a cellulose separator can exhibit a high capacity of 947 mAh g⁻¹ after 100 cycles, which is much higher than that of the Li-S battery with a Celgard 2500 separator (lower than 600 mAh g⁻¹). The enhanced performance of Li-S batteries equipped with the cellulose separator is attributed to the blockage of soluble polysulfides and suppression of formation of Li dendrites.

As well as natural polymer-based separators, some novel synthetic polymers, such as Nafion, poly(methyl methacrylate) (PMMA), polyacrylonitrile (PAN), polyetherimide, polyimide (PI), polyvinylidene fluoride (PVDF), PEO, and their composites have been widely used for the fabrication of separators.^{192–198} The lithiated Nafion ionomer was utilized as a functional separator in Li-S batteries as early as 2012.¹⁹² The high transference number of Li ions of the lithiated Nafion ionomer-based separators can efficiently prevent the crossover of soluble polysulfides and thus greatly enhance the cycling performance of Li-S batteries. For some other polymers with polar groups, such as hydroxyl (-OH), carboxyl (-COOH), imine (-NH-), amine (-NH₂), and nitrile (-C≡N), the strong polar-polar bonds between these groups and polysulfides can effectively retard the irreversible diffusion of soluble sulfur species. Recently, a nonflammable and multifunctional separator prepared by the electrospun PAN@ammonium polyphosphate (PAN@APP) nanofibers was reported for stable and safe Li-S batteries (Figure 7C).¹⁹⁰ Because of the existence of rich amine groups and phosphate radicals in APP, the PAN@APP separator has strong binding interactions with polysulfides (Figure 7D). In addition, the PAN@APP separator is observed to be nonflammable because of the introduction of the flame-retardant APP, while the PP and PAN separators combust on ignition, and are burned up within a few seconds, even the lighter is removed (Figure 7E). Meanwhile, the PAN@APP separator was found to have excellent heat tolerance and, even under 200°C, the PAN@APP separator remains uniform and intact. As a result, the Li-S batteries with the PAN@APP separator display a stable capacity from room temperature to 100°C. In contrast, the capacity of Li-S batteries with the PP and PAN separators deteriorates sharply when the temperature is increased to 100°C.

Inorganic materials with high thermal stability and high Young's modulus also present a potential for the construction of separators. For example, glass fiber-based membranes with high porosity, superior thermal stability, low cost, and excellent electrolyte wettability have been successfully demonstrated in Li-S batteries.¹⁹⁹ The porous ceramic Li_{6.4}La₃Zr_{1.4}Ta_{0.6}O₁₂ membrane, with a strong affinity for polysulfides and a high mechanical strength to block Li dendrites, was reported to be a separator for Li-S batteries, which leads to significantly enhanced electrochemical performance and safety.²⁰⁰ As well as the above-mentioned conventional polymers and inorganics, some novel functional materials, such as MOFs, have been delicately designed for the preparation of high-performance separators in Li-S batteries.^{201,202} Because of the 3D channel structure that contains highly ordered micropores with a smaller pore size than the diameters of polysulfides (Li₂S_x, 4 ≤ x ≤ 8), the MOF, Cu₃(BTC)₂ (HKUST-1), was selected to build the MOF@GO separator in Li-S batteries to selectively sieve Li ions while hindering the shuttle of polysulfides (Figure 7F).¹⁹¹ Without any complex preparation and elaborate surface modification of the sulfur cathode, the Li-S batteries with the MOF@GO separator display a moderate drop within the first 100 cycles, and show a high capacity of 855 mAh g⁻¹ after running 1,500 cycles, with a fading rate as low as 0.019% per cycle (Figure 7G). In contrast, the Li-S batteries with the GO separator display a rather dramatic capacity decay, and only a low capacity of 234 mAh g⁻¹ can be retained after 1,000 cycles. To further avoid the initial "sulfur loss" caused by the strong interaction between polysulfides and metal sites in MOFs, a negatively charged sulfonic polymer was introduced into the microchannels of MOFs to restrain the bonded polysulfides and facilitate the transport kinetics of Li ions.²⁰³ As a result, a high capacity of 1,017 mAh g⁻¹ after 1,000 cycles at 1 C can be achieved. These strategies could guide us in developing advanced functional separators using other ordered mesoporous materials for high-performance Li-S batteries.

Design of the electrolyte

It has been proven that the stability of both the sulfur cathode and the Li metal anode in traditional liquid organic electrolytes is still insufficient for long-term operation of Li-S batteries. Recent investigations on manipulation of electrolyte components (solvents and Li salts) to improve sulfur utilization and enhance Li anode reversibility have achieved great progress.^{204–206} The selection of solvents is critical to determine the polysulfide solubility and the stability of the Li metal anode. Until now, various solvents, such as ethers, carbonates, sulfones, and ILs, have been investigated in Li-S batteries. Despite the fact that carbonate-based electrolytes have been successfully applied in Li ion batteries, most are incompatible with Li metal anodes and S₈ cathodes. The severe side reactions between Li metals/soluble polysulfides and carbonates greatly impede their further development in Li-S batteries. Although few specific sulfur cathodes, such as sulfur-pyrolyzed polyacrylonitrile (S@pPAN) and small sulfur molecules (S_{2–4}), display acceptable electrochemical performance under the premise of Li metal-free anodes or Li metal protection, much effort still needs to be dedicated to improving the compatibility between electrodes and carbonate solvents.^{207,208} Sulfone-based electrolytes have been applied in Li-S batteries due to their favorable thermal stability and high dielectric constant.²⁰⁹ Nevertheless, it is seldom reported that the sulfone-based solvents with high viscosity and high polysulfide solubility can be used alone in Li-S batteries to achieve high performance. The sulfone-based solvents are usually mixed with ethers to balance viscosity and polysulfide solubility.²¹⁰ The practical application of sulfone-based electrolytes still has a long way to go. As alternative safe electrolyte solvents, ILs are usually used in Li-S batteries due to their limited polysulfide solubility because of their relatively weak Lewis acidity/basicity. However, the ILs with a high viscosity suffer from a poor rate capability owing to their slow Li ion diffusion kinetics and low Li ion transference number.²¹¹ Based on the above, we emphasize the review of ether-based electrolytes in this section.

As mentioned above, although the DOL/DME-based electrolyte systems have been widely used in Li-S batteries, their development is still limited by the high dissolution of polysulfides and the instability of the Li anode, which eventually has side effects on the cycling stability of Li-S batteries. One of the effective strategies of component regulation to improve the electrochemical performance of Li-S batteries is using highly concentrated electrolytes (HCEs). The concept of HCEs was first investigated in tetraglyme-Li salt equimolar complexes.²¹² Because the coordination number of Li ions is typically 4–5, the long-chain tetraglyme is favorable for the solvation of Li ions because its Lewis-basic oxygen atoms can generate a 1:1 complex cation of [Li(tetraglyme)]⁺. As a result, [Li(tetraglyme)]⁺ and TFSI[−] behave as discrete ions, similar to the ILs, and the polysulfide dissolution is thus suppressed. Another successful example of HCEs in Li-S batteries is the 7 M LiTFSI in the DOL/DME electrolyte.³⁸ In these “solvent-in-salt” electrolytes (SIS-7#), the number of solvated Li ions is decreased, and a number of Li-ether complex pairs generate because of the incomplete solvation shell, which can effectively mitigate the dissolution of polysulfides. Also, the Li metal anode shows a high stability in SIS-7#, which is attributed to the minimized space charge near the Li anode and an enhanced Li diffusion rate. As a result, the Li-S batteries with SIS-7# show a high capacity of 770 mAh g^{−1} after 100 cycles. However, the “two plateau” voltage profile remains, which is a typical characteristic of catholyte sulfur electrochemistry, implying that a low electrolyte to sulfur (E/S) ratio cannot be realized in these electrolyte systems.

To decouple the electrolyte and sulfur use and suppress the growth of Li dendrites, a novel highly concentrated diethylene glycol DME system (G2:LiTFSI) was developed

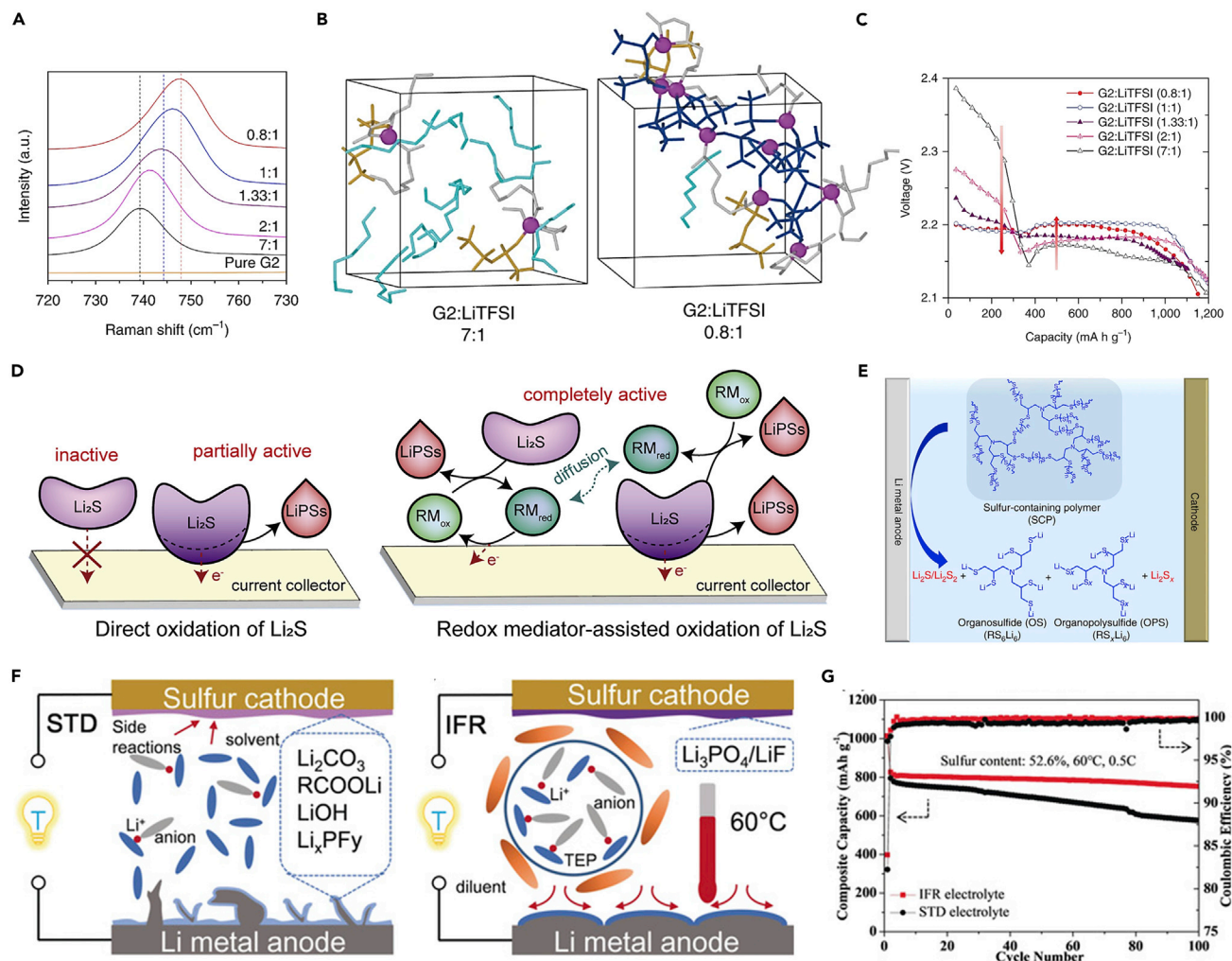


Figure 8. Regulation of liquid electrolyte components and additives for Li-S batteries

(A) Raman spectra of the TFSI⁻ band for pure G2 and different G2:LiTFSI electrolytes.

(B) Snapshots from the AIMD trajectories for the two end-member electrolytes (Li ion: purple; free and coordinated G2 molecules: cyan and gray, respectively; contact-ion-pairs and aggregates of TFSI⁻ anions: gold and blue, respectively).

(C) Typical discharge profiles of different G2:LiTFSI electrolytes. Reproduced with permission from Pang et al.²¹³ Copyright 2018, Springer Nature.

(D) Schematic illustration of direct Li₂S oxidation and RM-assisted Li₂S oxidation in Li-S batteries. Reproduced with permission from Tsao et al.²¹⁶ Copyright 2019, Elsevier.

(E) Schematic illustration showing the formation of stable SEI layers containing organic units (organosulfide/organopolysulfide) and inorganic units (Li₂S/Li₂S₂) Reproduced with permission from Li et al.²¹⁷ Copyright 2017, Springer Nature.

(F) Schematic illustration of structure evolution of sulfur cathode and Li anode in IFR and STD electrolytes.

(G) Cycling performance of the Li-S batteries with the IFR and STD electrolytes. Reproduced with permission from Yang et al.²¹⁸ Copyright 2019, Wiley-VCH Verlag GmbH & Co. KGaA.

to convert the dissolution-precipitation mechanism of sulfur to a quasi-solid-state conversion.²¹³ Raman spectra reveal that the TFSI⁻ band shifts toward a higher wavenumber with the decrease of the G2:LiTFSI ratio, which suggests a stronger interaction of TFSI⁻ and Li ions through the Li-O bond (Figure 8A). It was also found that G2-LiTFSI (0.8:1) has the highest solvent-Li ion coordination, and that the solvation symmetry of Li ions decreases with the decrease of the G2:LiTFSI ratio. AIMD simulation results show that the number of O (TFSI⁻) around the Li ions reaches 2.55 for the G2-LiTFSI (0.8:1) electrolyte from 1 for the G2-LiTFSI (7:1) electrolyte. In the G2-LiTFSI (0.8:1) electrolyte, each TFSI⁻ binds with multiple Li ions to build

a 3D network, leading to low solvent activity (Figure 8B). The voltage profiles clearly demonstrate that the first voltage plateau decreases and that the second voltage plateau increases with the decrease of the G2:LiTFSI ratio (Figure 8C), and that the voltage profile of G2-LiTFSI (0.8:1) is different from both that of the solid-solid conversion and the conventional “two plateau” conversion. Verified by the electrochemical results, a novel quasi-solid-solid reaction pathway ($S_8 + 4e^- + 4Li^+ \rightarrow 2Li_2S_4$) and subsequent disproportionation reactions ($Li_2S_4 + 2e^- + 2Li^+ \rightarrow Li_2S_3 + Li_2S$; $4Li_2S_3 \rightarrow 4Li_2S + S_8$) are proposed. Benefiting from the unique electrolyte structure of G2-LiTFSI (0.8:1), the polysulfide dissolution and shuttle and parasitic reactions of Li metal anode are effectively inhibited. As a result, a greatly improved capacity retention of the Li-S batteries can be achieved (720 mAh g^{-1} over 100 cycles) with the G2-LiTFSI (0.8:1) electrolyte using a low E/S ratio of $5 \mu\text{L mg}^{-1}$. Furthermore, to reduce the cost and improve the ionic conductivity and wettability of HCEs, a new concept of localized high-concentration electrolytes (LHCEs), diluting the HCEs with an “inert” diluent, such as 1H,1H,5H-octafluoropentyl-1,1,2,2-tetrafluoroethyl ether, has been proposed,²¹⁴ and has been successfully demonstrated in Li-S batteries.²¹⁵ The so-called inert diluent usually does not dissolve the Li salt but is miscible with the solvent, which means that the original Li ion-solvent coordination in the HCEs will not be affected. In particular, the ideal inert diluent in LHCEs for Li-S batteries should possess a low donor number and viscosity, high wettability, and favorable compatibility with Li to prevent the dissolution of polysulfides and enhance Li reversibility.

As well as manipulating the solvents and Li salts, the addition of additives in electrolytes has been regarded as another facile yet effective strategy to improve the utilization of sulfur cathodes and protect Li metal anodes. Among various additives to upgrade utilization of sulfur, RMs have triggered increased attention because they can facilitate electrochemical conversion of Li_2S and thus enhance the capacity and rate performance of Li-S batteries (Figure 8D). However, the exploration of RMs in Li-S batteries is still in its infancy. So far, only a few RMs, including some specific organosulfide compounds and metallocenes, have been successfully applied in Li-S batteries.^{219–222} Recently, a novel RM concept based on quinone redox chemistry has been proposed in Li-S batteries.²¹⁶ By tailoring the redox potential, stability, and solubility of quinones using molecular engineering, 1,5-bis(2-(2-methoxyethoxy)ethoxy)ethoxy anthra-9,10-quinone (AQT) was synthesized as a new RM, which can boost the initial oxidation of Li_2S below 2.5 V at a high rate of 0.5 C. Moreover, it has been confirmed that AQT can suppress polysulfide dissolution and enable the controlled deposition of Li_2S and sulfur during cycling. As a result, with the assistance of AQT, the thick Li_2S electrode, with a high mass loading of 6 mg cm^{-2} , can achieve a discharge capacity retention of 606 mAh g^{-1} with an average Coulombic efficiency of 92.8% after 100 cycles.

In Li-S batteries, the conventional SEI layers on Li metal anodes mainly consist of organic components that possess poor mechanical properties and continuously break and repair during cycling. Suitable additives in electrolytes can also help to form a robust SEI layer on Li metal anodes. The working mechanisms of these additives to protect the Li metal anodes are either the participation of robust SEI layer formation through the decomposition of additives or smoothing of SEI layers through electrostatic shielding and homogenizing near-surface Li ion flux. As well as the inorganic salts and inorganic solid nanoparticles mentioned previously, some organic additives for Li anode protection have been also demonstrated in Li-S batteries.^{223,224} For example, a novel sulfur-containing polymer of poly(sulfur-random-triallylamine) with a sulfur content of 90 wt % (PST-90) was regarded as a

high-performance additive to protect the Li metal anode in Li-S batteries.²¹⁷ In PST-90, numerous sulfur chains are connected with organic components to form a 3D interconnected network. The self-formation of inorganic (Li_2S ; Li_2S_2 ; Li_2S_x) and organic (organosulfides and organopolysulfides) hybrids through the decomposition of PST-90 contributes to the generation of a stable and flexible SEI layer on Li metal anodes (Figure 8E). The organic components in the hybrid could improve the flexibility and toughness of SEI layers, while the inorganic components could offer conductive pathways for the Li ions. Benefiting from the synergistic effect of organic and inorganic components in the SEI layers, the Li metal anode exhibits a high average Coulombic efficiency of 99% over 400 cycles (2 mA cm^{-2} , 1 mAh cm^{-2}) and an average Coulombic efficiency of 98.6% over 220 cycles (2 mA cm^{-2} , 3 mAh cm^{-2}). Furthermore, the Li-S batteries with PST-90 additives can maintain a capacity of 735 mAh g^{-1} with a Coulombic efficiency of 99.9% over 1,000 cycles, while the capacity of Li-S batteries with only the LiNO_3 additives deteriorate rapidly within the first 200 cycles. The strategy to build a robust SEI layer using organic electrolyte additives could be a promising research direction for the development of advanced Li metal-based battery systems.

Safety concerns, in particular with regard to the volatile and flammable liquid organic electrolytes, pose a great challenge for the practical applications of Li-S batteries. Addition of fire-retardant additives in electrolytes is taken as a simple yet effective strategy to address the safety issues of Li-S batteries. Until now, few additives of phosphorus-rich compounds have been introduced in Li-S batteries to enhance the safety and compatibility with electrodes.^{225,226} For example, an intrinsic flame-retardant (IFR) electrolyte solvent was prepared by adding the fire-retardant additive, triethyl phosphate (TEP), in TTE for safe Li-S batteries.²¹⁸ Electrolyte ignition tests confirmed the superior fire-retardant property of the 1.1 M LiFSI/TEP-3TTE electrolytes, while standard carbonate (STD) electrolytes kept on burning. Furthermore, it has been found that a protection layer containing Li_3PO_4 and LiF was formed both on the cathode and the anode when using the IFR electrolyte (Figure 8F). The Li_3PO_4 and LiF layers on the Li anode can serve as electronic insulators to prevent electrolyte consumption and regulate the dendrite-free Li deposition. Meanwhile, the Li_3PO_4 and LiF layers on the S@pPAN cathode can inhibit the side reactions between the sulfur species and the electrolyte. In addition, the enhanced TEP-Li ion solvation can avoid attack by polysulfides, leading to a stable electrolyte even at high temperatures. As a result, the S@pPAN (52.6 wt %) cathode in the IFR electrolyte can safely work over 100 cycles, with a capacity retention of 92.4% under a high temperature of 60°C (Figure 8G). In contrast, the S@pPAN (52.6 wt %) cathode in the STD electrolyte shows much worse stability under temperatures less than 60°C .

Despite much progress on liquid organic electrolyte-based Li-S batteries, their electrode stability remains to be improved. Utilizing solid-state electrolytes with high ionic conductivity and superior chemical/electrochemical stability to replace the conventional liquid organic electrolytes is a promising strategy to build high-performance solid-state Li-S batteries.^{227–229} Solid-state electrolytes can be usually categorized into gel polymer electrolytes (GPEs), solid polymer electrolytes (SPEs), and solid inorganic electrolytes (SIEs). The polymer-based electrolytes commonly have favorable flexibility and low interface resistance, while the inorganic ceramic-based electrolytes have high Young's modulus and high ionic conductivity at room temperature. These three types of solid-state electrolytes generate different interfacial properties with both the Li anodes and the sulfur cathodes. For the GPEs, the liquid plasticizers, such as ethers or ILs, fill in the polymer matrices, such as PEO, PVDF-HFP, and PMMA, to form the so-called quasi-solid-state

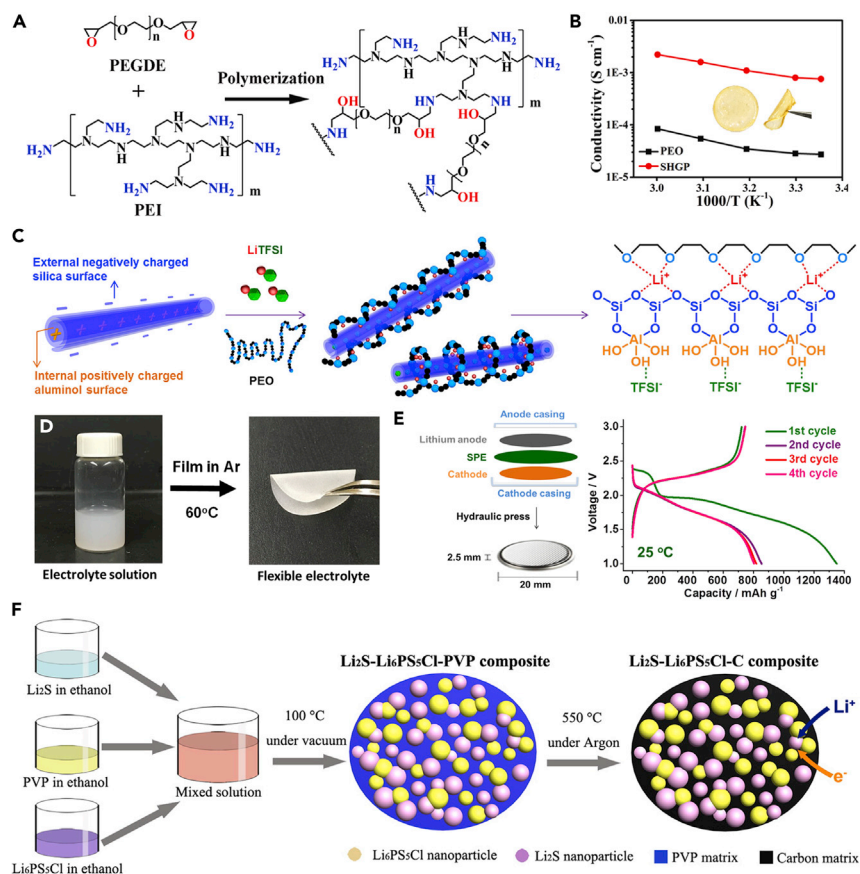


Figure 9. Design of advanced solid-state electrolytes for Li-S batteries

(A) Synthesis scheme of the polymerization of PEGDE and PEI.

(B) Ionic conductivities of the SHGP electrolyte and PEO gel polymer under different temperatures. Reproduced with permission from Zhou et al.²³⁴ Copyright 2019, Elsevier.

(C) Schematic illustration of the effect of HNT on the ionic conductivity.

(D) Photographs of the electrolyte solution containing HNT, LiTFSI, and PEO and flexible electrolyte thin film.

(E) Schematic illustration of all-solid-state Li-S batteries based on the PEO/LiTFSI/HNT electrolyte and corresponding charge/discharge curves. Reproduced with permission from Lin et al.²³⁵ Copyright 2017, Elsevier.

(F) Schematic illustration of the fabrication of Li_2S nanocomposite electrode. Reproduced with permission from Han et al.²³⁶ Copyright 2016, American Chemical Society.

electrolytes.^{230–233} In general, GPEs possess high ionic conductivity and favorable interfacial compatibility. For example, a new kind of super-high conductive gel polymer (SHGP) electrolyte for high-performance quasi-solid-state Li-S batteries was demonstrated recently using a ring-opening polymerization between poly(ethylene glycol) diglycidyl ether (PEGDE) and branched polyethylenimine (PEI) (Figure 9A).²³⁴ The ether chains of PEGDE and N atoms from amino groups on PEI can strongly interact with Li ions to facilitate ion transport. In addition, the polar groups in the SHGP electrolyte have a strong chemical interaction with polysulfides, thus effectively suppressing polysulfide shuttling. The results of ionic conductivity measurements display that the ionic conductivity of the SHGP electrolyte is higher than that of the conventional PEO GPEs (Figure 9B). A high ionic conductivity of 0.75 mS cm^{-1} can be obtained for the SHGP electrolyte, which is comparable with that of liquid electrolytes. In particular, the Li-S batteries using the SHGP electrolyte exhibited a high capacity retention of 85% over 400 cycles at 1.5 C.

Although the GPEs possess a high ionic conductivity, the problems of Li anodes and sulfur cathodes in liquid organic electrolytes also exist in GPEs, even if the situation is mitigated. Generally, the SPEs have better ability to shield polysulfides and suppress Li dendrites compared with the GPEs because of the lack of liquid electrolytes. Among the various SPEs, PEO-based SPEs with good chemical and electrochemical stability have gained much attention.²³⁷ Nevertheless, the extremely low ionic conductivity of PEO at room temperature (10^{-8} – 10^{-7} S cm⁻¹) greatly limits its applications in Li-S batteries. Although the PEO electrolytes can exhibit an acceptable ionic conductivity of above 10^{-4} S cm⁻¹ over 60°C, the dissolution of polysulfides in the partially molten PEO matrices is largely increased. Moreover, the poor mechanical properties of PEO electrolytes under high temperature can lead to safety hazards. To address the above issues, constructing PEO-based composite SPEs, such as using interpenetrating network SPEs, copolymer SPEs, and organic-inorganic hybrid SPEs, is an effective strategy.^{238–241} For example, the halloysite nanotube (HNT), with oppositely charged surfaces, could be introduced into the PEO matrices to prepare the PEO-based composite SPEs.²³⁵ The opposite surface charge of the HNT could effectively help to dissociate Li salts into Li ions that interact with the negatively charged silica outer layers and TFSI⁻ anions, which are adsorbed onto the aluminol groups at the inner layers of HNT (Figure 9C). In addition, the introduction of HNT can decrease the degree of crystallinity of PEO and reduce the phase transition temperature of PEO. These effects can lower ionic coupling and accelerate ion transport. As a result, the flexible PEO/LiTFSI/HNT SPE displays high ionic conductivities of 1.11×10^{-4} and 2.14×10^{-3} S cm⁻¹ at 25°C and 100°C, respectively (Figure 9D). Also, the assembled all-solid-state Li-S batteries with PEO/LiTFSI/HNT SPEs can deliver a high discharge capacity of 854 mAh g⁻¹ at room temperature (Figure 9E). Even under 100°C, the Li-S batteries can still operate safely over 400 cycles with a capacity retention of 386 mAh g⁻¹. It should be mentioned that the ratio of inorganic fillers in SPEs should be seriously controlled. Overfilled fillers could cause deterioration of the interfacial issues and lower the energy density of Li-S cells. Insufficient fillers could lead to limited enhancements in mechanical properties and ionic conductivity. Therefore, the ionic conductivity at room temperature and interfacial problems for SPEs are still important issues that need to be addressed.

Constructing all-solid-state Li-S batteries based on the SIEs is considered to be the ultimate solution to the polysulfide shuttling, Li dendrite growth, and high electrolyte flammability. However, it remains a huge challenge to build well-contacted interfaces at both sulfur cathodes and Li anodes to achieve high-rate and high-capacity all-solid-state Li-S batteries.²⁴² To obtain an intimate contact for the interface between SIEs and sulfur cathodes, nano-engineering is one of the most effective approaches. It follows that high-energy ball milling and high pressure have been usually required to obtain homogeneous and dense electrode structures. For the interfaces between SIE and Li anodes, the point-to-point contact is usually generated between the solid Li anodes and non-flowable ceramic electrolytes, leading to a large interface impedance. In addition, most SIEs are liable to be reduced by the highly reactive Li metal anode to form various by-products with a low ionic conductivity, further causing deterioration of the interface contact. To address these issues, various function layers, such as polymer interlayers, *in-situ*-formed inorganic coatings, and Li alloys have been successfully used to lower the interface impedance and enhance the compatibility.^{243–247} A few SIEs, such as hydrides (LiBH₄ and LiBH₄-LiCl)^{248,249} and sulfides (Li₁₀GeP₂S₁₂, Li₁₀SnP₂S₁₂ and Li₃PS₄),^{250–253} have been successfully used for all-solid-state Li-S batteries. Sulfide-based SIEs, in particular, have attracted much attention in the field of all-solid-state Li-S batteries, due to their impressively high ionic conductivity, stable electrochemical window, proper

elastic modulus, and favorable processability. For example, a high-performance all-solid-state Li-S battery was successfully built using $\text{Li}_2\text{S-Li}_6\text{PS}_5\text{Cl-C}$ as the cathode, $80\text{Li}_2\text{S} \cdot 20\text{P}_2\text{S}_5$ glass ceramic as the solid electrolyte, and Li-In alloy as the anode.²³⁶ The $\text{Li}_2\text{S-Li}_6\text{PS}_5\text{Cl-C}$ composite cathode was prepared by mixing the Li_2S , PVP, and $\text{Li}_6\text{PS}_5\text{Cl}$ in ethanol, followed by a high-temperature calcination under argon atmosphere (Figure 9F). The uniform and nanoscale distribution of Li_2S , $\text{Li}_6\text{PS}_5\text{Cl}$, and carbon in the composite cathode contributes to both continuous Li ion and electron transport. Owing to the optimized mixed ionic/electronic conductivity, the all-solid-state Li-S battery using the $\text{Li}_2\text{S-Li}_6\text{PS}_5\text{Cl-C}$ cathode can display an initial capacity of 648 mAh g^{-1} and then stabilize at about 830 mAh g^{-1} at 50 mA g^{-1} after 60 cycles.

Although the all-solid-state battery systems based on the SIEs are a promising strategy to solve the stability and safety problems of Li-S batteries, it is still difficult to give full play to the capacity and rate performance of Li-S batteries so far. As a compromise strategy, the SIEs are usually combined with liquid electrolytes or GPEs (so-called hybrid electrolytes) to ensure good interfacial contact and electrode wettability, in particular for the sulfur cathodes.^{254–257} Under these circumstances, a high capacity and a favorable rate performance can be obtained. However, it cannot be ignored that these hybrid electrolytes make it difficult to immobilize the flowable liquid electrolyte in the actual battery configurations, which would inevitably increase the complexity of structure design and preparation. Therefore, great efforts should be still devoted to seeking advanced materials or new fabrication techniques to realize all-solid-state Li-S batteries without compromising the electrochemical performance.

Design of the Li anode

Metallic Li (an indispensable component in Li-S battery systems) possesses the lowest electrochemical potential, highest theoretical specific energy, and low density, which has long been regarded as the “Holy Grail” of battery chemistry. However, before the Li metal anode can become a viable choice in Li-S batteries, some challenges need to be overcome.^{258–260} With regard to the infinite shape change, material design, and structure optimization for 3D hosts to accommodate the metallic Li and mitigate the thickness fluctuation during cycling have been taken as promising approaches to the practical use of Li metal anodes, although further improvements are still desired. Until now, various 3D host materials, such as carbons (graphene aerogels, carbon nanofibers, CNT sponges, carbon felts, carbon clothes, and carbonized wood),^{261–266} polymers (polyimide nanofibers, PAN nanofibers, and polyethylenimine sponge),^{267–269} and conductive metals and metal compounds (Ni foams, Cu foams, and MXene aerogels),^{270–272} have been reported to regulate the stripping/plating behavior of Li metal anodes.

In one example, molten Li can be infused into a layered reduced graphene oxide (rGO) film by capillarity to form the Li-rGO composite anode.²⁷³ The stable rGO film host can effectively minimize the Li volume fluctuation and suppress Li dendrites due to the reduced current density and homogenized ion flux. Another new report has shown that Li atoms tend to be stripped and deposited at the upper surface of highly tortuous hosts, such as horizontally aligned layered rGO, because of the extended ion transport pathways to the bottom part of hosts (Figure 10A).²⁷⁴ As a result, the deposited Li on the top surface will further block ion access to the internal host, in turn causing deterioration of the upper overgrowth of Li and breaking the SEI layers. When stripping, the uneven shape and increased current density caused by the decreased surface can easily lead to the formation of dead Li, degrading the

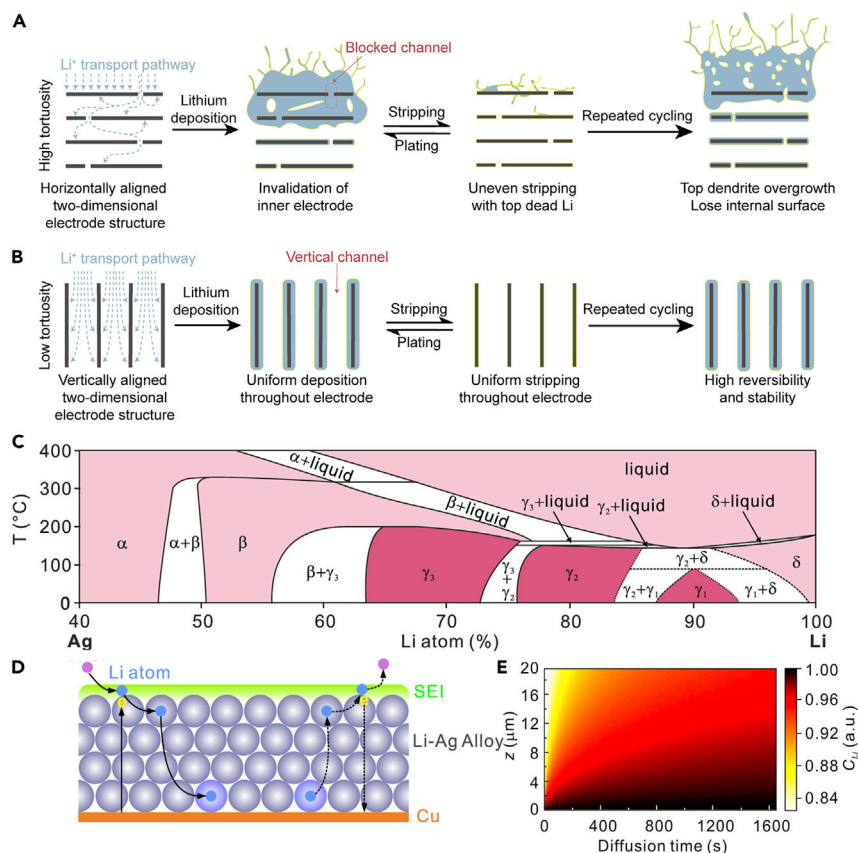


Figure 10. Design of advanced 3D Li hosts and Li alloys for Li-S batteries

- (A) Schematic illustration of structure evolution of Li in a horizontally aligned 3D host.
 (B) Schematic illustration of structure evolution of Li in a vertically aligned 3D host. Reproduced with permission from Chen et al.²⁷⁴ Copyright 2020, Elsevier.
 (C) Li-Ag binary phase diagram.
 (D) Schematic illustration of Li atom deposition and diffusion in Li-Ag alloy.
 (E) Normalized Li atom concentration as a function of diffusion time and depth in a Li₂₀Ag alloy through theoretical calculation. Reproduced with permission from Jin et al.²⁷⁵ Copyright 2020, American Chemical Society.

reversibility of the Li anode. In contrast, the vertically aligned rGO hosts with straight and low-tortuosity Li ion transport pathways can ensure reversible and uniform Li stripping/plating throughout the entire 3D matrix (Figure 10B). It has been shown that an 80- μm -thick upper Li dendrite layer was coated on the highly tortuous rGO hosts after only one plating step, and that a rapid Coulombic efficiency decay of 98.6%–90% was observed for the rGO hosts after 24 cycles. For the vertically aligned rGO hosts, a high Coulombic efficiency of $\sim 99.1\%$ over 150 cycles can be obtained, further proving the necessity of low tortuosity for stable Li metal anodes.

As well as the regulation of the microstructure of 3D hosts, the chemical modification of the surface of hosts is also an important strategy for the construction of stable Li metal anodes. For example, for carbon hosts with pre-stored Li through molten infusion before battery assembly, surface functionalization using metal oxides, such as ZnO, SnO₂, and MgO, is an effective way to improve the lithiophilicity of hosts, which contributes to building uniform and integrated composite Li anodes.^{276–278} As for the hosts with post-stored Li using electroreduction methods, increasing and homogenizing the Li nucleation sites by introducing lithiophilic heteroatoms (O, N,

P, and S) and metal nanoparticles/nanoclusters/single atoms (Au, Ag, and Zn) are commonly utilized to facilitate the uniform stripping/plating of Li anodes.^{279–284} In a representative work, ultrafine Ag nanoparticles with a diameter of ~ 40 nm were synthesized using a rapid Joule heating method, which can act as nanoseeds to direct the deposition of Li within the 3D hosts based on the interconnected carbon nanofibers.²⁸⁵ In this way, the nucleation overpotential of Li was greatly reduced, and the metallic Li was uniformly deposited into the 3D carbon matrix. As a result, the Li anode with the Ag nanoseeds could achieve a high Coulombic efficiency of $\sim 98\%$, while the Li anode on bare carbon nanofibers only exhibited a Coulombic efficiency of $\sim 96\%$.

The formation of Li alloys is also an effective strategy to regulate the stripping/plating behavior of the Li anode that has attracted much attention in the past several years.^{286–292} For example, a nanostructured Li metal foil interpenetrated with *in-situ*-formed 3D interconnected, mixed electron and Li ion conductive $\text{Li}_{22}\text{Sn}_5$ alloy networks was prepared using a facile repeated calendaring and folding method.²⁹³ The 3D $\text{Li}_{22}\text{Sn}_5$ alloy networks in the composite Li anode can facilitate both Li ion diffusion and electron conduction, and the metallic Li in the composite Li anode serves as a “Li reservoir” to provide an Li source. In addition, owing to the potential difference (~ 0.3 V) between the metallic Li and the $\text{Li}_{22}\text{Sn}_5$ alloy, a number of Li/ $\text{Li}_{22}\text{Sn}_5$ interfaces contribute to forcing Li diffusion within the entire electrode. As a result, the obtained Li/ $\text{Li}_{22}\text{Sn}_5$ nanocomposite anode can remain stable over 200 cycles with a low overpotential of 20 mV even under an ultrahigh current density of 30 mA cm^{-2} and a high areal capacity of 5 mAh cm^{-2} . In general, the electrochemical Li alloy reactions can be divided into a reconstitution reaction and a solid-solution reaction. The reconstitution reaction usually involves significant phase change and takes place at a higher potential than Li/Li⁺ redox, thus leading to obvious charge/discharge voltage hysteresis and sacrificing energy density. In contrast, the solid-solution reaction suffers from much less structure evolution and can take place with a low charge/discharge voltage hysteresis at a potential close to that of Li/Li⁺ redox. If the lithiation/delithiation process is based on the solid-solution reaction, the deposited Li atoms on the surface of Li anodes can rapidly diffuse into the anode matrix to form an alloy phase rather than accumulating on the surface to generate metallic Li, which can effectively facilitate uniform Li stripping/plating and suppress the formation of Li dendrites.

As a representative example, a new type of Li_{20}Ag metal anode that enables fast and uniform inward-growth plating of Li atoms was successfully synthesized using a facile melt mixing method.²⁷⁵ As shown in the binary phase diagram of a Li-Ag alloy (Figure 10C), a solid solution with a cubic structure, including the δ , γ_1 , γ_2 , and γ_3 phases, covers a wide range from 63 to 100 at % of Li. In particular, the lattice constants of the γ_1 , γ_2 , and γ_3 phases are quite close (0.980, 0.968, and 0.949 nm for γ_1 , γ_2 , and γ_3 phases, respectively). *In situ* X-ray diffraction studies have revealed that the delithiation/lithiation process for the Li_{20}Ag alloy is accompanied by the evolution of Li-Ag alloy phases and no Li metal signal is observed when cycling, which is in accordance with the phase diagram of the Li-Ag alloy. Because the Li-Ag alloy is electronically conductive, the Li ions should go through the SEI layers and be reduced to form Li atoms on the surface of the Li-Ag alloy before diffusing inside it (Figure 10D). It follows that the diffusion coefficient of Li atoms in the Li-Ag alloy is critical factor for determining the inward transport rate of Li. Based on the results of the galvanostatic intermittent titration technique, the diffusion coefficient of the Li atom in the Li-Ag alloy was calculated to be $\sim 10^{-8} \text{ cm}^2 \text{ s}^{-1}$, much higher than that in bulk metallic Li ($5.7 \times 10^{-11} \text{ cm}^2 \text{ s}^{-1}$). The high diffusion coefficient of the Li atom in

the Li-Ag alloy can effectively avoid the formation of Li and ensure stable cycling. The simulated normalized concentration of Li atoms in the Li_{20}Ag alloy as a function of diffusion time and thickness is shown in Figure 10E. It was observed that the composition at the bottom of delithiated Li-Ag alloy ($\text{Li}_{4.7}\text{Ag}$) can be restored to Li_{20}Ag alloy after 1,650 s. The results indicate that the Li concentration gradient can facilitate the inward diffusion of Li atoms rather than surface accumulation during the lithiation process. These new findings of Li storage in alloy anodes can provide some useful solutions to improve the reversibility of metallic Li.

In addition to the construction of bulk Li alloys, surface coating using Li alloys is also a facile yet effective approach to regulating the stripping/plating behavior of Li.²⁹⁴ For instance, a surface composite film, comprised of respective Li-rich Li_xM alloy ($\text{M} = \text{In}, \text{Zn}, \text{Bi}, \text{or As}$) and electronically insulating LiCl, was *in situ* formed on Li metals through a simple reduction of metal chlorides by metallic Li. The function of the composite films that allow uniform Li stripping/plating is ascribed to the following factors. First, the insulating LiCl could build a potential gradient across the composite film to force diffusion of Li ions through the layer and prevent the reduction of Li ions on the surface. Second, the Li-rich Li_xM alloys with a high diffusion coefficient can offer pathways for downward transport of Li to the underlying Li metals. Benefitting from the synergistic effect, the Li alloy-coated Li metal anodes can deliver a super-long cycling lifespan of 1,400 h at a high current density of 2 mA cm^{-2} in a symmetric cell. Moreover, another novel Li-Hg alloy film coated on the metallic Li was also prepared using a facile coating followed by self-alloying.²⁹⁵ The protective Li-Hg alloy film could act as a flexible buffer to accommodate huge volume change during cycling. In the symmetric cells, the Li-Hg alloy-protected Li anode displays a stable cycling over 750 cycles at 8 mAh cm^{-2} and 8 mA cm^{-2} . Despite the great success having been achieved, in-depth mechanisms of Li dendrite suppression using Li alloys still need to be investigated. Inspired by the diffusion barrier theory, the correlation of Li alloy surface diffusion properties and dendrite suppression was investigated in detail by Liang and colleagues.²⁹⁶ It was found that the diffusion energy barriers on specific phases of these alloys, such as LiZn, $\text{Li}_{13}\text{In}_3$, Li_3As , and Li_3Bi , are comparable with metallic Mg, which is known for its dendrite-free electrodeposition, and are much lower than that of metallic Li. The electrodeposition process on the alloy-coated Li metals can be described as fast migration on the surface of Li alloys without further nucleation and subsequent inward diffusion through the Li alloys. These findings could help to further understand the intrinsic mechanisms of Li alloys on the enhancement of the reversibility of Li metal anodes.

As well as the *in-situ*-formed SEI layers on Li metal anodes by reactions between Li anodes and organic solvents, Li salts, and electrolyte additives, the construction of artificial SEI layers before cell assembly is another effective strategy to improve the electrochemical performance of Li anodes. Usually, the conventional mosaic-like SEI layers are heterogeneous in both structure and chemical composition, and their poor mechanical properties easily lead to repeated fracture and reconstruction during cycling, which will continuously consume the liquid organic electrolyte. The artificial SEI layers are supposed to not only prevent the side reactions with electrolytes and soluble polysulfides, but also induce uniform Li stripping/plating. Ideally, the artificial SEI layers should possess the following properties: (1) favorable chemical and electrochemical stability to avoid decomposition; (2) high Li ion conductivity and low electronic conductivity to enable Li ion diffusion through SEI layers and deposition on the surface of metallic Li; and (3) high enough mechanical strength to withstand the volume change and inhibit dendrite growth. The artificial SEI layers can be divided into three categories: inorganic artificial SEI layers, such as BN, LiF,

Li_3N , Al_2O_3 , Li_2S , Li_3PO_4 , metal chloride perovskite, garnet-type $\text{Li}_{6.4}\text{La}_3\text{Zr}_{1.4}\text{Ta}_{0.6}\text{O}_{12}$ ^{297–304}; organic artificial SEI layers, such as lithiated Nafion, LiPAA, PI, PEO, PDMS, β -PVDF, and P(S-DVB)^{305–312}; composite artificial SEI layers, such as SiO_2 @PMMA, PVDF-HFP/LiF, PEDOT-co-PEG/AlF₃, and $\text{Li}_{1.5}\text{Al}_{0.5}\text{Ge}_{1.5}(\text{PO}_4)_3$ /PVDF.^{313–316} Different sorts of artificial SEI layers have specific advantages and disadvantages in protecting Li metal anodes.

Inorganic artificial SEI layers commonly exhibit high elastic modulus and favorable chemical/electrochemical stability. For example, a facile surface fluorination treatment to generate a uniform and dense inorganic LiF layer on Li metal anodes was developed recently (Figures 11A).³¹⁷ CYTOP is a typical fluoropolymer that can decompose and release pure fluorine gas at a relatively low temperature, which can prevent direct contact with the extremely toxic fluorine gas. The homogeneous and conformal LiF coating acts as mechanically robust and chemically stable protection layer for Li metal anodes by preventing side reactions with electrolytes and inhibiting dendrite growth. As a result, the LiF-coated Li metal anodes can maintain stability over 300 cycles at current densities of 1 and 5 mA cm⁻² even in carbonate electrolytes. The functions of the LiF layers on Li metal anodes have been further investigated in Li/polysulfides batteries. To better highlight the protection effect of the dense LiF layers, an ether electrolyte without a LiNO₃ additive was utilized. A higher capacity retention above 1,000 mAh g⁻¹ after 100 cycles can be obtained for Li/polysulfides cells based on LiF-coated Li anodes (Figure 11B). Furthermore, the LiF coating greatly enhances the average Coulombic efficiency from ~95.7% to ~99.0%.

Admittedly, these inorganic artificial SEI layers could effectively decrease the corrosion reactions and suppress the formation of Li dendrites, particularly at the early stage of cycling. However, the intrinsic brittle nature of inorganic artificial SEI layers makes them liable to fracture when a huge volume change of Li metal occurs. Although the Young's modulus of organic artificial SEI layers is usually inferior to that of their inorganic counterparts, their high flexibility, favorable shape adaption, and excellent processability contribute to achieving intimate interfacial contact and regulating uniform Li stripping/plating. The organic artificial SEI layers either possess porous structures or have ionic conductive groups, such as -O-, -CF, -C=O, and -C≡N, and charged groups (-COO⁻, -SO₃⁻, -O⁻, and -PO₃⁻) to provide Li ion transfer channels.³²⁰ For example, a Li metal anode featuring superior air resistance and waterproof properties using the PEO-based artificial SEI layers was prepared using a facile tip and coating method.³¹⁸ The functions of the wax-PEO hybrid artificial SEI layers are demonstrated in Figure 11C. The surface of a bare Li anode is unstable and could become rough when exposed to air and water due to its high reactivity. In contrast, the Li metal anode covered by a wax-PEO artificial SEI layer shows excellent surface stability in water and air because of the good sealing of the wax. In addition, the uniform distributed polar segments of PEO grafted with numerous -O- groups in the wax-PEO hybrid artificial SEI layers could regulate the homogeneous Li ion flux, leading to uniform Li stripping/plating. Therefore, the Li metal anode protected by the wax-PEO hybrid artificial SEI layers can remain stable in air (relative humidity 70%) for 24 h while a high retention capacity of 85% can be obtained. Furthermore, Li-S batteries have been assembled to investigate the effect of the wax-PEO hybrid artificial SEI layers on electrochemical performance. A high discharge capacity of 776 mAh g⁻¹ after 300 cycles can be achieved for the wax-PEO hybrid artificial SEI layer-coated Li anode, while only 390 mAh g⁻¹ after 150 cycles is obtained for the bare Li anode. The greatly enhanced cycling stability is attributed to the inhibition of corrosion reactions between polysulfides and Li anodes.

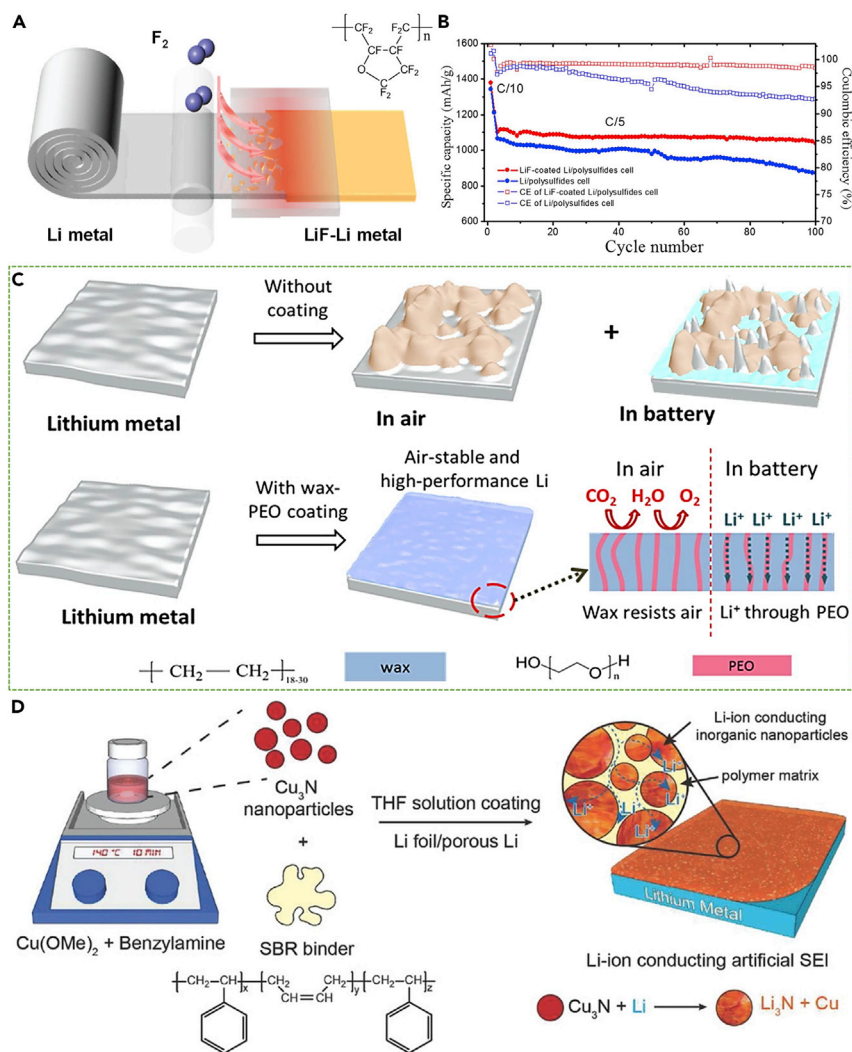


Figure 11. Design of advanced artificial SEI layers on Li metal anode for Li-S batteries

(A) Schematic illustration showing the LiF coating on a Li metal anode through the F_2 release by the decomposition of fluoropolymer, CYTOP.

(B) Cycling performance of the LiF-coated Li/polysulfides and Li/polysulfide cells. Reproduced with permission from Zhao et al.³¹⁷ Copyright 2017, American Chemical Society.

(C) Schematic illustration of the structure evolution of Li metal anode without and with the wax-PEO coating. Reproduced with permission from Zhang et al.³¹⁸ Copyright 2019, Elsevier.

(D) Schematic illustration of the preparation of the Cu_3N /SBR composite artificial SEI layers. Reproduced with permission from Liu et al.³¹⁹ Copyright 2016, Wiley-VCH Verlag GmbH & Co. KGaA.

Due to their high ionic conductivity, polymers with charged groups have been also extensively investigated as artificial SEI layers for Li anode protection. In a representative example, a dynamic single-ion-conductive network (DSN)-based organic artificial SEI layer, created by incorporating the negatively charged tetrahedral Al-O centers and soft fluorinated linkers, was prepared using a solution-processed coating method.³²¹ The tetrahedral $\text{Al}(\text{OR})_4^-$ (R = soft fluorinated linker) centers enable single-ion conductivity and flowability, while the fluorinated linkers can block the solvent and offer chain mobility. Benefiting from these unique features, the Li anode, protected by the DSN layers, shows a superior stripping/plating stability over 400 cycles in an asymmetric Li//Cu cell. It should be mentioned that two special

organic compounds, MOFs and COFs with tunable microstructures (specific surface area and pore size) and chemical components, have also been utilized to construct the artificial SEI layers.^{322–324} A representative example is that a thin UiO-66 MOF-based artificial SEI layer was prepared to act as an ion transport rectifier to regulate Li stripping/plating. The high Li ion transference number enabled by the strong binding of anions to the exposed Zr sites, high diffusion coefficient, and high mechanical modulus of the UiO-66 MOF-based artificial SEI layer can effectively inhibit uneven Li deposition and prevent dendrite growth.³²⁵

By combining the advantages of inorganic and organic artificial SEI layers, composite artificial SEI layers are a more promising choice for protecting the Li metal anodes. Recently, a composite artificial SEI layer composed of Cu₃N nanoparticles embedded in a styrene butadiene rubber (SBR) matrix was developed using a simple drop casting approach (Figure 11D).³¹⁹ The Cu₃N nanoparticles will react with metallic Li to form Li ion conductors of Li₃N ($\approx 10^{-3}$ – 10^{-4} S cm⁻¹) at room temperature, which can lead to uniform Li ion flux. Compared with single-component artificial SEI layers, pronounced synergistic effects can be exhibited in the Cu₃N-SBR composite artificial SEI layer. The densely stacked inorganic Li₃N can provide ion transport pathways and enhance the mechanical stiffness to prevent propagation of Li dendrites. Meanwhile, the flexible polymer of SBR can accommodate the volume change of Li anodes and maintain the integrity of the SEI layers without rupture during cycling. Because of the high Li ion conductivity and outstanding mechanical properties of the Cu₃N-SBR composite artificial SEI layer, the coated Li metal anode displays a high average Coulombic efficiency of 97.6% over 150 cycles in an asymmetric Li//Cu cell using a DOL/DME electrolyte, while the Coulombic efficiency of bare Li rapidly decreases after 75 cycles.

As well as the multicomponent mixed structure design of the composite artificial SEI layers, the natural SEI-inspired multilayer design is another effective strategy to construct high-performance composite artificial SEI layers. In a typical study, a bilayered composite artificial SEI layer was built using the sequence of atomic layer deposition (ALD) and molecular layer deposition (MLD).³²⁶ A dense inorganic Al₂O₃ coating prepared using the ALD method as the inner SEI layer can be utilized to conduct Li ions while blocking electron transfer. The highly flexible and porous organic alucone layer prepared using the MLD method is taken as the outer shell to allow electrolyte diffusion and relieve the change of surface stress. Through the thickness optimization for both the inorganic and organic layers, the natural SEI-inspired bilayered artificial SEI layer exhibited a superior structure stability during long-term electrochemical stripping/plating processing, and dendrite-inhibited Li deposition can be achieved under the protection of the bilayered artificial SEI layer. Moreover, Li-S batteries with a bilayered artificial SEI layer-coated Li anode showed a high capacity retention of 711.4 mAh g⁻¹ after 350 cycles, while only 236.9 mAh g⁻¹ can be obtained for Li-S batteries with bare Li anodes. The results further confirm that the designed bilayered artificial SEI layer can greatly improve the stability of Li anodes and enhance the lifetime of Li-S batteries by suppression of the side reactions between polysulfides and Li anodes.

CRITICAL CONCERNS FOR COMMERCIALIZATION

The critical concerns with regard to the practical use of rechargeable batteries basically include energy density, power capability, rechargeability, cost, and safety.³²⁷ In terms of energy density, it is generally accepted that Li-S batteries exhibit favorable performance due to their intrinsically unique conversion reactions of active sulfur

cathodes and the stripping/plating mechanism of Li metal anodes. Nevertheless, to realize the high gravimetric energy density of Li-S battery systems in reality ($\geq 500 \text{ Wh kg}^{-1}$), some prerequisites, including high sulfur:carbon ratio ($\geq 4:1$), low electrolyte:sulfur ratio ($\leq 3 \mu\text{L}/1 \text{ mg}$), low excess of Li ($\leq 50\%$), high mass loading of sulfur ($\geq 5 \text{ mg cm}^{-2}$), and high sulfur utilization ($\geq 80\%$), usually need to be met simultaneously. So far, for Li-S batteries, meeting all these conditions to achieve a high gravimetric energy density has not been easy.³²⁸ The resulting problems of passivation of the sulfur cathode, increased viscosity and decreased ionic conductivity of the electrolyte, electrolyte consumption, and pulverization of Li anodes under these conditions greatly hinder the practical application of high-energy-density Li-S batteries. More fundamental research on the optimization of sulfur cathodes, exploration of novel electrolytes, and enhancement of the reversibility of Li metal anodes are to be encouraged in the future to promote the practical development of Li-S batteries.

Despite the fact that Li-S batteries hold a potentially higher gravimetric energy density than that of Li ion batteries, the volumetric energy density of Li-S batteries is comparable with, or probably even lower than that of Li ion batteries. This is attributed to the large number of porous carbon additives that is required to enhance the conductivity of active sulfur and host the reaction intermediates, leading to a relatively low tapping density. In addition, owing to the low stripping/plating efficiency of Li metal anode, quite an excess of Li metal is required in the anode to replenish the loss of Li during the cycling process.³²⁹ More importantly, a considerable amount of electrolyte is needed to facilitate the solution-based conversion reactions of the sulfur cathode, increasing the volume and weight of cell devices by some degree, thus decreasing the energy density. Despite the weak volumetric energy density, Li-S batteries still hold great promise as a next-generation energy storage device, particularly in the application fields that give priority to weight and are less sensitive to volume, such as unmanned aerial vehicles.

The power capability of Li-S batteries is generally limited by the sulfur cathodes due to their inferior electronic conductivity and slow conversion kinetics, and hence the electrochemical measurement is rarely carried out above 5 C. The power capability of Li-S batteries can be boosted through enhanced mass transfer and redox reaction rates by increasing the content of the electrolyte and conductive additives; however, the energy density would accordingly decrease. Consequently, it is important to optimize the electron and Li ion transport pathways by developing advanced electrode materials with rational microstructures to achieve high rate performance without sacrificing energy density.

The rechargeability of Li-S batteries can be evaluated using round-trip efficiency, Coulombic efficiency, and cycle lifespan. The round-trip efficiency is determined by the overpotential of charge and discharge reactions and can be characterized by the ratio of discharge voltage/charge voltage under the same current density.³³⁰ The round-trip efficiency of Li-S batteries mainly depends on stage II, which is related with the sluggish solid-solid conversion reactions. Therefore, effective material and structure design are required to enhance the conversion kinetics of insoluble sulfur species to improve the energy-utilization efficiency of Li-S batteries. The Coulombic efficiency is represented by the capacity loss within a single cycle and can be defined as the ratio between discharge capacity and charge capacity. The Coulombic efficiency of Li-S batteries is greatly affected by the reversibility of the Li metal anode and the sulfur cathode, and can directly determine the cycle lifespan. So far, the cycle stability of Li-S batteries under practical conditions (usually lower than 500 cycles) is barely comparable with Li ion batteries based on the intercalation mechanism.

Barriers to the improvement of the cycle stability of Li-S batteries include various degradation mechanisms involving irreversible loss of active sulfur, inhomogeneous deposition/dissolution of Li metal anodes, and decomposition of electrolytes. Future efforts could take into account the novel material and structure designs that prevent the diffusion of soluble polysulfides, protect the highly reactive Li metal anodes, and stabilize the electrolytes.

Cost is another key factor that needs to be considered with regard to the practical application of Li-S batteries. Li ion battery packs cost over $\$1,000 \text{ kWh}^{-1}$ in 2010, and their price decreased by almost 8-fold to about $\$150 \text{ kWh}^{-1}$ in 2019. Despite this decrease, Li ion batteries still account for nearly 30%–40% of the cost of electric vehicles. Li-S batteries assembled with the earth-abundant element sulfur seem to have the potential to deal with this dilemma. The non-toxic sulfur has an average cost of $\$0.2 \text{ kg}^{-1}$, which is much lower than that of lithium cobalt oxide ($\sim\$30 \text{ kg}^{-1}$) and lithium nickel cobalt manganate oxide ($\sim\$20 \text{ kg}^{-1}$). The recycle technique for elemental sulfur, which involves solubilization and sublimation, is more facile and cost-effective than that of transition metal oxide cathodes in Li ion batteries, making Li-S batteries more competitive in terms of cost.³²⁷ However, it cannot be ignored that the higher cost of Li metal ($\sim\$70 \text{ kg}^{-1}$) over graphite ($\sim\10 kg^{-1}) and higher electrolyte consumption will inevitably somewhat offset the cost advantages of Li-S batteries. Several companies have been able to produce Li-S batteries on a certain scale. For example, in 2016, the British firm OXIS Energy successfully developed prototype Li-S batteries with a capacity of 1.2 kWh and anticipated that their Li-S batteries will only cost about $\$200 \text{ kWh}^{-1}$ in mass production, which is an inspiring prospect. Nevertheless, it should be noted that it is still difficult at this stage to accurately assess the cost of Li-S batteries, since they have not really been commercialized on a large scale until now. Even so, it can be predicted that the cost of Li-S batteries can be further reduced in the future by improving electrode performance and optimizing the electrolyte.

Apart from the above concerns, safety is also a critical factor for the commercialization of Li-S batteries. Unfortunately, so far, Li-S batteries have more potentially severe safety hazards compared with commercialized Li ion batteries due to the use of highly reactive Li metal anodes. The formation of Li dendrites, unstable SEI layers, and infinite shape changes lead to low Coulombic efficiency, inferior cycle life, and even internal short circuiting. Moreover, the currently used electrolyte in Li-S batteries is highly volatile and flammable (boiling points for DOL and DME are 78°C and 83°C at 100 kPa, respectively). This greatly increases the risk of thermal runaway and explosion of Li-S batteries under extreme use and external stimulus conditions. Consequently, it is extremely necessary to develop novel electrolyte systems for Li-S batteries with high boiling point, high chemical stability, and favorable compatibility with Li metal anode.

SUMMARY AND OUTLOOK

With the increasing demand for high energy density in electric vehicles and large-scale energy storage markets, and while the energy storage performance of current LIBs is approaching its ceiling, Li-S batteries with a potentially higher energy density have attracted extensive research interest worldwide. In this review, we first look back at the history of the development of Li-S batteries, and selectively list some pioneering and landmark achievements. The timeline for the development of Li-S batteries reveals the gradual transformation from basic scientific research to application-oriented research along the way. Subsequently, the fundamental reaction mechanisms of the Li-S battery chemistry are discussed in detail. While the multi-

electron conversion reactions of sulfur endow it with its high specific capacity, they also increase the complexity and uncertainty of Li-S battery chemistry. The existing scientific challenges facing the development of Li-S batteries, including the sulfur cathode, separator, electrolyte, and Li metal anode, are then systematically summarized. Representative strategies of material design and structure optimization to accordingly solve the existing scientific problems are comprehensively presented. Finally, some critical concerns on the practical applications of Li-S batteries are discussed. Although many significant advances have been achieved in Li-S batteries over the past few decades, there is still a long way to go before the commercialization of Li-S battery technology can be realized. Here, we outline some possible research directions for future studies of Li-S batteries, which may pave the ways for practical applications of Li-S batteries.

Sulfur cathode

Given the significant effect of the microstructure of carbon hosts on the performance of Li-S batteries, the manipulation and optimization of the microstructure, including macropores, mesopores, and micropores, needs to be further investigated. Carbon hosts with outer micropores and inner macro/mesopores could be an effective design strategy for high-loading and long-term stable sulfur cathodes. On the other hand, novel conductive materials other than carbons need to be developed to accommodate the active sulfur while improving the tap density and decreasing the proportion of inert materials. Ionic and electronic mixed conductor additives, such as TiS_2 and Mo_6S_8 , can be a promising choice in sulfur cathodes because they can decrease the porosity of electrodes, reduce electrolyte amount, and provide extra capacity, which can effectively improve the energy density of Li-S batteries. From the perspective of fundamental research, although significant improvements in Li-S batteries have been achieved by using solid heterogeneous mediators and electrocatalysts, their classification is arbitrary. In-depth molecular level evidence on the conversion process of polysulfide intermediates on solid additives are necessary to identify their exact functionality. Therefore, a series of advanced *ex situ* and *in situ* characterization techniques, such as synchrotron and *in situ* Raman, need to be developed to characterize and analyze polysulfide intermediates. Moreover, a strong polysulfide binding energy is not suggested to be utilized for screening the solid additives. Ideal solid additives should possess an appropriate polysulfide binding energy that is neither too high nor too low for reversible polysulfide adsorption and desorption. Importantly, in the future, more efforts should be devoted to the investigation of Li-S batteries with practically high mass loading and high sulfur content under a lean electrolyte to promote the practical development of Li-S battery technology.

Separator

Significant progress has been achieved in enhancing selective polysulfide blockage and regulating Li stripping/plating in Li-S batteries by functionalizing the separators. Nevertheless, the existing strategies of material design and structure optimization for separators cannot fully meet the requirements of Li-S batteries. First, the inert weight of various designed separators needs to be further reduced. Introducing an extra functional layer will increase the insert volume and weight and compromise the energy density of Li-S batteries. Although several thin functional layers have been reported to have little effect on the weight and volume of separators, their scale-up fabrication remains in doubt. Second, the mechanical properties of these designed separators need to be further improved. Particularly in liquid organic electrolytes, some functional separators can swell and deform, bringing great safety hazards. Last but not the least, the thermal stability of the separators needs to be

studied further at different operating temperatures. The operating temperature can have a great effect on the microstructures of separators, and thus influence their mechanical properties and functions. For future research, the effects of temperature on the performance of separators need to be systematically investigated.

Electrolyte

The electrolyte plays an extremely critical role in the practical applications of Li-S batteries. For the liquid organic electrolyte systems, novel solvents, Li salts and additives, and an appropriate component ratio should be explored to improve the stability of sulfur cathode/Li anodes while maintaining fast reaction kinetics of sulfur species. In-depth understanding of polysulfide chemistry in liquid organic electrolytes contributes to the design of advanced electrolytes to enhance sulfur utilization and suppress polysulfide shuttling. The development of novel sparingly/non-solvating electrolyte systems to mitigate the dissolution of polysulfides while remaining compatible with Li anodes can be a promising strategy to reduce the amount of electrolyte and then realize long-term stability and high energy density for Li-S batteries. The investigation of Li-S batteries under a lean electrolyte is still lacking. Future investigations on the evolution of surface/interfacial composition and structure of Li anodes and sulfur cathodes under lean electrolytes need to be conducted. The ultimate solution to address the problems of sulfur cathodes and Li anodes in Li-S batteries is to deploy solid-state electrolytes. Nevertheless, to date, none of the solid-state electrolyte systems has been able to demonstrate an electrochemical performance that is comparable with the liquid organic electrolyte systems. For SIEs, future efforts should be focused on the major disadvantages, such as fragility at a small thickness and poor interfacial properties between electrodes and electrolytes. For SPEs, improving room temperature ionic conductivity and mechanical properties are top priority issues for achieving high-performance Li-S batteries.

Li anode

Li metal anode has become a bottleneck problem with regard to the eventual commercialization of Li-S batteries. Compared with the progress achieved in sulfur cathodes, the advances in Li metal anodes in Li-S batteries are quite inadequate. In this review, several strategies for the protection of Li anodes in Li-S batteries, including electrolyte-modulated *in situ* SEI formation, 3D hosts, alloying treatment, and artificial SEI layers have been introduced. The optimization of electrolytes by manipulating the solvents, Li salts, and additives to facilitate the *in situ* formation of SEI layers on the surface of Li anodes is a facile yet effective approach for protection of Li anodes, and this can be potentially implemented in industrial production. However, the *in situ* formation of SEI layers through tuning the electrolyte component is not stable enough. Moreover, their composition and microstructure are still indistinct, and the accurate composition-structure-function relationship has not yet been established. Various artificial SEI layers with definite composition and structure have been proved to be effective for uniform Li stripping/plating. However, their mechanical properties, such as flexibility and stiffness, still need to be further optimized for adapting the shape change of Li and suppressing Li dendrites. In addition, the artificial SEI layers on Li metal anodes would usually increase the interface impedance, leading to increased polarization of Li-S batteries. Therefore, developing a thin artificial SEI layer with superior mechanical properties and high Li ion conductivity is a highly important research direction in the field of protection of Li anodes.

Although the strategy of building 3D hosts is indeed capable of mitigating the volume fluctuation of Li anodes and suppressing Li dendrites to a certain extent, the

increased surface area of Li anodes can cause more Li anode side reactions and consequently lead to a negative effect on the improvement of Coulombic efficiency. Combining interphase engineering with the 3D host strategy might provide a new way to solve this issue in the future. With regard to the alloying treatment strategy, it has been confirmed that Li alloys could alleviate Li corrosion due to reduced Li reactivity and regulate uniform Li stripping/plating due to the high Li ion bulk diffusion coefficient and low surface diffusion barrier. Nevertheless, the introduction of inert metal components in Li alloys would inevitably decrease the specific capacity of Li anodes to a certain extent. Furthermore, the stability of Li alloys in liquid organic electrolytes still needs to be further improved. It should be pointed out that, although these strategies can more or less enhance the reversibility of Li metal anode, so far it appears that there has been no report of the average Coulombic efficiency of Li metal anodes reaching 99.9%. Great efforts are still needed to further improve the Coulombic efficiency of Li metal anodes in the near future. Furthermore, advanced characterization techniques, such as cryogenic transmission electron microscopy are encouraged to be utilized to investigate the composition and structure of SEI layers and nucleation processing of Li metal.

ACKNOWLEDGMENTS

This study was financially supported by the National Science Fund for Distinguished Young Scholars (no. 52025133), the Tencent Foundation through the XPLOER PRIZE, the Beijing Natural Science Foundation (JQ18005), the National Key R&D Program of China (no. 2017YFA0206701), and BIC-ESAT funding. The authors also acknowledge the financial support of the Initiative Postdocs Supporting Program (BX20180001) and the China Postdoctoral Science Foundation (2018M640024).

AUTHOR CONTRIBUTIONS

S.G. and Y.L. discussed, co-wrote, and revised the manuscript.

REFERENCES

- Nitta, N., Wu, F., Lee, J.T., and Yushin, G. (2015). Li-ion battery materials: present and future. *Mater. Today* 18, 252–264.
- Liu, K., Liu, Y., Lin, D., Pei, A., and Cui, Y. (2018). Materials for lithium-ion battery safety. *Sci. Adv.* 4, eaas9820.
- Manthiram, A. (2017). An outlook on lithium ion battery technology. *ACS Cent. Sci.* 3, 1063–1069.
- Turcheniuk, K., Bondarev, D., Singhal, V., and Yushin, G. (2018). Ten years left to redesign lithium-ion batteries. *Nature* 559, 467–470.
- Marom, R., Amalraj, S.F., Leifer, N., Jacob, D., and Aurbach, D. (2011). A review of advanced and practical lithium battery materials. *J. Mater. Chem.* 21, 9938–9954.
- Fotouhi, A., Auger, D.J., Propp, K., Longo, S., and Wild, M. (2016). A review on electric vehicle battery modelling: from lithium-ion toward lithium-sulphur. *Renew. Sustain. Energy Rev.* 56, 1008–1021.
- Fotouhi, A., Auger, D.J., O'Neill, L., Cleaver, T., and Walus, S. (2017). Lithium-sulfur battery technology readiness and applications-a review. *Energies* 10, 1937.
- Ma, L., Hendrickson, K.E., Wei, S., and Archer, L.A. (2015). Nanomaterials: science and applications in the lithium-sulfur battery. *Nano Today* 10, 315–338.
- Bresser, D., Passerini, S., and Scrosati, B. (2013). Recent progress and remaining challenges in sulfur-based lithium secondary batteries-a review. *Chem. Commun.* 49, 10545–10562.
- Yin, Y.X., Xin, S., Guo, Y.G., and Wan, L.J. (2013). Lithium-sulfur batteries: electrochemistry, materials, and prospects. *Angew. Chem. Int. Ed.* 52, 13186–13200.
- Fang, R., Zhao, S., Sun, Z., Wang, D.W., Cheng, H.M., and Li, F. (2017). More reliable lithium-sulfur batteries: status, solutions and prospects. *Adv. Mater.* 29, 1606823.
- Manthiram, A., Fu, Y., Chung, S.-H., Zu, C., and Su, Y.-S. (2014). Rechargeable lithium-sulfur batteries. *Chem. Rev.* 114, 11751–11787.
- Yang, X., Li, X., Adair, K., Zhang, H., and Sun, X. (2018). Structural design of lithium-sulfur batteries: from fundamental research to practical application. *Electrochem. Energy Rev.* 1, 239–293.
- Nazar, L.F., Cuisinier, M., and Pang, Q. (2014). Lithium-sulfur batteries. *MRS Bull.* 39, 436–442.
- Danuta, H., Juliusz, U., Herbert, D., and Ulam, J. (1962). Electric dry cells and storage batteries. US Pat 3043896.
- Bhaskara, R.M.L. (1968). Organic electrolyte cells. US Pat 3413154.
- Martin, R.P., Doub, W.H., Roberts, J.L., and Sawyer, D.T. (1973). Electrochemical reduction of sulfur in aprotic solvents. *Inorg. Chem.* 12, 1921–1925.
- Rauh, R.D., Abraham, K.M., Pearson, G.F., Surprenant, J.K., and Brummer, S.B. (1979). A lithium/dissolved sulfur battery with an organic electrolyte. *J. Electrochem. Soc.* 126, 523–527.
- Peled, E., Sternberg, Y., Gorenshstein, A., and Lavi, Y. (1989). Lithium-sulfur battery: evaluation of doxolane-based electrolytes. *J. Electrochem. Soc.* 136, 1621–1625.
- Peled, E., Gorenshstein, A., Segal, M., and Sternberg, Y. (1989). Rechargeable lithium-sulfur battery. *J. Power Sources* 26, 269–271.
- Hayashi, A., Ohtomo, T., Mizuno, F., Tadanaga, K., and Tatsumisago, M. (2003). All-solid-state Li/S batteries with highly conductive glass-ceramic electrolytes. *Electrochem. Commun.* 5, 701–705.

22. Chu, M.Y. (1998). Rechargeable positive electrodes. US Pat 5789108.
23. Wang, J.L., Yang, J., Xie, J.Y., Xu, N.X., and Li, Y. (2002). Sulfur-carbon nano-composite as cathode for rechargeable lithium battery based on gel electrolyte. *Electrochem. Commun.* 4, 499–502.
24. Wang, J., Yang, J., Xie, J., and Xu, N. (2002). A novel conductive polymer-sulfur composite cathode material for rechargeable lithium batteries. *Adv. Mater.* 14, 963–965.
25. Ji, X., Lee, K.T., and Nazar, L.F. (2009). A highly ordered nanostructured carbon-sulphur cathode for lithium-sulphur batteries. *Nat. Mater.* 8, 500–506.
26. Chen, S., Sun, B., Xie, X., Mondal, A.K., Huang, X., and Wang, G. (2015). Multi-chambered micro/mesoporous carbon nanocubes as new polysulfides reservoirs for lithium-sulfur batteries with long cycle life. *Nano Energy* 16, 268–280.
27. Zhang, C., Wu, H.B., Yuan, C., Guo, Z., and Lou, X.W. (2012). Confining sulfur in double-shelled hollow carbon spheres for lithium-sulfur batteries. *Angew. Chem. Int. Ed.* 51, 9592–9595.
28. Li, G., Sun, J., Hou, W., Jiang, S., Huang, Y., and Geng, J. (2016). Three-dimensional porous carbon composites containing high sulfur nanoparticle content for high-performance lithium-sulfur batteries. *Nat. Commun.* 7, 10601.
29. Sun, L., Li, M., Jiang, Y., Kong, W., Jiang, K., Wang, J., and Fan, S. (2014). Sulfur nanocrystals confined in carbon nanotube network as a binder-free electrode for high-performance lithium sulfur batteries. *Nano Lett.* 14, 4044–4049.
30. Lyu, Z., Xu, D., Yang, L., Che, R., Feng, R., Zhao, J., Li, Y., Wu, Q., Wang, X., and Hu, Z. (2015). Hierarchical carbon nanocages confining high-loading sulfur for high-rate lithium-sulfur batteries. *Nano Energy* 12, 657–665.
31. Mikhaylik, Y.V., and Akridge, J.R. (2004). Polysulfide shuttle study in the Li/S battery system. *J. Electrochem. Soc.* 151, A1969.
32. Yu, X., Xie, J., Yang, J., Huang, H., Wang, K., and Wen, Z. (2004). Lithium storage in conductive sulfur-containing polymers. *J. Electroanal. Chem.* 573, 121–128.
33. Aurbach, D., Pollak, E., Elazari, R., Salitra, G., Kelley, C.S., and Affinito, J. (2009). On the surface chemical aspects of very high energy density, rechargeable Li-sulfur batteries. *J. Electrochem. Soc.* 156, A694.
34. Ji, X., and Nazar, L.F. (2010). Advances in Li-S batteries. *J. Mater. Chem.* 20, 9821–9826.
35. Lee, Y.M., Choi, N.-S., Park, J.H., and Park, J.-K. (2003). Electrochemical performance of lithium/sulfur batteries with protected Li anodes. *J. Power Sources* 119, 964–972.
36. Hassoun, J., and Scrosati, B. (2010). Moving to a solid-state configuration: a valid approach to making lithium-sulfur batteries viable for practical applications. *Adv. Mater.* 22, 5198–5201.
37. Jin, B., Kim, J.-U., and Gu, H.-B. (2003). Electrochemical properties of lithium-sulfur batteries. *J. Power Sources* 117, 148–152.
38. Suo, L., Hu, Y.-S., Li, H., Armand, M., and Chen, L. (2013). A new class of solvent-in-salt electrolyte for high-energy rechargeable metallic lithium batteries. *Nat. Commun.* 4, 1481.
39. Huang, J.-Q., Zhang, Q., Peng, H.-J., Liu, X.-Y., Qian, W.-Z., and Wei, F. (2014). Ionic shield for polysulfides towards highly-stable lithium-sulfur batteries. *Energy Environ. Sci.* 7, 347–353.
40. Li, Z., Zhang, J.T., Chen, Y.M., Li, J., and Lou, X.W. (2015). Pie-like electrode design for high-energy density lithium-sulfur batteries. *Nat. Commun.* 6, 8850.
41. Sun, X.-G., Wang, X., Mayes, R.T., and Dai, S. (2012). Lithium-sulfur batteries based on nitrogen-doped carbon and an ionic-liquid electrolyte. *ChemSusChem* 5, 2079–2085.
42. Su, Y.-S., and Manthiram, A. (2012). A new approach to improve cycle performance of rechargeable lithium-sulfur batteries by inserting a free-standing MWCNT interlayer. *Chem. Commun.* 48, 8817–8819.
43. Xin, S., Gu, L., Zhao, N.-H., Yin, Y.-X., Zhou, L.-J., Guo, Y.-G., and Wan, L.-J. (2012). Smaller sulfur molecules promise better lithium-sulfur batteries. *J. Am. Chem. Soc.* 134, 18510–18513.
44. Evers, S., Yim, T., and Nazar, L.F. (2012). Understanding the nature of absorption/adsorption in nanoporous polysulfide sorbents for the Li-S battery. *J. Phys. Chem. C* 116, 19653–19658.
45. Al Salem, H., Babu, G.V., Rao, C., and Arava, L.M.R. (2015). Electrocatalytic polysulfide traps for controlling redox shuttle process of Li-S batteries. *J. Am. Chem. Soc.* 137, 11542–11545.
46. Babu, G., Ababtain, K., Ng, K.Y.S., and Arava, L.M.R. (2015). Electrocatalysis of lithium polysulfides: current collectors as electrodes in Li/S battery configuration. *Sci. Rep.* 5, 8763.
47. Bai, S., Zhu, K., Wu, S., Wang, Y., Yi, J., Ishida, M., and Zhou, H. (2016). A long-life lithium-sulphur battery by integrating zinc-organic framework based separator. *J. Mater. Chem. A* 4, 16812–16817.
48. Ghazi, Z.A., He, X., Khattak, A.M., Khan, N.A., Liang, B., Iqbal, A., Wang, J., Sin, H., Li, L., and Tang, Z. (2017). MoS₂/Celgard separator as efficient polysulfide barrier for long-life lithium-sulfur batteries. *Adv. Mater.* 29, 1606817.
49. Xu, G., Yan, Q.-b., Kushima, A., Zhang, X., Pan, J., and Li, J. (2017). Conductive graphene oxide-polyacrylic acid (GOPAA) binder for lithium-sulfur battery. *Nano Energy* 31, 568–574.
50. Chen, W., Lei, T., Qian, T., Lv, W., He, W., Wu, C., Liu, X., Liu, J., Chen, B., Yan, C., et al. (2018). A new hydrophilic binder enabling strongly anchoring polysulfides for high-performance sulfur electrodes in lithium-sulfur battery. *Adv. Energy Mater.* 8, 1702889.
51. Xiao, Z., Li, Z., Li, P., Meng, X., and Wang, R. (2019). Ultrafine Ti₃C₂ MXene nanodots-interspersed nanosheet for high-energy-density lithium-sulfur batteries. *ACS Nano* 13, 3608–3617.
52. Tao, X., Wang, J., Ying, Z., Cai, Q., Zheng, G., Gan, Y., Huang, H., Xia, Y., Liang, C., Zhang, W., et al. (2014). Strong sulfur binding with conducting Magnéli-phase Ti_{1-x}O_{2n-1} nanomaterials for improving lithium-sulfur batteries. *Nano Lett.* 14, 5288–5294.
53. Huang, C., Xiao, J., Shao, Y., Zheng, J., Bennett, W.D., Lu, D., Saraf, L.V., Engelhard, M., Ji, L., Zhang, J., et al. (2014). Manipulating surface reactions in lithium-sulphur batteries using hybrid anode structures. *Nat. Commun.* 5, 3015.
54. Cao, R., Xu, W., Lv, D., Xiao, J., and Zhang, J.-G. (2015). Anodes for rechargeable lithium-sulfur batteries. *Adv. Energy Mater.* 5, 1402273.
55. Cheng, X.-B., Yan, C., Chen, X., Guan, C., Huang, J.-Q., Peng, H.-J., Zhang, R., Yang, S.-T., and Zhang, Q. (2017). Implantable solid electrolyte interphase in lithium-metal batteries. *Chem* 2, 258–270.
56. Dörfler, S., Althues, H., Härtel, P., Abendroth, T., Schumm, B., and Kaskel, S. (2020). Challenges and key parameters of lithium-sulfur batteries on pouch cell level. *Joule* 4, 539–554.
57. Pan, H., Han, K.S., Engelhard, M.H., Cao, R., Chen, J., Zhang, J.-G., Mueller, K.T., Shao, Y., and Liu, J. (2018). Addressing passivation in lithium-sulfur battery under lean electrolyte condition. *Adv. Funct. Mater.* 28, 1707234.
58. Fang, R., Zhao, S., Hou, P., Cheng, M., Wang, S., Cheng, H.-M., Liu, C., and Li, F. (2016). 3D interconnected electrode materials with ultrahigh areal sulfur loading for Li-S batteries. *Adv. Mater.* 28, 3374–3382.
59. Xue, W., Shi, Z., Suo, L., Wang, C., Wang, Z., Wang, H., So, K.P., Maurano, A., Yu, D., Chen, Y., et al. (2019). Intercalation-conversion hybrid cathodes enabling Li-S full-cell architectures with jointly superior gravimetric and volumetric energy densities. *Nat. Energy* 4, 374–382.
60. Zhao, M., Li, B.-Q., Peng, H.-J., Yuan, H., Wei, J.-Y., and Huang, J.-Q. (2020). Lithium-sulfur batteries under lean electrolyte conditions: challenges and opportunities. *Angew. Chem. Int. Ed.* 59, 12636–12652.
61. Wang, Q., Zheng, J., Walter, E., Pan, H., Lv, D., Zuo, P., Chen, H., Deng, Z.D., Liaw, B.Y., Yu, X., et al. (2015). Direct observation of sulfur radicals as reaction media in lithium sulfur batteries. *J. Electrochem. Soc.* 162, A474–A478.
62. Li, G., Wang, S., Zhang, Y., Li, M., Chen, Z., and Lu, J. (2018). Revisiting the role of polysulfides in lithium-sulfur batteries. *Adv. Mater.* 30, 1705590.
63. Huang, L., Li, J., Liu, B., Li, Y., Shen, S., Deng, S., Lu, C., Zhang, W., Xia, Y., Pan, G., et al. (2020). Electrode design for lithium-sulfur batteries: problems and solutions. *Adv. Funct. Mater.* 30, 1910375.

64. Maihom, T., Kaewruang, S., Phattharasupakun, N., Chiochan, P., Limtrakul, J., and Sawangphruk, M. (2018). Lithium bond impact on lithium polysulfide adsorption with functionalized carbon fiber paper interlayers for lithium-sulfur batteries. *J. Phys. Chem. C* 122, 7033–7040.
65. Ren, W., Ma, W., Zhang, S., and Tang, B. (2019). Recent advances in shuttle effect inhibition for lithium sulfur batteries. *Energy Storage Mater.* 23, 707–732.
66. Shaibani, M., Mirshekarloo, M.S., Singh, R., Easton, C.D., Cooray, M.C.D., Eshraghi, N., Abendroth, T., Dörfler, S., Althues, H., Kaskel, S., et al. (2020). Expansion-tolerant architectures for stable cycling of ultrahigh-loading sulfur cathodes in lithium-sulfur batteries. *Sci. Adv.* 6, eaay2757.
67. Zhang, Q., Wang, Y., Seh, Z.W., Fu, Z., Zhang, R., and Cui, Y. (2015). Understanding the anchoring effect of two-dimensional layered materials for lithium-sulfur batteries. *Nano Lett.* 15, 3780–3786.
68. Liang, X., Hart, C., Pang, Q., Garsuch, A., Weiss, T., and Nazar, L.F. (2015). A highly efficient polysulfide mediator for lithium-sulfur batteries. *Nat. Commun.* 6, 5682.
69. Wang, D.-Y., Guo, W., and Fu, Y. (2019). Organosulfides: an emerging class of cathode materials for rechargeable lithium batteries. *Acc. Chem. Res.* 52, 2290–2300.
70. Wang, J., Li, M., Liu, C., Liu, Y., Zhao, T., Zhai, P., and Wang, J. (2019). An electronegative modified separator with semifused pores as a selective barrier for highly stable lithium-sulfur batteries. *Ind. Eng. Chem. Res.* 58, 14538–14547.
71. Huang, X., He, R., Li, M., Chee, M.O.L., Dong, P., and Lu, J. (2020). Functionalized separator for next-generation batteries. *Mater. Today*. <https://doi.org/10.1016/j.mattod.2020.07.015>.
72. Wang, L., Ye, Y., Chen, N., Huang, Y., Li, L., Wu, F., and Chen, R. (2018). Development and challenges of functional electrolytes for high-performance lithium-sulfur batteries. *Adv. Funct. Mater.* 28, 1800919.
73. Xiong, S., Regula, M., Wang, D., and Song, J. (2018). Toward better lithium-sulfur batteries: functional non-aqueous liquid electrolytes. *Electrochem. Energy Rev.* 1, 388–402.
74. Chen, W., Lei, T., Wu, C., Deng, M., Gong, C., Hu, K., Ma, Y., Dai, L., Lv, W., He, W., et al. (2018). Designing safe electrolyte systems for a high-stability lithium-sulfur battery. *Adv. Energy Mater.* 8, 1702348.
75. Azimi, N., Weng, W., Takoudis, C., and Zhang, Z. (2013). Improved performance of lithium-sulfur battery with fluorinated electrolyte. *Electrochem. Commun.* 37, 96–99.
76. Cuisinier, M., Cabelguen, P.E., Adams, B.D., Garsuch, A., Balasubramanian, M., and Nazar, L.F. (2014). Unique behaviour of nonsolvents for polysulphides in lithium-sulphur batteries. *Energy Environ. Sci.* 7, 2697–2705.
77. Park, J.-W., Ueno, K., Tachikawa, N., Dokko, K., and Watanabe, M. (2013). Ionic liquid electrolytes for lithium-sulfur batteries. *J. Phys. Chem. C* 117, 20531–20541.
78. Hu, J.J., Long, G.K., Liu, S., Li, G.R., and Gao, X.P. (2014). A LiFSI–LiTFSI binary-salt electrolyte to achieve high capacity and cycle stability for a Li–S battery. *Chem. Commun.* 50, 14647–14650.
79. Gupta, A., Bhargav, A., and Manthiram, A. (2019). Highly solvating electrolytes for lithium-sulfur batteries. *Adv. Energy Mater.* 9, 1803096.
80. Zhang, G., Peng, H.J., Zhao, C.Z., Chen, X., Zhao, L.D., Li, P., Huang, J.Q., and Zhang, Q. (2018). The radical pathway based on a lithium-metal-compatible high-dielectric electrolyte for lithium-sulfur batteries. *Angew. Chem. Int. Ed.* 130, 16974–16978.
81. Kim, J.-S., Yoo, D.-J., Min, J., Shakoore, R.A., Kahraman, R., and Choi, J.W. (2015). Poreless separator and electrolyte additive for lithium-sulfur batteries with high areal energy densities. *ChemNanoMat* 1, 240–245.
82. Ding, F., Xu, W., Graff, G.L., Zhang, J., Sushko, M.L., Chen, X., Shao, Y., Engelhard, M.H., Nie, Z., Xiao, J., et al. (2013). Dendrite-free lithium deposition via self-healing electrostatic shield mechanism. *J. Am. Chem. Soc.* 135, 4450–4456.
83. Jia, W., Fan, C., Wang, L., Wang, Q., Zhao, M., Zhou, A., and Li, J. (2016). Extremely accessible potassium nitrate (KNO₃) as the highly efficient electrolyte additive in lithium battery. *ACS Appl. Mater. Inter.* 8, 15399–15405.
84. Liu, S., Li, G.-R., and Gao, X.-P. (2016). Lanthanum nitrate as electrolyte additive to stabilize the surface morphology of lithium anode for lithium-sulfur battery. *ACS Appl. Mater. Interfaces* 8, 7783–7789.
85. Zeng, W., Cheng, M.M.-C., and Ng, S.K.-Y. (2019). Effects of transition metal cation additives on the passivation of lithium metal anode in Li-S batteries. *Electrochim. Acta* 319, 511–517.
86. Chen, W., Hu, Y., Lv, W., Lei, T., Wang, X., Li, Z., Zhang, M., Huang, J., Du, X., Yan, Y., et al. (2019). Lithiophilic montmorillonite serves as lithium ion reservoir to facilitate uniform lithium deposition. *Nat. Commun.* 10, 4973.
87. Li, J., Zhang, L., Qin, F., Hong, B., Xiang, Q., Zhang, K., Fang, J., and Lai, Y. (2019). ZrO(NO₃)₂ as a functional additive to suppress the diffusion of polysulfides in lithium-sulfur batteries. *J. Power Sources* 442, 227232.
88. Gerber, L.C.H., Frischmann, P.D., Fan, F.Y., Doris, S.E., Qu, X., Scheuermann, A.M., Persson, K., Chiang, Y.-M., and Helms, B.A. (2016). Three-dimensional growth of Li₂S in lithium-sulfur batteries promoted by a redox mediator. *Nano Lett.* 16, 549–554.
89. Li, Q., Yang, H., Naveed, A., Guo, C., Yang, J., Nuli, Y., and Wang, J. (2018). Duplex component additive of tris(trimethylsilyl) phosphite-vinylene carbonate for lithium sulfur batteries. *Energy Storage Mater.* 14, 75–81.
90. Wu, B., Pei, F., Wu, Y., Mao, R., Ai, X., Yang, H., and Cao, Y. (2013). An electrochemically compatible and flame-retardant electrolyte additive for safe lithium-ion batteries. *J. Power Sources* 227, 106–110.
91. Umeshbabu, E., Zheng, B., and Yang, Y. (2019). Recent progress in all-solid-state lithium-sulfur batteries using high Li-ion conductive solid electrolytes. *Electrochem. Energy Rev.* 2, 199–230.
92. Chen, W.J., Li, B.Q., Zhao, C.X., Zhao, M., Yuan, T.Q., Sun, R.C., Huang, J.Q., and Zhang, Q. (2020). Electrolyte regulation towards stable lithium-metal anodes in lithium-sulfur batteries with sulfurized polyacrylonitrile cathodes. *Angew. Chem. Int. Ed.* 132, 10821–10834.
93. Liu, S., Xie, K., Chen, Z., Li, Y., Hong, X., Xu, J., Zhou, L., Yuan, J., and Zheng, C. (2015). A 3D nanostructure of graphene interconnected with hollow carbon spheres for high performance lithium-sulfur batteries. *J. Mater. Chem. A* 3, 11395–11402.
94. Liu, S., Hong, X., Wang, D., Li, Y., Xu, J., Zheng, C., and Xie, K. (2018). Hollow carbon spheres with nanoporous shells and tailored chemical interfaces as sulfur host for long cycle life of lithium sulfur batteries. *Electrochim. Acta* 279, 10–18.
95. Jayaprakash, N., Shen, J., Moganty, S.S., Corona, A., and Archer, L.A. (2011). Porous hollow carbon@sulfur composites for high-power lithium-sulfur batteries. *Angew. Chem. Int. Ed.* 50, 5904–5908.
96. Qu, Y., Zhang, Z., Wang, X., Lai, Y., Liu, Y., and Li, J. (2013). A simple SDS-assisted self-assembly method for the synthesis of hollow carbon nanospheres to encapsulate sulfur for advanced lithium-sulfur batteries. *J. Mater. Chem. A* 1, 14306–14310.
97. Zhang, K., Zhao, Q., Tao, Z., and Chen, J. (2013). Composite of sulfur impregnated in porous hollow carbon spheres as the cathode of Li-S batteries with high performance. *Nano Res.* 6, 38–46.
98. Yang, D.-H., Zhou, H.-Y., Liu, H., and Han, B.-H. (2019). Hollow N-doped carbon polyhedrons with hierarchically porous shell for confinement of polysulfides in lithium-sulfur batteries. *iScience* 13, 243–253.
99. Dhawa, T., Chattopadhyay, S., De, G., and Mahanty, S. (2019). Carbon@carbon double hollow spheres as efficient cathode host for high rate LiS battery. *Mater. Chem. Phys.* 225, 309–315.
100. Zang, J., An, T., Dong, Y., Fang, X., Zheng, M., Dong, Q., and Zheng, N. (2015). Hollow-in-hollow carbon spheres with hollow foam-like cores for lithium-sulfur batteries. *Nano Res.* 8, 2663–2675.
101. Fu, A., Wang, C., Pei, F., Cui, J., Fang, X., and Zheng, N. (2019). Recent advances in hollow porous carbon materials for lithium-sulfur batteries. *Small* 15, 1804786.
102. Yu, Z., Liu, M., Guo, D., Wang, J., Chen, X., Li, J., Jin, H., Yang, Z., Chen, X.a., and Wang, S. (2020). Radially inwardly aligned hierarchical porous carbon for ultra-long-life lithium-sulfur batteries. *Angew. Chem. Int. Ed.* 59, 6406–6411.
103. Jung, D.S., Hwang, T.H., Lee, J.H., Koo, H.Y., Shakoore, R.A., Kahraman, R., Jo, Y.N., Park, M.-S., and Choi, J.W. (2014). Hierarchical porous carbon by ultrasonic spray pyrolysis

- yields stable cycling in lithium-sulfur battery. *Nano Lett.* **14**, 4418–4425.
104. Choudhury, S., Ebert, T., Windberg, T., Seifert, A., Göbel, M., Simon, F., Formanek, P., Stamm, M., Spange, S., and Ionov, L. (2018). Hierarchical porous carbon cathode for lithium-sulfur batteries using carbon derived from hybrid materials synthesized by twin polymerization. *Part. Part. Syst. Charact.* **35**, 1800364.
 105. Zhong, Y., Wang, S., Sha, Y., Liu, M., Cai, R., Li, L., and Shao, Z. (2016). Trapping sulfur in hierarchically porous, hollow indented carbon spheres: a high-performance cathode for lithium-sulfur batteries. *J. Mater. Chem. A* **4**, 9526–9535.
 106. Wang, H., Zhang, C., Chen, Z., Liu, H.K., and Guo, Z. (2015). Large-scale synthesis of ordered mesoporous carbon fiber and its application as cathode material for lithium-sulfur batteries. *Carbon* **81**, 782–787.
 107. Zhang, X.-Q., He, B., Li, W.-C., and Lu, A.-H. (2018). Hollow carbon nanofibers with dynamic adjustable pore sizes and closed ends as hosts for high-rate lithium-sulfur battery cathodes. *Nano Res.* **11**, 1238–1246.
 108. Elazari, R., Salitra, G., Garsuch, A., Panchenko, A., and Aurbach, D. (2011). Sulfur-impregnated activated carbon fiber cloth as a binder-free cathode for rechargeable Li-S batteries. *Adv. Mater.* **23**, 5641–5644.
 109. Zhang, Y.-Z., Zhang, Z., Liu, S., Li, G.-R., and Gao, X.-P. (2018). Free-standing porous carbon nanofiber/carbon nanotube film as sulfur immobilizer with high areal capacity for lithium-sulfur battery. *ACS Appl. Mater. Interfaces* **10**, 8749–8757.
 110. Zhao, Y., Wu, W., Li, J., Xu, Z., and Guan, L. (2014). Encapsulating MWNTs into hollow porous carbon nanotubes: a tube-in-tube carbon nanostructure for high-performance lithium-sulfur batteries. *Adv. Mater.* **26**, 5113–5118.
 111. Wang, H., Yang, Y., Liang, Y., Robinson, J.T., Li, Y., Jackson, A., Cui, Y., and Dai, H. (2011). Graphene-wrapped sulfur particles as a rechargeable lithium-sulfur battery cathode material with high capacity and cycling stability. *Nano Lett.* **11**, 2644–2647.
 112. Yu, M., Li, R., Wu, M., and Shi, G. (2015). Graphene materials for lithium-sulfur batteries. *Energy Storage Mater.* **1**, 51–73.
 113. Chen, H., Zhou, G., Boyle, D., Wan, J., Wang, H., Lin, D., Mackanic, D., Zhang, Z., Kim, S.C., Lee, H.R., et al. (2020). Electrode design with integration of high tortuosity and sulfur-philicity for high-performance lithium-sulfur battery. *Matter* **2**, 1605–1620.
 114. Guo, J., Zhang, J., Jiang, F., Zhao, S., Su, Q., and Du, G. (2015). Microporous carbon nanosheets derived from corncobs for lithium-sulfur batteries. *Electrochim. Acta* **176**, 853–860.
 115. Ma, J., Yu, M., Ye, H., Song, H., Wang, D., Zhao, Y., Gong, W., and Qiu, H. (2019). A 2D/2D graphitic carbon nitride/N-doped graphene hybrid as an effective polysulfide mediator in lithium-sulfur batteries. *Mater. Chem. Front.* **3**, 1807–1815.
 116. Li, G., Sun, J., Hou, W., Jiang, S., Huang, Y., and Geng, J. (2016). Three-dimensional porous carbon composites containing high sulfur nanoparticle content for high-performance lithium-sulfur batteries. *Nat. Commun.* **7**, 10601.
 117. Liu, S., Zhao, T., Tan, X., Guo, L., Wu, J., Kang, X., Wang, H., Sun, L., and Chu, W. (2019). 3D pomegranate-like structures of porous carbon microspheres self-assembled by hollow thin-walled highly-graphitized nanoballs as sulfur immobilizers for Li-S batteries. *Nano Energy* **63**, 103894.
 118. Wang, H., Zhang, W., Liu, H., and Guo, Z. (2016). A strategy for configuration of an integrated flexible sulfur cathode for high-performance lithium-sulfur batteries. *Angew. Chem. Int. Ed.* **55**, 3992–3996.
 119. Pei, F., Lin, L., Ou, D., Zheng, Z., Mo, S., Fang, X., and Zheng, N. (2017). Self-supporting sulfur cathodes enabled by two-dimensional carbon yolk-shell nanosheets for high-energy-density lithium-sulfur batteries. *Nat. Commun.* **8**, 482.
 120. He, G., Mandlmeier, B., Schuster, J., Nazar, L.F., and Bein, T. (2014). Bimodal mesoporous carbon nanofibers with high porosity: freestanding and embedded in membranes for lithium-sulfur batteries. *Chem. Mater.* **26**, 3879–3886.
 121. Gueon, D., Hwang, J.T., Yang, S.B., Cho, E., Sohn, K., Yang, D.-K., and Moon, J.H. (2018). Spherical macroporous carbon nanotube particles with ultrahigh sulfur loading for lithium-sulfur battery cathodes. *ACS Nano* **12**, 226–233.
 122. Tao, X., Chen, X., Xia, Y., Huang, H., Gan, Y., Wu, R., Chen, F., and Zhang, W. (2013). Highly mesoporous carbon foams synthesized by a facile, cost-effective and template-free Pechini method for advanced lithium-sulfur batteries. *J. Mater. Chem. A* **1**, 3295–3301.
 123. Zhang, B., Qin, X., Li, G.R., and Gao, X.P. (2010). Enhancement of long stability of sulfur cathode by encapsulating sulfur into micropores of carbon spheres. *Energy Environ. Sci.* **3**, 1531–1537.
 124. Li, Z., Jiang, Y., Yuan, L., Yi, Z., Wu, C., Liu, Y., Strasser, P., and Huang, Y. (2014). A highly ordered meso@microporous carbon-supported sulfur@smaller sulfur core-shell structured cathode for Li-S batteries. *ACS Nano* **8**, 9295–9303.
 125. Li, Z., Yuan, L., Yi, Z., Sun, Y., Liu, Y., Jiang, Y., Shen, Y., Xin, Y., Zhang, Z., and Huang, Y. (2014). Insight into the electrode mechanism in lithium-sulfur batteries with ordered microporous carbon confined sulfur as the cathode. *Adv. Energy Mater.* **4**, 1301473.
 126. Wu, F., Chen, S., Srot, V., Huang, Y., Sinha, S.K., van Aken, P.A., Maier, J., and Yu, Y. (2018). A sulfur-limonene-based electrode for lithium-sulfur batteries: high-performance by self-protection. *Adv. Mater.* **30**, 1706643.
 127. Tao, X., Wang, J., Liu, C., Wang, H., Yao, H., Zheng, G., Seh, Z.W., Cai, Q., Li, W., Zhou, G., et al. (2016). Balancing surface adsorption and diffusion of lithium-polysulfides on nonconductive oxides for lithium-sulfur battery design. *Nat. Commun.* **7**, 11203.
 128. Naoi, K., Kawase, K.i., and Inoue, Y. (1997). A new energy storage material: organosulfur compounds based on multiple sulfur-sulfur bonds. *J. Electrochem. Soc.* **144**, L170–L172.
 129. Wang, D.-Y., Si, Y., Li, J., and Fu, Y. (2019). Tuning the electrochemical behavior of organodisulfides in rechargeable lithium batteries using N-containing heterocycles. *J. Mater. Chem. A* **7**, 7423–7429.
 130. Visco, S.J., and DeJonghe, L.C. (1988). Ionic conductivity of organosulfur melts for advanced storage electrodes. *J. Electrochem. Soc.* **135**, 2905–2909.
 131. Wu, M., Cui, Y., Bhargav, A., Losovyj, Y., Siegel, A., Agarwal, M., Ma, Y., and Fu, Y. (2016). Organotrithiulfide: a high capacity cathode material for rechargeable lithium batteries. *Angew. Chem. Int. Ed.* **55**, 10027–10031.
 132. Wu, M., Bhargav, A., Cui, Y., Siegel, A., Agarwal, M., Ma, Y., and Fu, Y. (2016). Highly reversible diphenyl trisulfide catholyte for rechargeable lithium batteries. *ACS Energy Lett.* **1**, 1221–1226.
 133. Bhargav, A., Ma, Y., Shashikala, K., Cui, Y., Losovyj, Y., and Fu, Y. (2017). The unique chemistry of thiuram polysulfides enables energy dense lithium batteries. *J. Mater. Chem. A* **5**, 25005–25013.
 134. Fu, C., Li, G., Zhang, J., Cornejo, B., Piao, S.S., Bozhilov, K.N., Haddon, R.C., and Guo, J. (2016). Electrochemical lithiation of covalently bonded sulfur in vulcanized polyisoprene. *ACS Energy Lett.* **1**, 115–120.
 135. Wang, X., Qian, Y., Wang, L., Yang, H., Li, H., Zhao, Y., and Liu, T. (2019). Sulfurized polyacrylonitrile cathodes with high compatibility in both ether and carbonate electrolytes for ultrastable lithium-sulfur batteries. *Adv. Funct. Mater.* **29**, 1902929.
 136. Chen, X., Peng, L., Wang, L., Yang, J., Hao, Z., Xiang, J., Yuan, K., Huang, Y., Shan, B., Yuan, L., et al. (2019). Ether-compatible sulfurized polyacrylonitrile cathode with excellent performance enabled by fast kinetics via selenium doping. *Nat. Commun.* **10**, 1021.
 137. Zhou, J., Qian, T., Xu, N., Wang, M., Ni, X., Liu, X., Shen, X., and Yan, C. (2017). Selenium-doped cathodes for lithium-organosulfur batteries with greatly improved volumetric capacity and Coulombic efficiency. *Adv. Mater.* **29**, 1701294.
 138. Wang, H., Zhang, W., Xu, J., and Guo, Z. (2018). Advances in polar materials for lithium-sulfur batteries. *Adv. Funct. Mater.* **28**, 1707520.
 139. Hou, T.-Z., Chen, X., Peng, H.-J., Huang, J.-Q., Li, B.-Q., Zhang, Q., and Li, B. (2016). Design principles for heteroatom-doped nanocarbon to achieve strong anchoring of polysulfides for lithium-sulfur batteries. *Small* **12**, 3283–3291.
 140. Pang, Q., Tang, J., Huang, H., Liang, X., Hart, C., Tam, K.C., and Nazar, L.F. (2015). A nitrogen and sulfur dual-doped carbon derived from polyrhodanine@cellulose for advanced lithium-sulfur batteries. *Adv. Mater.* **27**, 6021–6028.
 141. Chen, L., Feng, J., Zhou, H., Fu, C., Wang, G., Yang, L., Xu, C., Chen, Z., Yang, W., and

- Kuang, Y. (2017). Hydrothermal preparation of nitrogen, boron co-doped curved graphene nanoribbons with high dopant amounts for high-performance lithium sulfur battery cathodes. *J. Mater. Chem. A* 5, 7403–7415.
142. Wang, W., Li, Y., Feng, Y., Han, J., Zhang, F., Long, P., Peng, C., Cao, C., Cao, Y., Yang, H., et al. (2018). Asymmetric self-supporting hybrid fluorinated carbon nanotubes/carbon nanotubes sponge electrode for high-performance lithium-polysulfide battery. *Chem. Eng. J.* 349, 756–765.
143. Wu, H., Xia, L., Ren, J., Zheng, Q., Xu, C., and Lin, D. (2017). A high-efficiency N/P co-doped graphene/CNT@porous carbon hybrid matrix as a cathode host for high performance lithium-sulfur batteries. *J. Mater. Chem. A* 5, 20458–20472.
144. Ding, B., Shen, L., Xu, G., Nie, P., and Zhang, X. (2013). Encapsulating sulfur into mesoporous TiO₂ host as a high performance cathode for lithium-sulfur battery. *Electrochim. Acta* 107, 78–84.
145. Choi, Y.J., Jung, B.S., Lee, D.J., Jeong, J.H., Kim, K.W., Ahn, H.J., Cho, K.K., and Gu, H.B. (2007). Electrochemical properties of sulfur electrode containing nano Al₂O₃ for lithium/sulfur cell. *Phys. Scr.* T129, 62–65.
146. Rehman, S., Guo, S., and Hou, Y. (2016). Rational design of Si/SiO₂@hierarchical porous carbon spheres as efficient polysulfide reservoirs for high-performance Li-S battery. *Adv. Mater.* 28, 3167–3172.
147. Xu, J., Zhang, W., Chen, Y., Fan, H., Su, D., and Wang, G. (2018). MOF-derived porous N-Co₃O₄@N-C nanododecahedra wrapped with reduced graphene oxide as a high capacity cathode for lithium-sulfur batteries. *J. Mater. Chem. A* 6, 2797–2807.
148. Zheng, J., Tian, J., Wu, D., Gu, M., Xu, W., Wang, C., Gao, F., Engelhard, M.H., Zhang, J.-G., Liu, J., et al. (2014). Lewis acid-base interactions between polysulfides and metal organic framework in lithium sulfur batteries. *Nano Lett.* 14, 2345–2352.
149. Xiao, Z., Li, L., Tang, Y., Cheng, Z., Pan, H., Tian, D., and Wang, R. (2018). Covalent organic frameworks with lithiophilic and sulfiphilic dual linkages for cooperative affinity to polysulfides in lithium-sulfur batteries. *Energy Storage Mater.* 12, 252–259.
150. Bao, W., Liu, L., Wang, C., Choi, S., Wang, D., and Wang, G. (2018). Facile synthesis of crumpled nitrogen-doped MXene nanosheets as a new sulfur host for lithium-sulfur batteries. *Adv. Energy Mater.* 8, 1702485.
151. Zhang, Z.-W., Peng, H.-J., Zhao, M., and Huang, J.-Q. (2018). Heterogeneous/homogeneous mediators for high-energy-density lithium-sulfur batteries: progress and prospects. *Adv. Funct. Mater.* 28, 1707536.
152. Liang, X., Kwok, C.Y., Lodi-Marzano, F., Pang, Q., Cuisinier, M., Huang, H., Hart, C.J., Houtarde, D., Kaup, K., Sommer, H., et al. (2016). Tuning transition metal oxide-sulfur interactions for long life lithium sulfur batteries: the “Goldilocks” principle. *Adv. Energy Mater.* 6, 1501636.
153. Zheng, C., Niu, S., Lv, W., Zhou, G., Li, J., Fan, S., Deng, Y., Pan, Z., Li, B., Kang, F., et al. (2017). Propelling polysulfides transformation for high-rate and long-life lithium-sulfur batteries. *Nano Energy* 33, 306–312.
154. He, J., Luo, L., Chen, Y., and Manthiram, A. (2017). Yolk-shelled C@Fe₃O₄ nanoboxes as efficient sulfur hosts for high-performance lithium-sulfur batteries. *Adv. Mater.* 29, 1702707.
155. Chang, Z., Dou, H., Ding, B., Wang, J., Wang, Y., Hao, X., and MacFarlane, D.R. (2017). Co₃O₄ nanoneedle arrays as a multifunctional “super-reservoir” electrode for long cycle life Li-S batteries. *J. Mater. Chem. A* 5, 250–257.
156. Wu, S., Wang, Y., Na, S., Chen, C., Yu, T., Wang, H., and Zang, H. (2017). Porous hollow carbon nanospheres embedded with well-dispersed cobalt monoxide nanocrystals as effective polysulfide reservoirs for high-rate and long-cycle lithium-sulfur batteries. *J. Mater. Chem. A* 5, 17352–17359.
157. Yuan, Z., Peng, H.-J., Hou, T.-Z., Huang, J.-Q., Chen, C.-M., Wang, D.-W., Cheng, X.-B., Wei, F., and Zhang, Q. (2016). Powering lithium-sulfur battery performance by propelling polysulfide redox at sulfiphilic hosts. *Nano Lett.* 16, 519–527.
158. He, J., and Manthiram, A. (2019). A review on the status and challenges of electrocatalysts in lithium-sulfur batteries. *Energy Storage Mater.* 20, 55–70.
159. He, J., Chen, Y., and Manthiram, A. (2019). Metal sulfide-decorated carbon sponge as a highly efficient electrocatalyst and adsorbent for polysulfide in high-loading Li₂S batteries. *Adv. Energy Mater.* 9, 1900584.
160. Tian, Y., Li, G., Zhang, Y., Luo, D., Wang, X., Zhao, Y., Liu, H., Ji, P., Du, X., Li, J., et al. (2020). Low-bandgap Se-deficient antimony selenide as a multifunctional polysulfide barrier toward high-performance lithium-sulfur batteries. *Adv. Mater.* 32, 1904876.
161. Zhou, F., Li, Z., Luo, X., Wu, T., Jiang, B., Lu, L.-L., Yao, H.-B., Antonietti, M., and Yu, S.-H. (2018). Low cost metal carbide nanocrystals as binding and electrocatalytic sites for high performance Li-S batteries. *Nano Lett.* 18, 1035–1043.
162. Sun, Z., Zhang, J., Yin, L., Hu, G., Fang, R., Cheng, H.-M., and Li, F. (2017). Conductive porous vanadium nitride/graphene composite as chemical anchor of polysulfides for lithium-sulfur batteries. *Nat. Commun.* 8, 14627.
163. Huang, S., Lim, Y.V., Zhang, X., Wang, Y., Zheng, Y., Kong, D., Ding, M., Yang, S.A., and Yang, H.Y. (2018). Regulating the polysulfide redox conversion by iron phosphide nanocrystals for high-rate and ultrastable lithium-sulfur battery. *Nano Energy* 51, 340–348.
164. Zhang, Z., Luo, D., Li, G., Gao, R., Li, M., Li, S., Zhao, L., Dou, H., Wen, G., Sy, S., et al. (2020). Tantalum-based electrocatalyst for polysulfide catalysis and retention for high-performance lithium-sulfur batteries. *Matter* 3, 920–934.
165. Li, B.-Q., Peng, H.-J., Chen, X., Zhang, S.-Y., Xie, J., Zhao, C.-X., and Zhang, Q. (2019). Polysulfide electrocatalysis on framework porphyrin in high-capacity and high-stable lithium-sulfur batteries. *CCS Chem.* 1, 128–137.
166. Peng, L., Wei, Z., Wan, C., Li, J., Chen, Z., Zhu, D., Baumann, D., Liu, H., Allen, C.S., and Xu, X. (2020). A fundamental look at electrocatalytic sulfur reduction reaction. *Nat. Catal.* 3, 762–770.
167. Du, Z., Chen, X., Hu, W., Chuang, C., Xie, S., Hu, A., Yan, W., Kong, X., Wu, X., Ji, H., et al. (2019). Cobalt in nitrogen-doped graphene as single-atom catalyst for high-sulfur content lithium-sulfur batteries. *J. Am. Chem. Soc.* 141, 3977–3985.
168. Zhang, L., Liu, D., Muhammad, Z., Wan, F., Xie, W., Wang, Y., Song, L., Niu, Z., and Chen, J. (2019). Single nickel atoms on nitrogen-doped graphene enabling enhanced kinetics of lithium-sulfur batteries. *Adv. Mater.* 31, 1903955.
169. Wang, J., Jia, L., Zhong, J., Xiao, Q., Wang, C., Zang, K., Liu, H., Zheng, H., Luo, J., Yang, J., et al. (2019). Single-atom catalyst boosts electrochemical conversion reactions in batteries. *Energy Storage Mater.* 18, 246–252.
170. Li, B.-Q., Kong, L., Zhao, C.-X., Jin, Q., Chen, X., Peng, H.-J., Qin, J.-L., Chen, J.-X., Yuan, H., Zhang, Q., and Huang, J.-Q. (2019). Expediting redox kinetics of sulfur species by atomic-scale electrocatalysts in lithium-sulfur batteries. *InfoMat* 1, 533–541.
171. Ye, H., and Lee, J.Y. (2020). Solid additives for improving the performance of sulfur cathodes in lithium-sulfur batteries—adsorbents, mediators, and catalysts. *Small Methods* 4, 1900864.
172. Wei, Z., Ren, Y., Sokolowski, J., Zhu, X., and Wu, G. (2020). Mechanistic understanding of the role separators playing in advanced lithium-sulfur batteries. *InfoMat* 2, 483–508.
173. Xing, L.-B., Xi, K., Li, Q., Su, Z., Lai, C., Zhao, X., and Kumar, R.V. (2016). Nitrogen, sulfur-codoped graphene sponge as electroactive carbon interlayer for high-energy and -power lithium-sulfur batteries. *J. Power Sources* 303, 22–28.
174. Huang, J.-Q., Xu, Z.-L., Abouali, S., Akbari Garakani, M., and Kim, J.-K. (2016). Porous graphene oxide/carbon nanotube hybrid films as interlayer for lithium-sulfur batteries. *Carbon* 99, 624–632.
175. Fan, L., Li, M., Li, X., Xiao, W., Chen, Z., and Lu, J. (2019). Interlayer material selection for lithium-sulfur batteries. *Joule* 3, 361–386.
176. Wang, Y., He, J., Zhang, Z., Liu, Z., Huang, C., and Jin, Y. (2019). Graphdiyne-modified polyimide separator: a polysulfide-immobilizing net hinders the shuttling of polysulfides in lithium-sulfur battery. *ACS Appl. Mater. Interfaces* 11, 35738–35745.
177. Qian, J., Wang, F., Li, Y., Wang, S., Zhao, Y., Li, W., Xing, Y., Deng, L., Sun, Q., Li, L., et al. (2020). Electrocatalytic interlayer with fast lithium-polysulfides diffusion for lithium-sulfur batteries to enhance electrochemical kinetics under lean electrolyte conditions. *Adv. Funct. Mater.* 30, 2000742.

178. Wei, B., Shang, C., Wang, X., and Zhou, G. (2020). Conductive FeOOH as multifunctional interlayer for superior lithium-sulfur batteries. *Small* 16, 2002789.
179. Guo, Y., Zhang, Y., Zhang, Y., Xiang, M., Wu, H., Liu, H., and Dou, S. (2018). Interwoven V₂O₅ nanowire/graphene nanoscroll hybrid assembled as efficient polysulfide-trapping-conversion interlayer for long-life lithium-sulfur batteries. *J. Mater. Chem. A* 6, 19358–19370.
180. Xue, W., Yu, D., Suo, L., Wang, C., Wang, Z., Xu, G., Xiao, X., Ge, M., Ko, M., Chen, Y., et al. (2019). Manipulating sulfur mobility enables advanced Li-S batteries. *Matter* 1, 1047–1060.
181. Qu, L., Liu, P., Yi, Y., Wang, T., Yang, P., Tian, X., Li, M., Yang, B., and Dai, S. (2019). Enhanced cycling performance for lithium-sulfur batteries by a laminated 2D g-C₃N₄/graphene cathode interlayer. *ChemSusChem* 12, 213–223.
182. Zang, Y., Pei, F., Huang, J., Fu, Z., Xu, G., and Fang, X. (2018). Large-area preparation of crack-free crystalline microporous conductive membrane to upgrade high energy lithium-sulfur batteries. *Adv. Energy Mater.* 8, 1802052.
183. Kim, P.-J.H., Seo, J., Fu, K., Choi, J., Liu, Z., Kwon, J., Hu, L., and Paik, U. (2017). Synergistic protective effect of a BN-carbon separator for highly stable lithium sulfur batteries. *NPG Asia Mater.* 9, e375.
184. Li, Y., Lin, S., Wang, D., Gao, T., Song, J., Zhou, P., Xu, Z., Yang, Z., Xiao, N., and Guo, S. (2020). Single atom array mimic on ultrathin MOF nanosheets boosts the safety and life of lithium-sulfur batteries. *Adv. Mater.* 32, 1906722.
185. Bauer, I., Thieme, S., Brückner, J., Althues, H., and Kaskel, S. (2014). Reduced polysulfide shuttle in lithium-sulfur batteries using Nafion-based separators. *J. Power Sources* 251, 417–422.
186. Yu, B.-C., Park, K., Jang, J.-H., and Goodenough, J.B. (2016). Cellulose-based porous membrane for suppressing Li dendrite formation in lithium-sulfur battery. *ACS Energy Lett.* 1, 633–637.
187. Pavlin, N., Hribernik, S., Kapun, G., Talian, S.D., Njil, C., Dedryvère, R., and Dominko, R. (2018). The role of cellulose based separator in lithium sulfur batteries. *J. Electrochem. Soc.* 166, A5237–A5243.
188. Jiang, F., Yin, L., Yu, Q., Zhong, C., and Zhang, J. (2015). Bacterial cellulose nanofibrous membrane as thermal stable separator for lithium-ion batteries. *J. Power Sources* 279, 21–27.
189. Kim, J.-K., Kim, D.H., Joo, S.H., Choi, B., Cha, A., Kim, K.M., Kwon, T.-H., Kwak, S.K., Kang, S.J., and Jin, J. (2017). Hierarchical chitin fibers with aligned nanofibrillar architectures: a nonwoven-mat separator for lithium metal batteries. *ACS Nano* 11, 6114–6121.
190. Lei, T., Chen, W., Hu, Y., Lv, W., Lv, X., Yan, Y., Huang, J., Jiao, Y., Chu, J., Yan, C., et al. (2018). A nonflammable and thermotolerant separator suppresses polysulfide dissolution for safe and long-cycle lithium-sulfur batteries. *Adv. Energy Mater.* 8, 1802441.
191. Bai, S., Liu, X., Zhu, K., Wu, S., and Zhou, H. (2016). Metal-organic framework-based separator for lithium-sulfur batteries. *Nat. Energy* 1, 16094.
192. Jin, Z., Xie, K., Hong, X., Hu, Z., and Liu, X. (2012). Application of lithiated Nafion ionomer film as functional separator for lithium sulfur cells. *J. Power Sources* 218, 163–167.
193. Hu, M., Ma, Q., Yuan, Y., Pan, Y., Chen, M., Zhang, Y., and Long, D. (2020). Grafting polyethyleneimine on electrospun nanofiber separator to stabilize lithium metal anode for lithium sulfur batteries. *Chem. Eng. J.* 388, 124258.
194. Deng, N., Kang, W., Liu, Y., Ju, J., Wu, D., Li, L., Hassan, B.S., and Cheng, B. (2016). A review on separators for lithium sulfur battery: progress and prospects. *J. Power Sources* 331, 132–155.
195. Cao, L., An, P., Xu, Z., and Huang, J. (2016). Performance evaluation of electrospun polyimide non-woven separators for high power lithium-ion batteries. *J. Electroanal. Chem.* 767, 34–39.
196. Liang, Y., Cheng, S., Zhao, J., Zhang, C., Sun, S., Zhou, N., Qiu, Y., and Zhang, X. (2013). Heat treatment of electrospun polyvinylidene fluoride fibrous membrane separators for rechargeable lithium-ion batteries. *J. Power Sources* 240, 204–211.
197. Wang, B., Richardson, T.J., and Chen, G. (2014). Electroactive polymer fiber separators for stable and reversible overcharge protection in rechargeable lithium batteries. *J. Electrochem. Soc.* 161, A1039–A1044.
198. Yvonne, T., Zhang, C., Zhang, C., Omollo, E., and Ncube, S. (2014). Properties of electrospun PVDF/PMMA/CA membrane as lithium based battery separator. *Cellulose* 21, 2811–2818.
199. Zhu, J., Yanilmaz, M., Fu, K., Chen, C., Lu, Y., Ge, Y., Kim, D., and Zhang, X. (2016). Understanding glass fiber membrane used as a novel separator for lithium-sulfur batteries. *J. Membr. Sci.* 504, 89–96.
200. Qu, H., Ju, J., Chen, B., Xue, N., Du, H., Han, X., Zhang, J., Xu, G., Yu, Z., Wang, X., et al. (2018). Inorganic separators enable significantly suppressed polysulfide shuttling in high-performance lithium-sulfur batteries. *J. Mater. Chem. A* 6, 23720–23729.
201. He, Y., Chang, Z., Wu, S., Qiao, Y., Bai, S., Jiang, K., He, P., and Zhou, H. (2018). Simultaneously inhibiting lithium dendrites growth and polysulfides shuttle by a flexible MOF-based membrane in Li-S batteries. *Adv. Energy Mater.* 8, 1802130.
202. Li, M., Wan, Y., Huang, J.-K., Assen, A.H., Hsiung, C.-E., Jiang, H., Han, Y., Eddaoudi, M., Lai, Z., Ming, J., et al. (2017). Metal-organic framework-based separators for enhancing Li-S battery stability: mechanism of mitigating polysulfide diffusion. *ACS Energy Lett.* 2, 2362–2367.
203. Chang, Z., Qiao, Y., Wang, J., Deng, H., He, P., and Zhou, H. (2020). Fabricating better metal-organic frameworks separators for Li-S batteries: pore sizes effects inspired channel modification strategy. *Energy Storage Mater.* 25, 164–171.
204. Carbone, L., Gobet, M., Peng, J., Devany, M., Scrosati, B., Greenbaum, S., and Hassoun, J. (2015). Comparative study of ether-based electrolytes for application in lithium-sulfur battery. *ACS Appl. Mater. Interfaces* 7, 13859–13865.
205. Zhang, S., Ueno, K., Dokko, K., and Watanabe, M. (2015). Recent advances in electrolytes for lithium-sulfur batteries. *Adv. Energy Mater.* 5, 1500117.
206. Cheng, L., Curtiss, L.A., Zavadil, K.R., Gewirth, A.A., Shao, Y., and Gallagher, K.G. (2016). Sparingly solvating electrolytes for high energy density lithium-sulfur batteries. *ACS Energy Lett.* 1, 503–509.
207. Shi, L., Liu, Y., Wang, W., Wang, A., Jin, Z., Wu, F., and Yang, Y. (2017). High-safety lithium-ion sulfur battery with sulfurized polyacrylonitrile cathode, prelithiated SiOx/C anode and carbonate-based electrolyte. *J. Alloys Compd.* 723, 974–982.
208. Takahashi, T., Yamagata, M., and Ishikawa, M. (2015). A sulfur-microporous carbon composite positive electrode for lithium/sulfur and silicon/sulfur rechargeable batteries. *Prog. Nat. Sci. Mater. Int.* 25, 612–621.
209. Pan, H., Wei, X., Henderson, W.A., Shao, Y., Chen, J., Bhattacharya, P., Xiao, J., and Liu, J. (2015). On the way toward understanding solution chemistry of lithium polysulfides for high energy Li-S redox flow batteries. *Adv. Energy Mater.* 5, 1500113.
210. Yoon, S., Lee, Y.-H., Shin, K.-H., Cho, S.B., and Chung, W.J. (2014). Binary sulfone/ether-based electrolytes for rechargeable lithium-sulfur batteries. *Electrochim. Acta* 145, 170–176.
211. Pang, Q., Liang, X., Kwok, C.Y., and Nazar, L.F. (2016). Advances in lithium-sulfur batteries based on multifunctional cathodes and electrolytes. *Nat. Energy* 1, 16132.
212. Tachikawa, N., Yamauchi, K., Takashima, E., Park, J.-W., Dokko, K., and Watanabe, M. (2011). Reversibility of electrochemical reactions of sulfur supported on inverse opal carbon in glyme-Li salt molten complex electrolytes. *Chem. Commun.* 47, 8157–8159.
213. Pang, Q., Shyamsunder, A., Narayanan, B., Kwok, C.Y., Curtiss, L.A., and Nazar, L.F. (2018). Tuning the electrolyte network structure to invoke quasi-solid state sulfur conversion and suppress lithium dendrite formation in Li-S batteries. *Nat. Energy* 3, 783–791.
214. Yu, L., Chen, S., Lee, H., Zhang, L., Engelhard, M.H., Li, Q., Jiao, S., Liu, J., Xu, W., and Zhang, J.-G. (2018). A localized high-concentration electrolyte with optimized solvents and lithium difluoro(oxalate)borate additive for stable lithium metal batteries. *ACS Energy Lett.* 3, 2059–2067.
215. Zheng, J., Ji, G., Fan, X., Chen, J., Li, Q., Wang, H., Yang, Y., DeMella, K.C., Raghavan, S.R., and Wang, C. (2019). High-fluorinated electrolytes for Li-S batteries. *Adv. Energy Mater.* 9, 1803774.

216. Tsao, Y., Lee, M., Miller, E.C., Gao, G., Park, J., Chen, S., Katsumata, T., Tran, H., Wang, L.-W., Toney, M.F., et al. (2019). Designing a quinone-based redox mediator to facilitate Li_2S oxidation in Li-S batteries. *Joule* 3, 872–884.
217. Li, G., Gao, Y., He, X., Huang, Q., Chen, S., Kim, S.H., and Wang, D. (2017). Organosulfide-plasticized solid-electrolyte interphase layer enables stable lithium metal anodes for long-cycle lithium-sulfur batteries. *Nat. Commun.* 8, 850.
218. Yang, H., Guo, C., Chen, J., Naveed, A., Yang, J., Nuli, Y., and Wang, J. (2019). An intrinsic flame-retardant organic electrolyte for safe lithium-sulfur batteries. *Angew. Chem. Int. Ed.* 58, 791–795.
219. Meini, S., Elazari, R., Rosenman, A., Garsuch, A., and Aurbach, D. (2014). The use of redox mediators for enhancing utilization of Li_2S cathodes for advanced Li-S battery systems. *J. Phys. Chem. Lett.* 5, 915–918.
220. Chen, S., Gao, Y., Yu, Z., Gordin, M.L., Song, J., and Wang, D. (2017). High capacity of lithium-sulfur batteries at low electrolyte/sulfur ratio enabled by an organosulfide containing electrolyte. *Nano Energy* 31, 418–423.
221. Chen, S., Dai, F., Gordin, M.L., Yu, Z., Gao, Y., Song, J., and Wang, D. (2016). Functional organosulfide electrolyte promotes an alternate reaction pathway to achieve high performance in lithium-sulfur batteries. *Angew. Chem. Int. Ed.* 55, 4231–4235.
222. Zhao, M., Li, B.-Q., Chen, X., Xie, J., Yuan, H., and Huang, J.-Q. (2020). Redox mediation with organopolysulfides in working lithium-sulfur batteries. *Chem.* <https://doi.org/10.1016/j.chempr.2020.09.015>.
223. Wang, Q., Yang, C., Yang, J., Wu, K., Hu, C., Lu, J., Liu, W., Sun, X., Qiu, J., and Zhou, H. (2019). Dendrite-free lithium deposition via a superfilling mechanism for high-performance Li-metal batteries. *Adv. Mater.* 31, 1903248.
224. Wei, J.-Y., Zhang, X.-Q., Hou, L.-P., Shi, P., Li, B.-Q., Xiao, Y., Yan, C., Yuan, H., and Huang, J.-Q. (2020). Shielding polysulfide intermediates by an organosulfur-containing solid electrolyte interphase on the lithium anode in lithium-sulfur batteries. *Adv. Mater.* 32, 2003012.
225. Lin, F., Wang, J., Jia, H., Monroe, C.W., Yang, J., and Nuli, Y. (2013). Nonflammable electrolyte for rechargeable lithium battery with sulfur based composite cathode materials. *J. Power Sourc.* 223, 18–22.
226. Chen, J., Yang, H., Zhang, X., Lei, J., Zhang, H., Yuan, H., Yang, J., Nuli, Y., and Wang, J. (2019). Highly reversible lithium-metal anode and lithium-sulfur batteries enabled by an intrinsic safe electrolyte. *ACS Appl. Mater. Interfaces* 11, 33419–33427.
227. Lei, D., Shi, K., Ye, H., Wan, Z., Wang, Y., Shen, L., Li, B., Yang, Q.-H., Kang, F., and He, Y.-B. (2018). Progress and perspective of solid-state lithium-sulfur batteries. *Adv. Funct. Mater.* 28, 1707570.
228. Umeshbabu, E., Zheng, B., and Yang, Y. (2019). Recent progress in all-solid-state lithium-sulfur batteries using high Li-ion conductive solid electrolytes. *Electrochem. Energy Rev.* 2, 199–230.
229. Yang, X., Luo, J., and Sun, X. (2020). Towards high-performance solid-state Li-S batteries: from fundamental understanding to engineering design. *Chem. Soc. Rev.* 49, 2140–2195.
230. Li, W., Pang, Y., Zhu, T., Wang, Y., and Xia, Y. (2018). A gel polymer electrolyte based lithium-sulfur battery with low self-discharge. *Solid State Ionics* 318, 82–87.
231. Han, D.-D., Liu, S., Liu, Y.-T., Zhang, Z., Li, G.-R., and Gao, X.-P. (2018). Lithiophilic gel polymer electrolyte to stabilize the lithium anode for a quasi-solid-state lithium-sulfur battery. *J. Mater. Chem. A* 6, 18627–18634.
232. Yang, W., Yang, W., Feng, J., Ma, Z., and Shao, G. (2016). High capacity and cycle stability rechargeable lithium-sulfur batteries by sandwiched gel polymer electrolyte. *Electrochim. Acta* 210, 71–78.
233. Jiang, J.-H., Wang, A.-B., Wang, W.-K., Jin, Z.-Q., and Fan, L.-Z. (2020). P(VDF-HFP)-poly(sulfur-1,3-diisopropenylbenzene) functional polymer electrolyte for lithium-sulfur batteries. *J. Energy Chem.* 46, 114–122.
234. Zhou, J., Ji, H., Liu, J., Qian, T., and Yan, C. (2019). A new high ionic conductive gel polymer electrolyte enables highly stable quasi-solid-state lithium sulfur battery. *Energy Storage Mater.* 22, 256–264.
235. Lin, Y., Wang, X., Liu, J., and Miller, J.D. (2017). Natural halloysite nano-clay electrolyte for advanced all-solid-state lithium-sulfur batteries. *Nano Energy* 31, 478–485.
236. Han, F., Yue, J., Fan, X., Gao, T., Luo, C., Ma, Z., Suo, L., and Wang, C. (2016). High-performance all-solid-state lithium-sulfur battery enabled by a mixed-conductive Li_2S nanocomposite. *Nano Lett.* 16, 4521–4527.
237. Judez, X., Zhang, H., Li, C., González-Marcos, J.A., Zhou, Z., Armand, M., and Rodriguez-Martinez, L.M. (2017). Lithium bis(fluorosulfonyl)imide/poly(ethylene oxide) polymer electrolyte for all solid-state Li-S cell. *J. Phys. Chem. Lett.* 8, 1956–1960.
238. Zhang, J., Yue, L., Hu, P., Liu, Z., Qin, B., Zhang, B., Wang, Q., Ding, G., Zhang, C., Zhou, X., et al. (2014). Taichi-inspired rigid-flexible coupling cellulose-supported solid polymer electrolyte for high-performance lithium batteries. *Sci. Rep.* 4, 6272.
239. Schulze, M.W., McIntosh, L.D., Hillmyer, M.A., and Lodge, T.P. (2014). High-modulus, high-conductivity nanostructured polymer electrolyte membranes via polymerization-induced phase separation. *Nano Lett.* 14, 122–126.
240. Zhu, P., Yan, C., Dirican, M., Zhu, J., Zang, J., Selvan, R.K., Chung, C.-C., Jia, H., Li, Y., Kiyak, Y., et al. (2018). $\text{Li}_{0.33}\text{La}_{0.557}\text{TiO}_3$ ceramic nanofiber-enhanced polyethylene oxide-based composite polymer electrolytes for all-solid-state lithium batteries. *J. Mater. Chem. A* 6, 4279–4285.
241. Goujon, L.J., Khaldi, A., Maziz, A., Plesse, C., Nguyen, G.T.M., Aubert, P.-H., Vidal, F., Chevrot, C., and Yessiad, D. (2011). Flexible solid polymer electrolytes based on nitrile butadiene rubber/poly(ethylene oxide) interpenetrating polymer networks containing either LiTFSI or EMITFSI. *Macromolecules* 44, 9683–9691.
242. Yan, M., Wang, W.-P., Yin, Y.-X., Wan, L.-J., and Guo, Y.-G. (2019). Interfacial design for lithium-sulfur batteries: from liquid to solid. *EnergyChem* 1, 100002.
243. Tan, D.H.S., Banerjee, A., Chen, Z., and Meng, Y.S. (2020). From nanoscale interface characterization to sustainable energy storage using all-solid-state batteries. *Nat. Nanotechnol.* 15, 170–180.
244. Lou, S., Zhang, F., Fu, C., Chen, M., Ma, Y., Yin, G., and Wang, J. (2020). Interface issues and challenges in all-solid-state batteries: lithium, sodium, and beyond. *Adv. Mater.* 2000721, <https://doi.org/10.1002/adma.202000721>.
245. Luo, W., Gong, Y., Zhu, Y., Li, Y., Yao, Y., Zhang, Y., Fu, K., Pastel, G., Lin, C.-F., Mo, Y., et al. (2017). Reducing interfacial resistance between garnet-structured solid-state electrolyte and Li-metal anode by a germanium layer. *Adv. Mater.* 29, 1606042.
246. Duan, H., Chen, W.-P., Fan, M., Wang, W.-P., Yu, L., Tan, S.-J., Chen, X., Zhang, Q., Xin, S., Wan, L.-J., et al. (2020). Building an air stable and lithium deposition regulable garnet interface from moderate-temperature conversion chemistry. *Angew. Chem. Int. Ed.* 59, 12069–12075.
247. Dong, D., Zhou, B., Sun, Y., Zhang, H., Zhong, G., Dong, Q., Fu, F., Qian, H., Lin, Z., Lu, D., et al. (2019). Polymer electrolyte glue: a universal interfacial modification strategy for all-solid-state Li batteries. *Nano Lett.* 19, 2343–2349.
248. Das, S., Ngene, P., Norby, P., Vegge, T., de Jongh, P.E., and Blanchard, D. (2016). All-solid-state lithium-sulfur battery based on a nanoconfined LiBH_4 electrolyte. *J. Electrochem. Soc.* 163, A2029–A2034.
249. Unemoto, A., Chen, C., Wang, Z., Matsuo, M., Ikeshoji, T., and Orimo, S.-i. (2015). Pseudo-binary electrolyte, $\text{LiBH}_4\text{-LiCl}$, for bulk-type all-solid-state lithium-sulfur battery. *Nanotechnol* 26, 254001.
250. Suzuki, K., Kato, D., Hara, K., Yano, T.-a., Hirayama, M., Hara, M., and Kanno, R. (2017). Composite sulfur electrode prepared by high-temperature mechanical milling for use in an all-solid-state lithium-sulfur battery with a $\text{Li}_{3.25}\text{Ge}_{0.25}\text{P}_{0.75}\text{S}_4$ electrolyte. *Electrochim. Acta* 258, 110–115.
251. Yi, J., Chen, L., Liu, Y., Geng, H., and Fan, L.-Z. (2019). High capacity and superior cyclic performances of all-solid-state lithium-sulfur batteries enabled by a high-conductivity $\text{Li}_{10}\text{SnP}_2\text{S}_{12}$ solid electrolyte. *ACS Appl. Mater. Interfaces* 11, 36774–36781.
252. Li, X., Liang, J., Luo, J., Wang, C., Li, X., Sun, Q., Li, R., Zhang, L., Yang, R., Lu, S., et al. (2019). High-performance Li-SeS_x all-solid-state lithium batteries. *Adv. Mater.* 31, 1808100.
253. Lin, Z., Liu, Z., Dudney, N.J., and Liang, C. (2013). Lithium superionic sulfide cathode for all-solid lithium-sulfur batteries. *ACS Nano* 7, 2829–2833.

254. Fu, K.K., Gong, Y., Xu, S., Zhu, Y., Li, Y., Dai, J., Wang, C., Liu, B., Pastel, G., Xie, H., et al. (2017). Stabilizing the garnet solid-electrolyte/poly sulfide interface in Li-S batteries. *Chem. Mater.* **29**, 8037–8041.
255. Fu, K., Gong, Y., Hitz, G.T., McOwen, D.W., Li, Y., Xu, S., Wen, Y., Zhang, L., Wang, C., Pastel, G., et al. (2017). Three-dimensional bilayer garnet solid electrolyte based high energy density lithium metal-sulfur batteries. *Energy Environ. Sci.* **10**, 1568–1575.
256. Xu, S., McOwen, D.W., Wang, C., Zhang, L., Luo, W., Chen, C., Li, Y., Gong, Y., Dai, J., Kuang, Y., et al. (2018). Three-dimensional, solid-state mixed electron-ion conductive framework for lithium metal anode. *Nano Lett.* **18**, 3926–3933.
257. Xu, S., McOwen, D.W., Zhang, L., Hitz, G.T., Wang, C., Ma, Z., Chen, C., Luo, W., Dai, J., Kuang, Y., et al. (2018). All-in-one lithium-sulfur battery enabled by a porous-dense-porous garnet architecture. *Energy Storage Mater.* **15**, 458–464.
258. Lee, M.-T., Liu, H., and Brandell, D. (2020). The surface chemistry of thin lithium metal electrodes in lithium-sulfur cells. *Batteries Supercaps.* <https://doi.org/10.1002/batt.202000145>.
259. Nanda, S., and Manthiram, A. (2020). Lithium degradation in lithium-sulfur batteries: insights into inventory depletion and interphasial evolution with cycling. *Energy Environ. Sci.* **13**, 2501–2514.
260. Yan, C., Zhang, X.-Q., Huang, J.-Q., Liu, Q., and Zhang, Q. (2019). Lithium-anode protection in lithium-sulfur batteries. *Trends Chem.* **1**, 693–704.
261. Huang, W., Yu, Y., Hou, Z., Liang, Z., Zheng, Y., Quan, Z., and Lu, Y.-C. (2020). Dendrite-free lithium electrode enabled by graphene aerogels with gradient porosity. *Energy Storage Mater.* **33**, 329–335.
262. Liu, L., Yin, Y.-X., Li, J.-Y., Li, N.-W., Zeng, X.-X., Ye, H., Guo, Y.-G., and Wan, L.-J. (2017). Free-standing hollow carbon fibers as high-capacity containers for stable lithium metal anodes. *Joule* **1**, 563–575.
263. Yang, G., Li, Y., Tong, Y., Qiu, J., Liu, S., Zhang, S., Guan, Z., Xu, B., Wang, Z., and Chen, L. (2019). Lithium plating and stripping on carbon nanotube sponge. *Nano Lett.* **19**, 494–499.
264. Yan, X., Zhang, H., Huang, M., Qu, M., and Wei, Z. (2019). Self-formed protection layer on a 3D lithium metal anode for ultrastable lithium-sulfur batteries. *ChemSusChem* **12**, 2263–2270.
265. Meng, J.-K., Wang, W.-W., Yue, X.-Y., Xia, H.-Y., Wang, Q.-C., Wang, X.-X., Fu, Z.-W., Wu, X.-J., and Zhou, Y.-N. (2020). Cotton-derived carbon cloth enabling dendrite-free Li deposition for lithium metal batteries. *J. Power Sources* **465**, 228291.
266. Zhang, Y., Luo, W., Wang, C., Li, Y., Chen, C., Song, J., Dai, J., Hitz, E.M., Xu, S., Yang, C., et al. (2017). High-capacity, low-tortuosity, and channel-guided lithium metal anode. *Proc. Natl. Acad. Sci. U S A* **114**, 3584–3589.
267. Liang, Z., Zheng, G., Liu, C., Liu, N., Li, W., Yan, K., Yao, H., Hsu, P.-C., Chu, S., and Cui, Y. (2015). Polymer nanofiber-guided uniform lithium deposition for battery electrodes. *Nano Lett.* **15**, 2910–2916.
268. Liu, Y., Lin, D., Liang, Z., Zhao, J., Yan, K., and Cui, Y. (2016). Lithium-coated polymeric matrix as a minimum volume-change and dendrite-free lithium metal anode. *Nat. Commun.* **7**, 10992.
269. Li, G., Liu, Z., Huang, Q., Gao, Y., Regula, M., Wang, D., Chen, L.-Q., and Wang, D. (2018). Stable metal battery anodes enabled by polyethylenimine sponge hosts by way of electrokinetic effects. *Nat. Energy* **3**, 1076–1083.
270. Chi, S.-S., Liu, Y., Song, W.-L., Fan, L.-Z., and Zhang, Q. (2017). Prestoring lithium into stable 3D nickel foam host as dendrite-free lithium metal anode. *Adv. Funct. Mater.* **27**, 1700348.
271. Zhao, H., Lei, D., He, Y.-B., Yuan, Y., Yun, Q., Ni, B., Lv, W., Li, B., Yang, Q.-H., Kang, F., et al. (2018). Compact 3D copper with uniform porous structure derived by electrochemical dealloying as dendrite-free lithium metal anode current collector. *Adv. Energy Mater.* **8**, 1800266.
272. Zhang, X., Lv, R., Wang, A., Guo, W., Liu, X., and Luo, J. (2018). MXene aerogel scaffolds for high-rate lithium metal anodes. *Angew. Chem. Int. Ed.* **57**, 15028–15033.
273. Lin, D., Liu, Y., Liang, Z., Lee, H.-W., Sun, J., Wang, H., Yan, K., Xie, J., and Cui, Y. (2016). Layered reduced graphene oxide with nanoscale interlayer gaps as a stable host for lithium metal anodes. *Nat. Nanotechnol.* **11**, 626–632.
274. Chen, H., Pei, A., Wan, J., Lin, D., Vilá, R., Wang, H., Mackanic, D., Steinrück, H.-G., Huang, W., Li, Y., et al. (2020). Tortuosity effects in lithium-metal host anodes. *Joule* **4**, 938–952.
275. Jin, S., Ye, Y., Niu, Y., Xu, Y., Jin, H., Wang, J., Sun, Z., Cao, A., Wu, X., Luo, Y., et al. (2020). Solid-solution-based metal alloy phase for highly reversible lithium metal anode. *J. Am. Chem. Soc.* **142**, 8818–8826.
276. Wang, L., Zhu, X., Guan, Y., Zhang, J., Ai, F., Zhang, W., Xiang, Y., Vijayan, S., Li, G., Huang, Y., et al. (2018). ZnO/carbon framework derived from metal-organic frameworks as a stable host for lithium metal anodes. *Energy Storage Mater.* **11**, 191–196.
277. Zhang, Y., Wang, C., Pastel, G., Kuang, Y., Xie, H., Li, Y., Liu, B., Luo, W., Chen, C., and Hu, L. (2018). 3D wettable framework for dendrite-free alkali metal anodes. *Adv. Energy Mater.* **8**, 1800635.
278. Jin, C., Sheng, O., Lu, Y., Luo, J., Yuan, H., Zhang, W., Huang, H., Gan, Y., Xia, Y., Liang, C., et al. (2018). Metal oxide nanoparticles induced step-edge nucleation of stable Li metal anode working under an ultrahigh current density of 15 mA cm⁻². *Nano Energy* **45**, 203–209.
279. Chen, X., Chen, X.-R., Hou, T.-Z., Li, B.-Q., Cheng, X.-B., Zhang, R., and Zhang, Q. (2019). Lithiophilicity chemistry of heteroatom-doped carbon to guide uniform lithium nucleation in lithium metal anodes. *Sci. Adv.* **5**, eaau7728.
280. Liu, Y., Qin, X., Zhang, S., Huang, Y., Kang, F., Chen, G., and Li, B. (2019). Oxygen and nitrogen co-doped porous carbon granules enabling dendrite-free lithium metal anode. *Energy Storage Mater.* **18**, 320–327.
281. Xue, P., Liu, S., Shi, X., Sun, C., Lai, C., Zhou, Y., Sui, D., Chen, Y., and Liang, J. (2018). A hierarchical silver-nanowire-graphene host enabling ultrahigh rates and superior long-term cycling of lithium-metal composite anodes. *Adv. Mater.* **30**, 1804165.
282. Lan, X., Ye, W., Zheng, H., Cheng, Y., Zhang, Q., Peng, D.-L., and Wang, M.-S. (2019). Encapsulating lithium and sodium inside amorphous carbon nanotubes through gold-seeded growth. *Nano Energy* **66**, 104178.
283. Tian, Y., An, Y., Wei, C., Xi, B., Xiong, S., Feng, J., and Qian, Y. (2019). Flexible and free-standing Ti₃C₂T_x MXene@Zn paper for dendrite-free aqueous zinc metal batteries and nonaqueous lithium metal batteries. *ACS Nano* **13**, 11676–11685.
284. Gu, J., Zhu, Q., Shi, Y., Chen, H., Zhang, D., Du, Z., and Yang, S. (2020). Single zinc atoms immobilized on MXene (Ti₃C₂Cl_x) layers toward dendrite-free lithium metal anodes. *ACS Nano* **14**, 891–898.
285. Yang, C., Yao, Y., He, S., Xie, H., Hitz, E., and Hu, L. (2017). Ultrafine silver nanoparticles for seeded lithium deposition toward stable lithium metal anode. *Adv. Mater.* **29**, 1702714.
286. Liu, S., Ma, Y., Zhou, Z., Lou, S., Huo, H., Zuo, P., Wang, J., Du, C., Yin, G., and Gao, Y. (2020). Inducing uniform lithium nucleation by integrated lithium-rich Li-In anode with lithiophilic 3D framework. *Energy Storage Mater.* **33**, 423–431.
287. Choudhury, S., Tu, Z., Stalin, S., Vu, D., Fawole, K., Gunceler, D., Sundararaman, R., and Archer, L.A. (2017). Electroless formation of hybrid lithium anodes for fast interfacial ion transport. *Angew. Chem. Int. Ed.* **56**, 13070–13077.
288. Ye, H., Zheng, Z.-J., Yao, H.-R., Liu, S.-C., Zuo, T.-T., Wu, X.-W., Yin, Y.-X., Li, N.-W., Gu, J.-J., Cao, F.-F., et al. (2019). Guiding uniform Li plating/stripping through lithium-aluminum alloying medium for long-life Li metal batteries. *Angew. Chem. Int. Ed.* **58**, 1094–1099.
289. Kim, M.S., Deepika, Lee, S.H., Kim, M.-S., Ryu, J.-H., Lee, K.-R., Archer, L.A., and Cho, W.I. (2019). Enabling reversible redox reactions in electrochemical cells using protected LiAl intermetallics as lithium metal anodes. *Sci. Adv.* **5**, eaax5587.
290. Lu, Z., Li, W., Long, Y., Liang, J., Liang, Q., Wu, S., Tao, Y., Weng, Z., Lv, W., and Yang, Q.-H. (2020). Constructing a high-strength solid electrolyte layer by *in vivo* alloying with aluminum for an ultrahigh-rate lithium metal anode. *Adv. Funct. Mater.* **30**, 1907343.
291. Kong, L.-L., Wang, L., Ni, Z.-C., Liu, S., Li, G.-R., and Gao, X.-P. (2019). Lithium-magnesium alloy as a stable anode for lithium-sulfur battery. *Adv. Funct. Mater.* **29**, 1808756.

292. Zhang, X., Wang, W., Wang, A., Huang, Y., Yuan, K., Yu, Z., Qiu, J., and Yang, Y. (2014). Improved cycle stability and high security of Li-B alloy anode for lithium-sulfur battery. *J. Mater. Chem. A* 2, 11660–11665.
293. Wan, M., Kang, S., Wang, L., Lee, H.-W., Zheng, G.W., Cui, Y., and Sun, Y. (2020). Mechanical rolling formation of interpenetrated lithium metal/lithium tin alloy foil for ultrahigh-rate battery anode. *Nat. Commun.* 11, 829.
294. Liang, X., Pang, Q., Kochetkov, I.R., Sempere, M.S., Huang, H., Sun, X., and Nazar, L.F. (2017). A facile surface chemistry route to a stabilized lithium metal anode. *Nat. Energy* 2, 17119.
295. He, G., Li, Q., Shen, Y., and Ding, Y. (2019). Flexible amalgam film enables stable lithium metal anodes with high capacities. *Angew. Chem. Int. Ed.* 58, 18466–18470.
296. Wang, R., Yu, J., Tang, J., Meng, R., Nazar, L.F., Huang, L., and Liang, X. (2020). Insights into dendrite suppression by alloys and the fabrication of a flexible alloy-polymer protected lithium metal anode. *Energy Storage Mater.* 32, 178–184.
297. Li, N.-W., Yin, Y.-X., Yang, C.-P., and Guo, Y.-G. (2016). An artificial solid electrolyte interphase layer for stable lithium metal anodes. *Adv. Mater.* 28, 1853–1858.
298. Yin, Y.-C., Wang, Q., Yang, J.-T., Li, F., Zhang, G., Jiang, C.-H., Mo, H.-S., Yao, J.-S., Wang, K.-H., Zhou, F., et al. (2020). Metal chloride perovskite thin film based interfacial layer for shielding lithium metal from liquid electrolyte. *Nat. Commun.* 11, 1761.
299. Chen, K., Pathak, R., Gurung, A., Adhamash, E.A., Bahrami, B., He, Q., Qiao, H., Smirnova, A.L., Wu, J.J., Qiao, Q., et al. (2019). Flower-shaped lithium nitride as a protective layer via facile plasma activation for stable lithium metal anodes. *Energy Storage Mater.* 18, 389–396.
300. Li, P., Dong, X., Li, C., Liu, J., Liu, Y., Feng, W., Wang, C., Wang, Y., and Xia, Y. (2019). Anchoring an artificial solid-electrolyte interphase layer on a 3D current collector for high-performance lithium anodes. *Angew. Chem. Int. Ed.* 58, 2093–2097.
301. Chen, H., Pei, A., Lin, D., Xie, J., Yang, A., Xu, J., Lin, K., Wang, J., Wang, H., Shi, F., et al. (2019). Uniform high ionic conducting lithium sulfide protection layer for stable lithium metal anode. *Adv. Energy Mater.* 9, 1900858.
302. Lin, C.-F., Kozen, A.C., Noked, M., Liu, C., and Rubloff, G.W. (2016). ALD protection of Li-metal anode surfaces—quantifying and preventing chemical and electrochemical corrosion in organic solvent. *Adv. Mater. Interfaces* 3, 1600426.
303. Yan, K., Lee, H.-W., Gao, T., Zheng, G., Yao, H., Wang, H., Lu, Z., Zhou, Y., Liang, Z., Liu, Z., et al. (2014). Ultrathin two-dimensional atomic crystals as stable interfacial layer for improvement of lithium metal anode. *Nano Lett.* 14, 6016–6022.
304. Yao, Y.-X., Zhang, X.-Q., Li, B.-Q., Yan, C., Chen, P.-Y., Huang, J.-Q., and Zhang, Q. (2020). A compact inorganic layer for robust anode protection in lithium-sulfur batteries. *InfoMat* 2, 379–388.
305. Lee, Y.M., Choi, N.-S., Park, J.H., and Park, J.-K. (2003). Electrochemical performance of lithium/sulfur batteries with protected Li anodes. *J. Power Sources* 119-121, 964–972.
306. Luo, J., Fang, C.-C., and Wu, N.-L. (2018). High polarity poly(vinylidene difluoride) thin coating for dendrite-free and high-performance lithium metal anodes. *Adv. Energy Mater.* 8, 1701482.
307. Lee, Y.-G., Ryu, S., Sugimoto, T., Yu, T., Chang, W.-s., Yang, Y., Jung, C., Woo, J., Kang, S.G., Han, H.N., et al. (2017). Dendrite-free lithium deposition for lithium metal anodes with interconnected microsphere protection. *Chem. Mater.* 29, 5906–5914.
308. Liu, W., Lin, D., Pei, A., and Cui, Y. (2016). Stabilizing lithium metal anodes by uniform Li-ion flux distribution in nanochannel confinement. *J. Am. Chem. Soc.* 138, 15443–15450.
309. Meng, J., Chu, F., Hu, J., and Li, C. (2019). Liquid polydimethylsiloxane grafting to enable dendrite-free Li plating for highly reversible Li-metal batteries. *Adv. Funct. Mater.* 29, 1902220.
310. Xu, R., Cheng, X.-B., Yan, C., Zhang, X.-Q., Xiao, Y., Zhao, C.-Z., Huang, J.-Q., and Zhang, Q. (2019). Artificial interphases for highly stable lithium metal anode. *Matter* 1, 317–344.
311. Feng, Y., Zhang, C., Jiao, X., Zhou, Z., and Song, J. (2020). Highly stable lithium metal anode with near-zero volume change enabled by capped 3D lithophilic framework. *Energy Storage Mater.* 25, 172–179.
312. Xiang, J., Zhao, Y., Yuan, L., Chen, C., Shen, Y., Hu, F., Hao, Z., Liu, J., Xu, B., and Huang, Y. (2017). A strategy of selective and dendrite-free lithium deposition for lithium batteries. *Nano Energy* 42, 262–268.
313. Liu, W., Li, W., Zhuo, D., Zheng, G., Lu, Z., Liu, K., and Cui, Y. (2017). Core-shell nanoparticle coating as an interfacial layer for dendrite-free lithium metal anodes. *ACS Cent. Sci.* 3, 135–140.
314. Xu, R., Zhang, X.-Q., Cheng, X.-B., Peng, H.-J., Zhao, C.-Z., Yan, C., and Huang, J.-Q. (2018). Artificial soft-rigid protective layer for dendrite-free lithium metal anode. *Adv. Funct. Mater.* 28, 1705838.
315. Kim, J.-H., Woo, H.-S., Kim, W.K., Ryu, K.H., and Kim, D.-W. (2016). Improved cycling performance of lithium-oxygen cells by use of a lithium electrode protected with conductive polymer and aluminum fluoride. *ACS Appl. Mater. Interfaces* 8, 32300–32306.
316. Sun, C., Huang, X., Jin, J., Lu, Y., Wang, Q., Yang, J., and Wen, Z. (2018). An ion-conductive $\text{Li}_{1.5}\text{Al}_{0.5}\text{Ge}_{1.5}(\text{PO}_4)_3$ -based composite protective layer for lithium metal anode in lithium-sulfur batteries. *J. Power Sources* 377, 36–43.
317. Zhao, J., Liao, L., Shi, F., Lei, T., Chen, G., Pei, A., Sun, J., Yan, K., Zhou, G., Xie, J., et al. (2017). Surface fluorination of reactive battery anode materials for enhanced stability. *J. Am. Chem. Soc.* 139, 11550–11558.
318. Zhang, Y., Lv, W., Huang, Z., Zhou, G., Deng, Y., Zhang, J., Zhang, C., Hao, B., Qi, Q., He, Y.-B., et al. (2019). An air-stable and waterproof lithium metal anode enabled by wax composite packaging. *Sci. Bull.* 64, 910–917.
319. Liu, Y., Lin, D., Yuen, P.-Y., Liu, K., Xie, J., Dauskardt, R.H., and Cui, Y. (2017). An artificial solid electrolyte interphase with high Li-ion conductivity, mechanical strength, and flexibility for stable lithium metal anodes. *Adv. Mater.* 29, 1605531.
320. Gao, S., Sun, F., Liu, N., Yang, H., and Cao, P.-F. (2020). Ionic conductive polymers as artificial solid electrolyte interphase films in Li metal batteries—a review. *Mater. Today*. <https://doi.org/10.1016/j.mattod.2020.06.011>.
321. Yu, Z., Mackanic, D.G., Michaels, W., Lee, M., Pei, A., Feng, D., Zhang, Q., Tsao, Y., Amanchukwu, C.V., Yan, X., et al. (2019). A dynamic, electrolyte-blocking, and single-ion-conductive network for stable lithium-metal anodes. *Joule* 3, 2761–2776.
322. Chen, D., Huang, S., Zhong, L., Wang, S., Xiao, M., Han, D., and Meng, Y. (2020). *In situ* preparation of thin and rigid COF film on Li anode as artificial solid electrolyte interphase layer resisting Li dendrite puncture. *Adv. Funct. Mater.* 30, 1907717.
323. Qian, J., Li, Y., Zhang, M., Luo, R., Wang, F., Ye, Y., Xing, Y., Li, W., Qu, W., Wang, L., et al. (2019). Protecting lithium/sodium metal anode with metal-organic framework based compact and robust shield. *Nano Energy* 60, 866–874.
324. Jiang, Z., Liu, T., Yan, L., Liu, J., Dong, F., Ling, M., Liang, C., and Lin, Z. (2018). Metal-organic framework nanosheets-guided uniform lithium deposition for metallic lithium batteries. *Energy Storage Mater.* 11, 267–273.
325. Xu, Y., Gao, L., Shen, L., Liu, Q., Zhu, Y., Liu, Q., Li, L., Kong, X., Lu, Y., and Wu, H.B. (2020). Ion-transport-rectifying layer enables Li-metal batteries with high energy density. *Matter*. <https://doi.org/10.1016/j.matt.2020.08.011>.
326. Zhao, Y., Amirmaleki, M., Sun, Q., Zhao, C., Codireni, A., Goncharova, L.V., Wang, C., Adair, K., Li, X., Yang, X., et al. (2019). Natural SEI-inspired dual-protective layers via atomic/molecular layer deposition for long-life metallic lithium anode. *Matter* 1, 1215–1231.
327. Li, G., Chen, Z., and Lu, J. (2018). Lithium-sulfur batteries for commercial applications. *Chem* 4, 3–7.
328. Peng, H.-J., Huang, J.-Q., Cheng, X.-B., and Zhang, Q. (2017). Review on high-loading and high-energy lithium-sulfur batteries. *Adv. Energy Mater.* 7, 1700260.
329. Chung, S.-H., and Manthiram, A. (2018). Designing lithium-sulfur cells with practically necessary parameters. *Joule* 2, 710–724.
330. Wang, H.-F., and Xu, Q. (2019). Materials design for rechargeable metal-air batteries. *Matter* 1, 565–595.